eman ta zabal zazu

Universidad del País Vasco
Euskal Herriko Unibertsitatea

Facultad de Medicina y Enfermería
Departamento de Neurociencias

Role of MCSF-activated microglia in amyloid-associated pathology

Tesis doctoral para optar al grado de Doctor, presentada por:

Jone Zuazo Ibarra

2022

Directores de tesis:

Dra. Estíbaliz Capetillo González de Zarate

Dr. Carlos Matute Almau

Esta tesis doctoral ha sido realizada gracias a una beca de contratación para la formación de personal investigador del Gobierno Vasco durante el periodo 2018-2021. El trabajo experimental ha sido financiado por el Centro de Investigación Biomédica en Red de Enfermedades Neurodegenerativas (CIBERNED), proyectos del Ministerio de Economía y Competitividad (SAF2016-7592-R), proyectos del Gobierno Vasco de grupos consolidados (IT02-13), de proyectos ELKARTEK: Ayudas a la investigación colaborativa en áreas estratégicas (KK2017/00067, KK2019/00058 y KK2020/00034) y de proyectos de Investigación Básica y/o Aplicada (PI-2016-1-0009).

Acknowledgements

Este trabajo es el resultado de 4 años de esfuerzo y dedicación. Voy a intentar plasmar brevemente todo lo vivido en estas páginas ya que tengo mucho que agradecer a esta etapa. Antes que nada, me gustaría reconocer a todos los animales que han contribuido en este proyecto. Ojalá se encuentre próximamente un método alternativo para evitar el uso de animales en experimentación.

A Esti, muchas gracias por confiar en mí y acompañarme en estos 5-6 años de experiencia científica. Gracias por enseñarme tanto científica y profesionalmente y por aportarme una formación tan amplia y diversa en nuestro campo, preocupándote siempre de mi formación, asistencia a congresos y estancia entre otras cosas. Sobre todo, en la estancia, no pude tener más suerte en el momento en que la realicé y en gran parte fue gracias a tu apoyo y preocupación desde la distancia. Siempre sabes elegir el camino correcto en cada reto que se nos presenta y con el mejor humor. Muchas gracias por tu disponibilidad, dedicación y empatía en este proyecto que hemos compartido. Eres una fantástica directora.

A Carlos, muchas gracias por darme la oportunidad de formar parte de tu equipo. Este grupo no solo me ha aportado muchísimo científica y profesionalmente, sino que personalmente ha sido un placer conocer a tanta gente de tan calidad humana que crea un entorno tan bueno de trabajo. En concreto, trabajar contigo ha sido un honor para mí y aprecio mucho tu cercanía, disponibilidad y disposición a reinventarse cada día como grupo y como centro de investigación.

A Magdalena, gracias por aceptarme en tu grupo de investigación a pesar del complicado momento que estábamos viviendo. Gracias por estar pendiente de mí y por enseñarme otra forma de trabajar en el mundo científico. Y muchas gracias al equipo de Imperial College por arroparme tan bien en el laboratorio: Bibiana, Nicola, Emily, Robertas y Laura, tuve muy buena experiencia trabajando con vosotros.

A Elena, muchas gracias por haberme introducido a este grupo de investigación, por tu apoyo profesional, por el conocimiento que me has transmitido, por confiar en mi para colaborar en tus proyectos, por estar siempre pendiente de nosotras y por tu cercanía. Fede, muchas gracias por tu naturalidad, por todo tu apoyo en mi proyecto de tesis, por tus consejos en cualquier momento y por tu paciencia enseñándome a

manejar el microscopio de dos fotones. Gracias a los demás compañeros del laboratorio: Fabio, por tu sentido del humor y cercanía trabajando; Vanja, por aportar tantas novedades al grupo y por tu cercanía trabajando; Asier, muchas gracias por enseñarme los cultivos de neuronas y apoyarnos cada lunes con el trabajo de laboratorio; Vicky, Fernando, Alberto, María y Susana, muchas gracias por contribuir a crear este equipo tan acogedor, completo y diverso.

A todos mis compañeros de Achucarro, gracias por crear un equipo tan bueno de trabajo, hacéis que venir a trabajar no sea una obligación. En especial a Laura Escobar, por estar siempre dispuesta a ayudar y apoyar mucho más de lo que te pedimos con el mejor humor; a Aitor, por estar siempre pendiente de todos nuestros requisitos con toda la paciencia del mundo; a Izaskun, por sacarnos una carcajada en cualquier momento del día.

A mi primera cuadrilla del laboratorio. Tania, tenerte como compañera de laboratorio y, además, coincidir en Londres viviendo unos meses juntas fue un regalo. Gracias por hacer de cualquier plan incluso en el peor momento de una pandemia algo para recordar siempre. Carolina, has sido la mejor mentora de laboratorio, y, además, siempre te tendré como un referente de organización. Me has enseñado mucho de cómo llevar una tesis de la mejor manera posible y me alegro mucho de haber compartido tantas horas de cultivos y laboratorio contigo. Hazel, gracias por ser un pilar fundamental para la organización de nuestro laboratorio y gracias por tu amistad dentro y fuera de él, siempre sabes mantener una amistad a pesar de la distancia. Ainara, tu apoyo como técnico fue imprescindible tanto como los buenos momentos vividos dentro y fuera de laboratorio. Paula, agradecerte en unas frases me parece que es quedarse muy corta. Me siento afortunada de haber coincidido mano a mano en el laboratorio y de haber podido vivir tantas experiencias juntas dentro y fuera del él, por seguir compartiendo muchísimo tiempo. Andrea, si algo me da pena de la tesis es de no haber coincidido más tiempo contigo porque lo habríamos pasado realmente bien. Gracias por las carcajadas que me provocas. Alazne, gracias por los buenos momentos dentro y fuera del laboratorio. En general, me siento muy afortunada de haber compartido esta etapa con vosotras.

A mi segunda cuadrilla del laboratorio. Adhara, tu llegada al laboratorio no pudo ser en mejor momento. Gracias por tu vitalidad, tus anécdotas, las risas interminables, los planes que tenemos pendientes, los avances técnicos que hemos aprendido juntas y porque mi llegada cada lunes al trabajo lo has hecho muy divertido con tus salseos de fin de semana. Eres un chute de energía personalizado. Uxue, gracias por tu sentido del humor, tus carcajadas, tu cariño y por estar siempre dispuesta a ayudar a todo el mundo en el laboratorio. Leire, gracias por tu apoyo, tu dulzura y tu espontaneidad tan graciosa. Irene, gracias por tu ternura, por tu atención, por todo lo que tenemos en común que siempre lo suelto de repente y por las carcajadas a cualquier momento del día. Carmen, gracias por darle un toque cómico cada día al laboratorio y las charlas a la hora de comer. Maialen y Nuria, aunque he coincidido con vosotras poco en el laboratorio, gracias por los buenos momentos que hemos compartido. Es una pena haberos conocido en una etapa tan tardía de la tesis, pero estoy segura de que aún nos quedan muchos momentos por compartir.

Muchas gracias al resto de compañeros del laboratorio. Fátima, gracias por ayudarnos tanto, me alegra mucho verte cada día llegar al labo tan animada y motivadora, ojalá tenerte siempre de compañera. Rafaela, muchas gracias por ser un apoyo en nuestro grupo tan fundamental y Celia, gracias por todas las novedades que aportas y todo lo que hemos avanzado juntas en la mejor compañía. Ane, aunque hayamos coincidido tan poco, qué bien me recibiste en el labo y qué divertido fue tenerte cada día contando cualquier anécdota. Álvaro y Alejandro, gracias por las risas que nos provocáis cada vez que venís por Achucarro. Laura, aunque coincidamos poco por en el labo, muchas gracias por tu sentido del humor, por tenernos siempre muy bien informadas de todo lo que pasa en la facultad y por crear tan buen rollo en el trabajo. Mónica, Anita, María, Ana, Juan Carlos, Zara, Paloma muchas gracias por crear un equipo tan organizado, motivante y divertido de trabajo.

A mi cuadrilla de San Fermín ikastola que me seguís desde hace mucho tiempo ya sea desde cerca o lejos para darme apoyo en cada momento de la vida y en especial, en mi tesis; a mi cuadrilla de Jaso ikastola, en especial a Cristina, Andrea y Jone, muchas gracias por todo vuestro apoyo y amistad y a mis amigas de Bilbao en especial a

Alejandra y Uxune, muchas gracias por apoyarme cada día, por seguir compartiendo etapas de vida.

A mis abuelos, muchas gracias por estar tan orgullosos de vuestra familia y darme tanto cariño y apoyo siempre. Siempre os tendré en mis recuerdos apoyándome y poniendo a vuestros nietos en lo más alto. Gracias al resto de mi familia, Yoli, Amaya, Martin, Juan Pedro, Edurne, Pedro, Carlos, Pierre, Fernan, Mertxe por vuestro cariño y apoyo constante.

Ama y Aita, para escribiros unos agradecimientos necesitaría mucho tiempo y espacio. Estoy ahora terminando esta experiencia gracias a todo vuestro esfuerzo, incondicionalidad, dedicación y cariño y no puedo estar más orgullosa, agradecida y feliz de que me acompañéis etapa tras etapa. A Miren, gracias por ser una muy buena compañera de vida y de carrera, me has apoyado mucho siempre. A los 3 os quiero tanto… siempre seréis mi mejor referente a seguir, el mejor team que se pueda tener.

Gurasoei

Table of contents

List of abbreviations

Abbreviation	
3xTg-AD	Triple transgenic mouse model of Alzheimer's disease
5XFAD	Transgenic mice with five familial Alzheimer's disease mutations
AICD	APP intracytoplasmic domain
Akt	Serine/threonine protein kinase
AD	Alzheimer's disease
Aβ	Amyloid β peptide
APP	Amyloid precursor protein
ApoE	Apolipoprotein E
BBB	Blood brain barrier
BSA	Bovine serum albumin
C1q	Complement factor 1q
C2	Complement factor 2
C3	Complement factor 3
C4	Complement factor 4
CD11b	Cluster of differentiation 11b
CD18	Cluster of differentiation 18
CD33	Cluster of differentiation 33
CD36	Cluster of differentiation 36
CD40	Cluster of differentiation 40
CD44	Cluster of differentiation 44
CD68	Cluster of differentiation 68
CD74	Cluster of differentiation 74
CD115	Cluster of differentiation 115
CD204	Cluster of differentiation 204
CERAD	Consortium to establish a registry for Alzheimer's disease
CLC-7	Chloride channel 7
CNS	Central nervous system
CR3	Complement receptor 3

CSF	Cerebrospinal fluid
Ct	Threshold cycle
DAM	Dissease associated microglia
DAP12	DNAX-activation protein 12
DAPI	4'-6-diamidino-2-phenylindale
DIV	Days *in vitro*
DMSO	Dimethyl sulfoxide
EDTA	Ethylenediamine tetraacetic acid
ELISA	Enzyme-linked immunosorbent assay
FBS	Fetal bovine serum
FDG	Fluorodeoxiglucose
FRL1 and 2	Formyl peptide receptor
GAPDH	Glyceraldehyde-3-phosphate dehydrogenase
GluR1	Glutamate receptor 1
GWAS	Genome-wide association study
HBSS	Hank's balanced salt solution
HFIP	Hexafluoroisopropanol
IDE	Insulin degrading enzyme
IRF8	Interferon regulatory factor 8
IL-4	Interleukin 4
IL-1β	Interleukin 1β
IL-10	Interleukin 10
IL-13	Interleukin 13
IL-34	Interleukin 34
IMDM	Iscove modified Dulbecco´s media
ITGAM	Integrin subunit αM
ITGB2	Integrin subunit β2
ITIM	Immunoreceptor tyrosine-based inhibition motifs
KDa	Kilodalton
LAMP1, 2 and 3	Lysosome membrane glycoproteins
LRP1	Lipoprotein receptor-related protein 1 receptor

LTP	Long-term potentiation
MAC-2	Macrophage antigen complex 2
MAPK	Mitogen-activated protein kinase
MCI	Mild cognitive impairment
MCSF	Macrophage colony stimulating factor
MG	Microglia
MGnD	Microglia neurodegenerative disease
MHC II	Major histocompatibility complex class II
MITF	Microphthalmia-associated transcription factor
MMP 2 and 9	Matrix metallopeptidase 2 and 9
MRC1	Mannose receptor C type 1
MRI	Magnetic resonance imaging
MSR1	Macrophage scavenger receptor 1
N	Neurons
N/MG	Neuronal-microglial co-culture
NFT	Neurofibrillary tangles
NGS	Normal goat serum
NMDA	N-methyl-D-aspartate
oAβ	Oligomeric β-amyloid peptide
ORG	Organotypic culture
OSTM1	Osteopetrosis-associated transmembrane protein 1
P2RY6	Purinergic receptor P2Y6
PB	Phosphate buffer
PBS	Phosphate saline buffer
PDL	Poly-D-Lysine
PFA	Paraformaldehyde
PLAT	Plasminogen activator tissue type
PTP-ɣ	Protein tyrosine phosphatase-ɣ
PSD95	Postsynaptic density protein 95
PSN 1 and 2	Presenilin 1 and 2
RAGE/AGER	Receptor for advanced glycation end products

RANK	Receptor activator of nuclear factor kB
ROI	Region of interest
ROS	Reactive oxygen species
RT	Room temperature
RT-PCR	Real Time-Polymerase Chain Reaction
SALL1	Spalt-like transcription factor
SCARA1	Scavenger receptor class A member 1
S.E.M.	Standard error of the mean
SiMOA	Single molecule assay
SR	Scavenger receptor
TFE3	Transcription factor binding to IGHM enhancer 3
TFEB	Transcription factor EB
TGFβ1 and -β3	Transforming growth factor β 1 and 3
TLRs	Toll-like receptors
TNFα	Tumor necrosis factor α
TREM2	Triggering receptor expressed on myeloid cells 2
TPP1	Tripeptidyl peptidase 1
Tyrobp	Transmembrane immune signaling adaptor
UPR	Ubiquitin proteasome system
Veh	3xTg-AD vehicle
WT	Wild type

Abstract

Accumulation of soluble oligomeric amyloid-β (oAβ) forms in the brain is a key early event in Alzheimer's disease (AD). In this study, we have investigated the role of macrophage colony-stimulating factor (MCSF) as a microglial modulator in the context of AD. In microglia primary cultures, we found that MCSF activation modulates several microglial functions. We have observed that MCSF treatment potentiated microglial receptor density and cytokine expression, promoting pro-inflammatory environment. In the presence of oAβ, however, reactive microglia, switch to an anti-inflammatory profile. Moreover, oAβ internalization and elimination was increased in the presence of MCSF and it attenuated synaptic damage associated to oAβ in a neuronal-microglial co-culture.

In organotypic brain slices, using two-photon time-lapse microscopy, we found that MCSF treatment reverted the alterations in microglial morphology and motility caused by oAβ. MCSF enhanced microglial surveillant activity and promoted microglial ramification. MCSF treatment also diminished micro- and astrogliosis, induced either by oAβ or Aβ pathology in 5XFAD mice.

When administered in adult 3xTg-AD mice, MCSF treatment reduced Aβ brain pathology and inflammation. It also mitigated synaptic alterations in the CA1 hippocampal region.

Finally, we observed a reduction in MCSF levels in hippocampal tissues extracted from AD patients, which came accompanied by an increase of CSF-1R expression, suggesting an alteration in the MCSF/CSF-1R axis during AD pathogenesis.

Overall, our results provide evidence supporting the hypothesis that MCSF promotes a more efficient and protective microglia phenotype against Aβ in AD models. The reduction of endogenous MCSF levels observed in AD patients might negatively contribute to AD progression. This doctoral thesis provides new knowledge with regards the role of microglia in the progression of AD and highlights the relevance of microglial modulation in Aβ-related AD pathology.

Introduction

1. Alzheimer's disease.

Alzheimer's disease (AD) is recognized by the World Health Organization as a global public health priority (Lane et al., 2018). Nowadays, it is the most common cause of dementia and the most prevalent neurodegenerative disorder.

Aloysius "Alois" Alzheimer (1864-1915), a german psychiatrist and neuropathologist first described AD as "presenile dementia" in 1907. He observed 51-year-old patient, Auguste Deter's symptomatology who presented hallucinations and loss of several mental functions such as memory and language impairment. He followed the course of the dementia disorder and after the death of Auguste, he continued with an anatomopathological analysis of her brain. *Post-mortem* analyses revealed the presence of general brain atrophy and abnormal intra- and extracellular aggregates being these features extensively used years later for AD diagnosis. Interestingly, it was later described that the extracellular aggregates that were observed by Alzheimer were insoluble aggregates of the amyloid β peptide (Aβ) called senile or amyloid plaques, and those intracellular were neurofibrillary tangles (NFT) composed by filamentous accumulations of hyperphosphorylated protein tau (Figure 1). After Auguste's death in 1906, her case was published under the title "On an Unusual Illness of the Cerebral Cortex" (from the German "Über eine eigenartige Erkrankung der Hirnrinde") (Alzheimer, 1907).

Besides the typical clinical presentation with irreversible memory impairment, atypical clinical presentation with focal cortical symptoms, for example, visual dysfunction, apraxia, dyscalculia, fluent and non-fluent aphasia, executive dysfunction, has also been reported (Cacace et al., 2016).

In turn, the progression of the disease has been associated with a gradual damage in function and structure of the hippocampus and neocortex, the vulnerable brain areas involved in memory and cognition (Scheff et al., 2006).

The main pathological features of AD pathology are amyloid plaques and NFTs. In addition, AD brains commonly display neuropil threads, dystrophic neurites, associated astrogliosis and microglial activation as well as cerebral amyloid angiopathy (Karch and Goate, 2015). The downstream consequences of these pathological

processes include synaptic and neuronal loss leading to neurodegeneration and macroscopic atrophy (Figure 1C) (Serrano-Pozo et al., 2011).

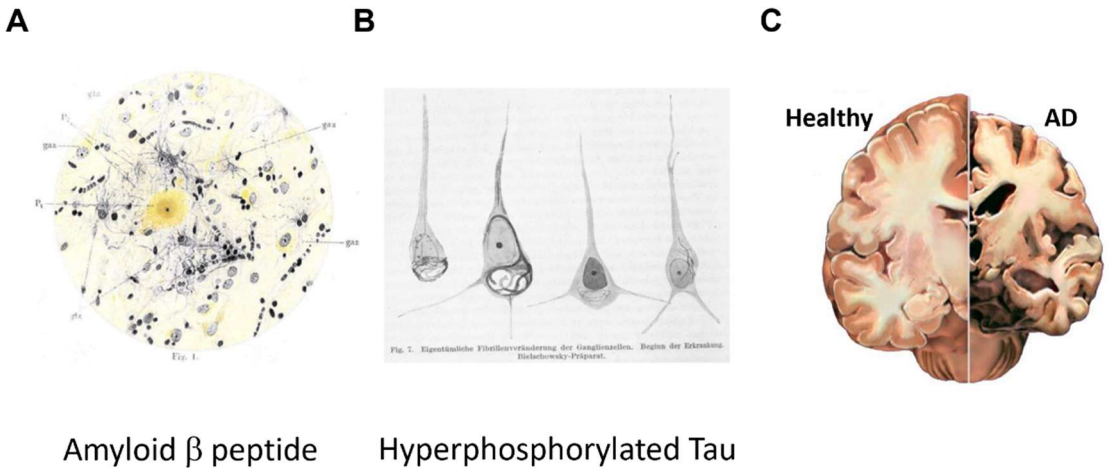

Figure 1. AD pathological features. Drawings of Alois Alzheimer showing senile plaques composed by amyloid β peptide (A) and neurons with intracellular tangles (B) present in AD patients. (A) Brain atrophy in AD brain compared with healthy brain. Adapted from (Kidd 2008) and (Alzheimer, 1907).

There are two classifications that grade the severity of AD pathology in various stages, and these stages are currently used as a reference of *post-mortem* studies. The first is based on the extend of neurofibrillary changes in the brain (occurred in form of neuritic plaques, NFT and neuropil threads) and a characteristic pattern in these parameters permitted the differentiation of six stages: stages I-II involve the transentorhinal region; the key feature of stages III-IV is that both the entorhinal and transentorhinal layer Pre-α area conspicuously affected along with a mild to moderate hippocampal and a still-low isocortical involvement; and the hallmark of stages V-VI is that the isocortex is extensively affected (Braak and Braak, 1991)(Figure 2A). This classification is known as the Braak stages and since it has been used as a diagnostic tool for *post-mortem* confirmation of the disease.

In 2002, a second classification based on Aβ deposition was reported. This parameter follows a distinct sequence in which the regions are hierarchically involved starting from the neocortex and expanding anterogradely into regions that receive neuronal projections from areas already exhibiting Aβ and ultimately the cerebellum. The extent of Aβ-deposition in the brain allows the distinction of five phases (Thal et al., 2002) that are frequently found in the cortex of non-demented individuals in the

absence of neurofibrillary changes, which are believed to appear after Aβ deposition (Duyckaerts et al., 1988) (Figure 2B).

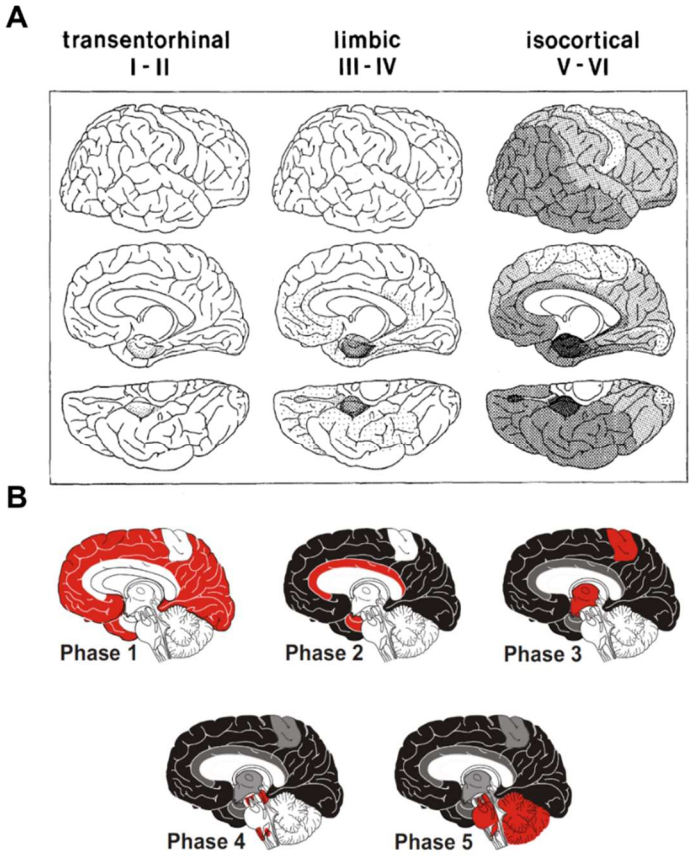

Figure 2. AD classification depending on neurofibrillary changes or amyloid deposition. Braak & Braak described six different stages for AD cases based on the extent of neurofibrillary changes in the brain (A). Thal et al. described five different stages for AD cases based on Aβ deposition sites in the brain (B). Images adapted from (Braak and Braak, 1991; Thal et al., 2002).

Since those two classifications required tissue for disease diagnosis, increasing efforts have been devoted to identifying biomarkers for early *in vivo* diagnosis. Figure 3 summarizes the current views on biomarker's progression in the pathophysiological pathway of the disease along with cognitive decline (Ingelsson et al., 2004; Jack et al., 2008, 2009; Mormino et al., 2009; Perrin et al., 2009). Abnormalities in cerebrospinal fluid (CSF) Aβ42 and amyloid PET tracer precede those of CSF tau and fluorodeoxiglucose (FDG) PET, followed by structural magnetic resonance imaging (MRI), and the emergence of clinical symptoms. Biomarker abnormality increases sequentially as the disease progresses (Jack et al., 2013). In addition, microglial activation precedes

alteration in biomarkers (Lautner et al., 2011) (Figure 3). This feature will be discussed in detail in the following chapters as it is a major topic in this thesis project.

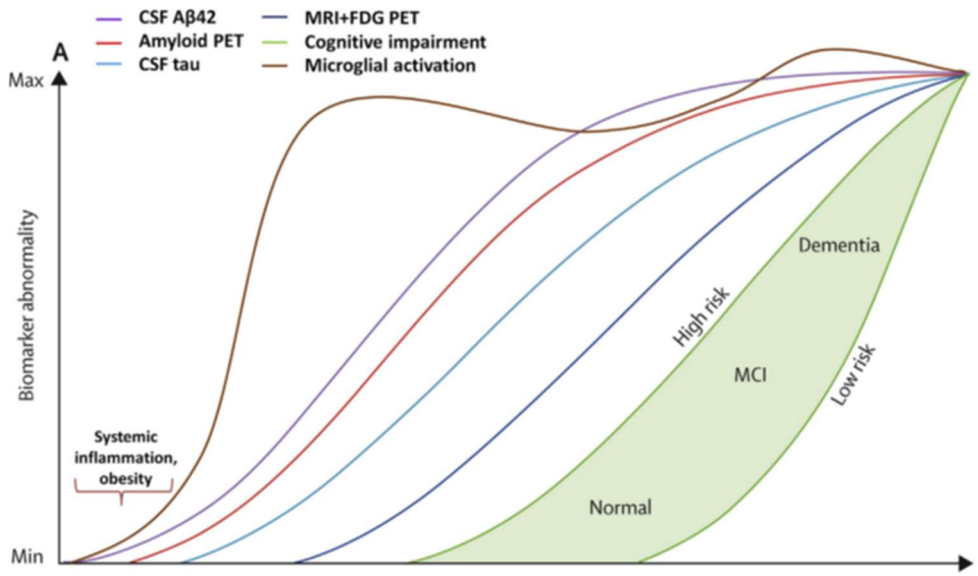

Figure 3. Model of biomarker progression in AD. The horizontal axis represents the progression of the disease and the vertical axis the biomarker abnormality. The abnormality begins with the reduction of Aβ in the CSF in conjunction with neuroinflammation and microglial activation. The later has a fluctuating trajectory. Subsequently, abnormalities involve amyloid PET, CSF tau and MRI and fluorodeoxiglucose PET, and finally cognitive impairment appears. Adapted from (Jack et al. 2013).

1.1. Alzheimer's disease subtypes.

AD has been classified mainly into two different forms, the early-onset (also known as familial AD) and the late-onset or sporadic AD.

Familial AD is the less prevalent subtype. It represents about 5% of all AD cases and, it usually develops earlier when compared with sporadic AD. Patients with familial AD experience their first symptoms at the age of 60. The genes causing early-onset AD are transmitted following Mendelian inheritance patterns and are responsible for Aβ formation such as the amyloid precursor protein (APP) gene on chromosome 21 (Goate et al., 1991) and presenilin-1 (PSN1) and -2 (PSN2) genes on chromosomes 14 and 1, respectively (Cruts et al., 1996). Mutations in the APP are transmitted to the offspring on an autosomal dominant fashion. To date, 52 pathogenic mutations in APP have been reported in 119 probands of autosomal dominant families (http://www.molgen.vib-ua.be/ADMutations) (Cruts et al., 2012). These mutations cause increased amyloidogenic processing of APP and increased oligomerization of the Aβ peptide. In

addition, mutations in PSN1 (180) and PSN2 (15) have been reported to promote AD (Sherrington et al., 1995; Cruts et al., 2012).

Late-onset or sporadic AD accounts for approximately 95% of clinical cases and first symptoms appear typically after the age of 65 years. The etiology of this AD subtype is unclear; it is likely driven by a complex interplay between genetic and environmental factors, being aging the main risk. Besides aging, the best characterized risk factor for AD is Apolipoprotein E (ApoE), which is the main cholesterol transporter in the brain, and it has been related to the transport and release of Aβ peptide (Bu, 2009). The gene encoding ApoE may present three different allelic variants, namely ApoEε2, ApoEε3 and ApoEε4. The ε4 variant, triples the probability of suffering AD in the case of heterozygotes and multiples it by 15 in the case of homozygotes, when compared with ApoEε2 and ApoEε3 haplotypes (Huang, 2006). In addition, by using genome-wide association studies (GWAS) a database has been generated gathering information on those genes with mutations associated to late-onset AD predisposition (http://www.alzgene.org) (Bertram et al., 2007). Moreover, recent functional studies implicated gene isoforms expressed in immune cells and microglia as possible contributors to late-onset AD pathology (Schwabe et al., 2020).

1.2. Amyloid β peptide.

The Aβ peptide is a 4.5 Kilodaltons (kDa) monomer originating from the proteolytic processing of the APP, a transmembrane glycoprotein with a large extracellular domain that carries out a wide range of biological functions in the central nervous system (CNS) (Zheng and Koo, 2011). Interestingly, APP is implicated in the regulation of neurites growth during development (Herms et al., 2004). In the adult brain, APP plays a role in cell adhesion, neuroprotection, synapse formation, and transcriptional modulation of several genes (Raychaudhuri and Mukhopadhyay, 2007). In addition, extracellular matrix proteins interact with APP and regulate its processing and intracellular signaling, which may be related to a role of APP as a cell surface receptor (Zheng and Koo, 2011).

The sequential proteolytic processing of APP can occur in two ways, namely non-amyloidogenically and amyloidogenically, giving rise to the Aβ peptide (Figure 4). The

non-amyloidogenic processing of APP is carried out by the α-secretase protease and generates soluble fragments APPsα (N-terminus) and CTFα (C-terminus), the latter remaining anchored to the cell membrane. CTFα is subsequently cleaved by other second enzyme, γ-secretase, producing two soluble peptides, namely p3 (for which its biological function is still poorly understood), and AICD (APP intracytoplasmic domain) which functions as a transcriptional regulator of several genes such as glycogen synthase kinase 3β or p53 (Kimberly et al., 2001; von Rotz et al., 2004).

In contrast, in the amyloidogenic cascade the first cleavage is performed by the protease β-secretase, generating APPsβ and CTFβ fragments. Further processing of CTFβ by γ-secretase produces AICD and the Aβ peptide, which is released extracellularly (Figure 4). Remarkably, while the non-amyloidogenic cascade is predominant in physiological conditions -presumably to avoid excessive production of Aβ peptide- the equilibrium between the two pathways seems altered in AD patients. In addition, there are several non-canonical pathways through which APP can be processed, some of them also contributing to Aβ peptide generation (Müller et al., 2017).

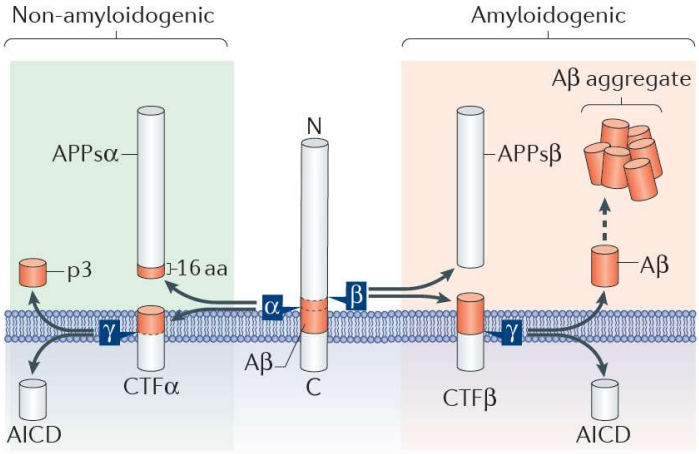

Figure 4. Schematic representation of canonical APP processing. The non-amyloidogenic (green background) and amyloidogenic (red background) pathways are shown. The proteolytic cleavage of APP by α- or β-secretase, and subsequently by γ-secretase, generates AICD, and p3 or Aβ peptides, respectively. Adapted from (Müller et al., 2017).

Since γ-secretases exhibit lack of specificity of the proteolytic cleavage of APP, the length of the Aβ peptide ranges between 37 and 49 amino acids (Weidemann et al., 2002). Most of the circulating Aβ peptide consists of 40 amino acid-long peptides, and to a great extent those formed by 42 or 43 amino acids ($Aβ_{1-40}$, $Aβ_{1-42}$ and $Aβ_{1-43}$,

respectively). In addition, shorter (38- or 39-amino acid-long) and longer (46 to 49-amino acid-long) peptides can also be found (Takami et al., 2009). Following APP processing, Aβ monomers, specially $Aβ_{1-42}$, tend to aggregate due to their structure, forming oligomers that will lead to protofibers and fibrils, and eventually generate senile plaques (Figure 5). Oligomeric Aβ species, resulting from the aggregation of Aβ monomers, have been reported to cause neurotoxic effects (Klein, 2002; Glabe, 2005).

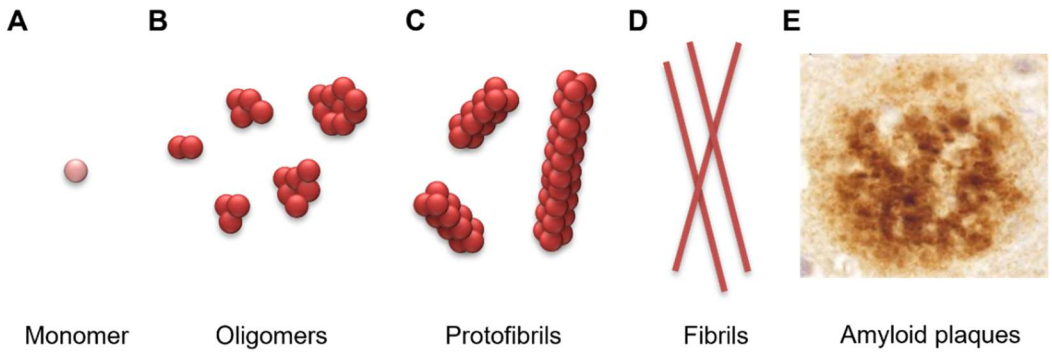

Figure 5. Oligomerization and aggregation of $Aβ_{1-42}$. Representation of the different products formed in APP processing and Aβ oligomerization and aggregation: monomer (A), oligomers (B), protofibrils (C), fibrils (D) and amyloid plaques (E). Image E adapted from (Querol-Vilaseca et al., 2019).

Aβ oligomers have been isolated from animal models of AD (Oddo et al., 2006; Tomiyama et al., 2010) and CSF and brains from AD patients (Bao et al., 2012). Oligomer tissue load correlates with disease progression (Santos et al., 2012). In fact, nanomolar concentrations of Aβ oligomers induce neuronal death in hippocampal organotypic slices (Lambert et al., 1998; Alberdi et al., 2010), inhibit long-term potentiation (LTP) (Lambert et al., 1998; Wang, 2004), alter Ca^{2+} homeostasis and disrupt cell membrane integrity (Demuro et al., 2005). Due to its biochemical and structural complexity, Aβ peptides are able to engage in a variety of signaling mechanisms through a repertoire of receptors and consequently promote a wide range of effects both in neurons and other cell types (Viola and Klein, 2015).

The identification of gene mutations related to Aβ synthesis in familial AD have led to formulate the amyloid cascade hypothesis (Selkoe, 1991; Hardy and Higgins, 1992). The hypothesis postulates that the accumulation of Aβ, which is due to an unbalance between its generation and elimination, leads to neurodegeneration and subsequent dementia (Glenner and Wong, 1984; Hardy and Allsop, 1991; Hardy, 2002).

This hypothesis proposes Aβ peptide as a candidate for initiating the disease, while NFTs appearing after Aβ-induced damage.

The increased Aβ accumulation can be caused, in familial AD, by missense mutations in APP and PS1 genes that increase Aβ production throughout life, and in case of sporadic AD, by failing Aβ clearance mechanisms leading to increasing Aβ concentration. This hypothesis suggests that the cerebral accumulation of Aβ triggers synaptotoxicity, a sustained and chronic inflammatory response, tau hyperphosphorylation, altered neuronal ionic homeostasis, oxidative injury, and consequently neuronal loss, thus leading to the progressive cognitive decline (Hardy, 2002; Haass and Selkoe, 2007; Jack et al., 2013) (Figure 6).

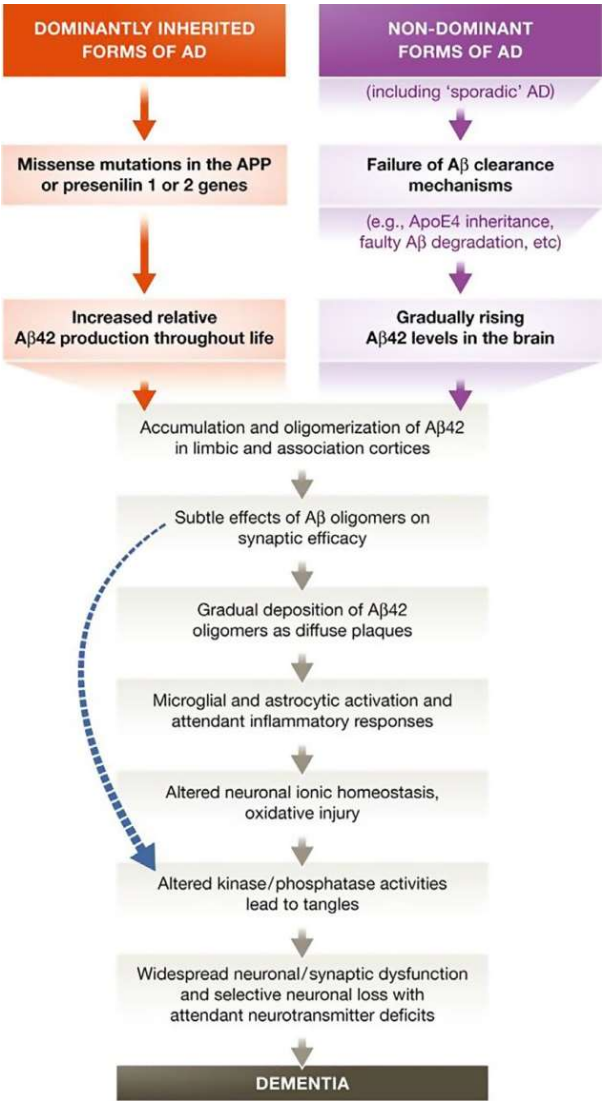

Figure 6. The sequence of major pathogenic events leading to AD proposed by the amyloid cascade hypothesis. The curved blue arrow indicates that Aβ oligomers may directly injure synapses and neurites of brain neurons, in addition to activate microglia and astrocytes. Adapted from (Selkoe and Hardy, 2016).

In 1993, Wertkin and collaborators published a seminal study which described the presence of Aβ within the cell (Wertkin et al., 1993). Yang et al. (1999) described a marked upregulation of newly generated intracellular $A\beta_{1-42}$ following treatment of cells with extracellular $A\beta_{1-42}$. A similar finding was reported in human samples (Gouras et al., 2000). AD transgenic mice showed physiological (Holcomb et al., 1998; Hsia et al., 1999; Moechars et al., 1999; Christensen et al., 2009) and neuritic alterations (Moolman et al., 2004; Capetillo-Zarate et al., 2006, 2012) prior to plaque formation, shifting the interest of the scientific community from fibrillar Aβ to soluble Aβ oligomers.

1.3. Hyperphosphorylated Tau.

The other main histopathological hallmark in AD is the intracellular accumulation of hyperphosphorylated tau. Tau is a microtubule-associated protein and the main component of NFT (Grundke-Iqbal et al., 1986; Kosik et al., 1986; Wood et al., 1986). Hyperphosphorylated tau is present in the brain as pre-tangles and neuropil threads decades before the onset of symptoms (Braak et al., 2006, 2011; Wharton et al., 2016). Even before the formation of tangles, tau undergoes a series of post-translational modifications, including hyperphosphorylation (Grundke-Iqbal et al., 1986), acetylation (Min et al., 2010), N-glycosylation (Wang et al., 1996) and truncation (Mena et al., 1996), which differentiate it from the normal tau predominant in healthy brains. As mentioned previously in section 1, deposition of tau aggregates in AD follows a highly specific pattern, beginning in the entorhinal cortex and hippocampus and progressing towards other regions (Figure 2A) (Braak and Braak, 1991, 1997). The mechanism underlying the spread of tau during disease progression is still known but it is proposed a cell-to-cell transfer of proteins in prion-like manner (reviewed at de Calignon et al., 2012).

Studies in AD transgenic mice harboring both Aβ and tau pathologies, support that Aβ is upstream of tau in AD pathogenesis, and that Aβ triggers the conversion of tau from a normal to a toxic state. However, toxic tau also enhances Aβ toxicity (Bloom, 2014). It is believed that AD pathology starts with the imbalance of Aβ, but tau pathology has a key role in the propagation of the disease.

1.4. Synaptic damage in AD.

A foundational principle of neuroscience is that synaptic function underlies cognition. There is a widespread acceptance of the premise that synapse damage or loss is a key hallmark of neurodegeneration, which in turn correlates strongly with cognitive decline in AD. This is supported by clinical, *post-mortem*, and non-clinical evidence (Colom-Cadena et al., 2020).

Synaptic dysfunction is reported as an early manifestation of AD (Selkoe, 2002; Milà-Alomà et al., 2020). Loss of synaptophysin has been shown to correlate well with Aβ accumulation (Selkoe, 2002; Oddo et al., 2003). In both human brain and mouse models expressing familial AD-associated APP and presenilin mutations, plaques are associated with local synapse loss (Spires, 2005; Koffie et al., 2009, 2012; Jackson et al., 2016; Yu et al., 2018) as well as memory and synaptic plasticity deficits (Ashe and Zahs, 2010; Saito et al., 2014; Sasaguri et al., 2017). However, total plaque load is not strongly correlated with cognitive decline (Nelson et al., 2012) or synaptic pathology in AD progression (Masliah et al., 1991; Blennow et al., 1996). Extensive research demonstrates that soluble forms of Aβ, rather than the large insoluble fibrils and plaques, are most toxic to synapses (Masliah et al., 1991; Cline et al., 2018). Moreover, alterations in postsynaptic density protein (PSD95) and glutamate receptor 1 (GluR1) are blocked by γ-secretase inhibition in APP mutant neurons, supporting the role of Aβ on synaptic dysfunction (Almeida et al., 2005).

There is ample evidence from both human brain and disease models supporting synaptotoxicity roles of soluble pathological forms of Aβ and tau, as well as glia-mediated neuroinflammation (Wilde et al., 2016). Particularly, microglia are likely key players in complement-mediated synapse loss in AD; they are the main source of C1q in the brain (Fonseca et al., 2017) and they phagocytose synapses during development (Stevens et al., 2007; Schafer et al., 2012; Sekar et al., 2016). Mouse models of β-amyloidosis exhibit elevated C1 levels, with increased synaptic localization of C1q even before plaques have formed (Hong et al., 2016). Genetic knockout of C1q or neutralizing antibodies against C1q protect against synapse loss observed in amyloid-bearing mice or induced by injected Aβ (Fonseca et al., 2004; Hong et al., 2016).

1.5. Inflammation in AD.

Inflammation is another key hallmark of AD. It is the body response to either intrinsic or extrinsic detrimental agents and is intended to be protective in the first place, although an excessive inflammatory response can cause or contribute to tissue damage and disease pathology (Lyman et al., 2014). Neuroinflammation refers to the inflammatory response that occurs within the CNS secondary to an insult. Astrocytes and microglial cells are the main cell types in charge of the inflammatory response in the CNS (Calsolaro and Edison, 2016). Aβ peptides and fibrils are potent glial activators, triggering an inflammatory response and microglial release of neurotoxic cytokines (Barger and Harmon, 1997). What is not well known yet is whether inflammation is a cause or a consequence of AD progression and whether its effect on disease progression depend on either its nature being acute or chronic. Moreover, the precise mechanism through which microglia contribute to AD-related inflammation remains to be elucidated. Inflammation, and in particular the role of microglia in AD is discussed more in detail in chapter 3.1.

2. Microglia and their functions.

Microglia are the main immune cells of the CNS and account for approximately 10% of the total CNS cell population, with regional variation in density (Lawson et al., 1990; Mittelbronn et al., 2001; Soulet and Rivest, 2008). Microglia terminology was firstly introduced by Pio del Rio Hortega in 1919 (Río-Hortega, 1919). After years of discussion, *in vivo* lineage tracing studies supported the hypothesis that microglial cells are of mesodermal origin and derive from primitive myeloid progenitors that arise before embryonic day 8 from the yolk sac (Ginhoux et al., 2010, 2013). The microglia lineage is similar but not identical to that of macrophages and is driven by the cytokine macrophage colony- stimulating factor (MCSF) (Ginhoux et al., 2010), the transcription factors Pu.1, interferon regulatory factor 8 (IRF8) (Kierdorf et al., 2013), and spalt-like transcription factor 1 (SALL1) (Buttgereit et al., 2016). As shown by parabiosis experiments, and unlike other myeloid cells, the adult microglia population does not renew from bone-marrow circulating progenitor cells (Ajami et al., 2007) but from local proliferation of resident cells, coupling apoptosis and mitosis (Askew et al., 2017).

Additional to its principal role in inflammation, microglia are implicated in diverse and important functions in the CNS such as neurogenesis (Walton et al., 2006; Cunningham et al., 2013), vasculogenesis (Checchin et al., 2006; Kubota et al., 2009), blood-brain barrier (BBB) permeability (Fernández-López et al., 2016), myelination/remyelination process (Wlodarczyk et al., 2017), surveillance, synapse monitoring and pruning, neuronal connectivity and function, and phagocytosis (Figure 7).

In homeostatic conditions, microglia continuously extend and retract their processes while maintaining their cell bodies relatively statical (Davalos et al., 2005; Nimmerjahn, 2005). This process movement, henceforth termed ‘‘**surveillance’’** of the brain, is assumed to play a key role in monitoring the ingress of bacteria, fungi, and viruses (Hanisch and Kettenmann, 2007). Also, microglial surveillance plays an important role in monitoring synaptic function and determining the ‘‘wiring’’ of the brain (Wake et al., 2009; Tremblay et al., 2010; Schafer et al., 2012). During postnatal development, synapses that are to be pruned become tagged with complement molecules and are thus removed by microglia (Stevens et al., 2007; Schafer et al., 2012) in a process called “**synaptic pruning”**.

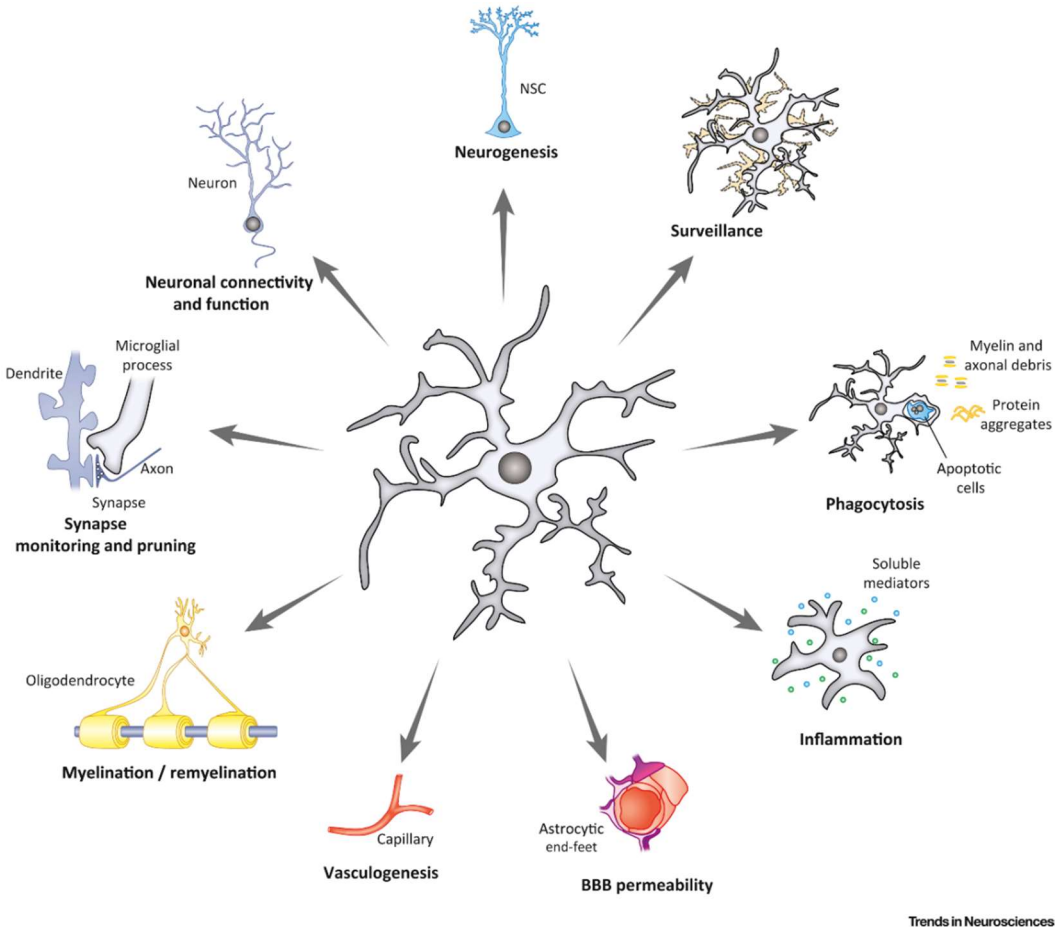

Figure 7. Microglia play several functions in the CNS. Microglia diverse roles in the CNS under physiological and pathological conditions: neurogenesis, surveillance, phagocytosis, inflammation, BBB permeability, vasculogenesis, myelination/remyelination, synapse monitoring and pruning and neuronal connectivity and function. Adapted from (Sierra et al., 2019).

In healthy homeostatic conditions, microglia have a small cell body and present highly ramified processes. However, in response to injury or pathogen invasion, microglia transform into phagocytic microglia (Stence et al., 2001), migrate, and accumulate at the site of injury through chemotaxis (Eugenin et al., 2001). These pro-inflammatory microglia are identified by their retracted processes and "amoeboid" morphology, release of both pro- and anti-inflammatory molecules and reactive oxygen species (ROS), and highly phagocytic towards apoptotic cells and debris (Gehrmann et al., 1995; Neumann et al., 2008).

Microglial **phagocytosis** relies on specific receptors expressed on the cell surface and downstream signaling pathways that contribute to the reorganization of actin protein and engulfment of harmful microparticles such as Aβ in AD. Microglial phagocytosis is modulated by several distinctive types of receptors: Toll-like receptors

(TLRs), triggering receptor expressed on myeloid cells 2 (TREM-2), Fc receptors, complement receptors, scavenger receptors (SR), purinergic receptor P2Y6 (P2RY6), macrophage antigen complex 2 (MAC-2), mannose receptor and lipoprotein receptor-related protein 1 (LRP1) receptor. They participate in microglial clearance of misfolded proteins, apoptotic cells and dead neurons, in both acute and chronic brain injury (Smith, 1999; Fu et al., 2014).

Microglia have been shown to play key roles in orchestrating brain **inflammation** that occurs during AD (Hemonnot et al., 2019). When an acute inflammatory injury occurs in the brain, there is an initial defensive glial response aimed to repair the tissue damage. However, if the "stimulus" persists, a chronic inflammatory condition develops, becoming harmful to the CNS and contributing to neuronal dysfunction, injury, and loss (Streit et al., 2004).

3. Dual role of microglia in AD.

Many studies have described microglia surrounding senile plaques both in AD patients and transgenic mouse models of AD (Itagaki et al., 1989; Frautschy et al., 1998; Meyer-Luehmann et al., 2008; Serrano-Pozo et al., 2011). Microglia associated with plaques present a specific, transformed morphology, which consists of a larger cell body and thicker processes, indicating pro-inflammatory activation (Wyss-Coray and Mucke, 2002; Prokop et al., 2013; Kamphuis et al., 2015, 2016). However, various GWAS studies have established that most AD risk loci are found in or near genes that are highly and sometimes uniquely expressed in microglia. Moreover, single cell transcriptome studies of microglial cells found extensive phenotypic heterogeneity of microglia from both AD patients (Young et al. 2021) and mouse models (Mathys et al., 2017), pointing towards temporal changes of microglia response to neurodegeneration. Microglia has been classified in different subgroups and cellular states in aging and AD such as Disease Associated Microglia (DAM) (Keren-Shaul et al., 2017) with phagocytic profile versus Microglial neurodegenerative Disease (MGnD) with dysfunctional phenotype (Krasemann et al., 2017). In relation to gender, while microglia from female mice seem to be more protective than microglia from males in healthy conditions, under pathological circumstances female ones seem to accelerate the course of the disease

(Sala Frigerio et al., 2019). Significantly, immune response pathways involving inflammation and/or clearance mechanisms line up with the genetics and pathological features of late-onset AD (reviewed at Tenner, 2020). This leads to the concept of microglia being critically involved in the early steps of the disease and identifying them as important potential therapeutic targets. Whether microglia reaction is beneficial, detrimental or both to AD progression is still unclear and the subject of intense debate (Combs et al., 2001; Qin, 2006; Hemonnot et al., 2019).

Microglia can play a dual role when interacting with Aβ in AD. Although microglia are able to phagocytose Aβ (Xu et al., 2020), with the progression of the disease, impairment of the phagocytosis has been described (Krabbe et al., 2013). Also, studies reported that microglia are not able to degrade Aβ efficiently unless activated by immunotherapy (Wilcock, 2004) or the action of cytokines (Monsonego et al., 2006; Medeiros et al., 2013) such as MCSF (Majumdar et al., 2007). On the other hand, microglia mediate synaptic loss in AD mouse models due to a pruning phenomenon (Hong et al., 2016). Importantly, pharmacological ablation of microglia or inhibition of their proliferation, prevented cognitive decline and slowed disease progression in AD models highlighting the contribution of microglia to AD (Gomez-Nicola et al., 2013; Dagher et al., 2015; Olmos-Alonso et al., 2016; Spangenberg et al., 2019) (Described in detail in chapter 5).

In the following subsections we will review some of microglial actions and functions related to amyloid pathology in AD such as inflammation, Aβ clearance and lysosomal biogenesis and function.

3.1. Contribution of microglia to AD-related inflammation.

Over the past two decades, researchers have determined that microglia are one of the key initiators of inflammation associated with neurodegenerative disease (Filipov, 2019). Microglia-driven inflammation was first identified in a number of seminal studies using mouse models of AD (Benzing et al., 1999; Yoshiyama et al., 2007). *Post-mortem* brains from AD patients as well as brains from APP transgenic mice show increased levels of pro-inflammatory cytokines as well as chemokines, including interferon γ (IFNγ), tumor necrosis factor α (TNFα), transforming growth factor β (TGFβ), interleukin 1β (IL-

1β), and interleukin 6 (IL-6) (Fillit et al., 1991; Vandenabeele and Fiers, 1991; Chao et al., 1992, 1994; van der Wal et al., 1993; T. Griffin et al., 1995; Prehn et al., 1996; Chong, 1997; Tarkowski et al., 1999; Sheng et al., 2001; Griffin et al., 2006; Hoozemans et al., 2006; Wyss-Coray, 2006; Heneka and O'Banion, 2007; Rojo et al., 2008). Nonetheless, some studies reported an association between low producing interleukin 10 (IL-10) genotypes and the risk of AD (Lio et al., 2003; Arosio et al., 2004).

Some microglial receptors can play different inflammation-related functions in response to Aβ. CD36 and cluster of differentiation 40 (CD40) can mediate production of ROS in response to Aβ fibrils (Coraci et al., 2002; el Khoury et al., 2003). Engagement of CD40 receptor with its ligand leads to the production of TNFα and IL-1β (Tan et al., 1999). Expression of CD40 receptor, as well as its ligand are increased around Aβ plaque deposits in the AD brain (Togo et al., 2000; Calingasan et al., 2002). Another receptor associated with Aβ is AGER or RAGE. AGER is a transmembrane receptor of the immunoglobulin superfamily that has been mainly involved in mediating the inflammatory cascade in activated microglia (Jones et al., 2013). Aβ induces kB nuclear factor (NF-kB) activation and promotes the production of pro-inflammatory molecules through the interaction with AGER (Doens and Fernández, 2014). Also, increased expression of cluster of differentiation 74 (CD74), a type II transmembrane protein which functions as a molecular chaperone of class II major histocompatibility complex (MHC II) (Matza, 2003), has been reported in AD cases relative to age-matched controls (Bryan et al., 2008).

Finally, the complement system is an essential component of the innate immune system and acts as a bridge between innate and adaptive immunity (reviewed at Shah et al., 2021). The levels of complement system factors are altered in AD, and *CR1* gene variant is linked to an increased risk for AD (Tremblay et al., 2011; Crehan et al., 2012). Knock out animals or Inhibition of C3, C1q, or complement system receptor 3 [CR3; constituted by cluster of differentiation 11b (CD11b) and cluster of differentiation 18 (CD18)] rescued early synapse loss (Hong et al., 2016). Also, increased C3 and C4 levels have been reported in AD patients and patients suffering from mild cognitive impairment (MCI) progressing to AD relative to patients suffering from MCI but not progressing to AD (Daborg et al., 2012).

3.2. Microglial contribution to Aβ clearance in AD.

Microglial cells play an important role during AD progression by interacting, internalizing and intracellularly degrading Aβ, and by secreting degrading enzymes involved in its extracellular degradation (Table 1). Indeed, the mechanisms of degradation by glial cells include the production of proteases, interaction with extracellular chaperones alone or in association with receptors or transporters that facilitate their exit to the blood circulation, autophagy, and internalization (Ries and Sastre, 2016).

- Aβ internalization.

Aβ can be internalized by microglia via pinocytosis, phagocytosis, or receptor-mediated endocytosis.

Pinocytosis is a non-selective process of extracellular fluid engulfment (Solé-Domènech et al., 2016). Soluble $A\beta_{1-42}$ is able to induce its **pinocytic** self-uptake by stimulating the P2Y4 receptor (Li et al., 2013).

Microglia cells express several receptors that modulate oligomeric and fibrillar Aβ recognition, internalization, and clearance as well as cell activation (Doens and Fernández, 2014). **Receptor-mediated Aβ endocytosis** can be mediated by Scavenger receptors (SR), cluster of differentiation 33 receptor (CD33), TREM2, TLRs, formyl peptide receptor (FRL1/FPR2), LRP1 and complement system receptors.

SRs are structurally diverse cell surface receptors that participate in cellular adhesion and uptake of ligands (Krieger and Krieger, 1994). The SR family can be classified into at least eight classes in mammalian species. Two of them have been described in AD: SR-A and SR-B.

SR-A [also called macrophage scavenger receptor (MSR1), scavenger receptor class A member 1 (SCARA1) and cluster of differentiation 204 (CD204)] can bind both soluble and fibrillar Aβ *in vitro* and facilitate its subsequent uptake (Khoury et al., 1996; Paresce et al., 1996; Yang et al., 2011; Frenkel et al., 2013). Moreover, increased microglial expression of MSR1 around Aβ plaques has been found in multiple AD

transgenic models (Bornemann et al., 2001; Wilkinson and el Khoury, 2012) as well as in human AD brains (Christie et al., 1996).

Table 1 . List of microglial Aβ internalization and clearance mechanisms involved in AD.

Mechanism		Proteins involved	Aβ species	References
Internalization	Pinocytosis	P2Y4 receptor	Soluble Aβ	(Li et al., 2013)
	Phagocytosis	SRA, SRB, complement receptors, (CR1, CR3, CR4), CD45, CD11b, CD11c	Soluble and fibrillar Aβ	(Reviewed at Solé-Domènech et al., 2016)
	Receptor-mediated endocytosis	SRA, SRB, CD33, TREM2, TLRs, FRL1/FPR2, LRP1, complement receptors (CR1, CR3, CR4)	Soluble and fibrillar Aβ	(Yang et al., 2011; Fu et al., 2012; Frenkel et al., 2013; Sheedy et al., 2013; Solé-Domènech et al., 2016; Wang et al., 2016b; Griciuc et al., 2020)
Intracellular degradation	Lysosome	Cathepsin B, D, TPP1	Soluble and fibrillar Aβ	(Cataldo et al., 1995; Mueller-Steiner et al., 2006; Solé-Domènech et al., 2018; Kim et al., 2021)
	UPS	β1i, β2i, β5i	Soluble and fibrillar Aβ	(Orre et al., 2013)
	Autophagy	ATG12-ATG5, LC3II	Fibrillar Aβ	(Cho et al., 2014)
Extracellular degradation	Metallopeptidases	Neprylisin, IDE	Soluble and fibrillar Aβ	(Zhao et al., 2007; Wang et al., 2010)
	Plasminogen activators	PLAT	Soluble and fibrillar Aβ	(Shibata et al., 2007)
	Matrix metalloproteinases	MMP2, MMP9	Soluble and fibrillar Aβ	(Gu et al., 2020; Wang et al., 2020)

SR-B or CD36 mediate phagocytosis of fibrillar $A\beta_{1-42}$ (Koenigsknecht, 2004; Wilkinson and el Khoury, 2012; Yu and Ye, 2015). CD36, also known to bind soluble $A\beta_{1-}$

$_{42}$ directly (Sheedy et al. 2013; Wilkinson K 2011), may play a redundant role in soluble $A\beta_{1-42}$ clearance (Frenkel et al., 2013). While CD36 confers neuroprotection through induction of Aβ removal, it also activates NLRP3 inflammasome in microglia and stimulates pro-inflammatory cytokine release (i.e. IL-1β, and ROS) (Sheedy et al. 2013).

Cluster of differentiation CD33 (CD33) receptor is a member of the sialic acid-binding immunoglobulin-like lectin family and it is thought to inhibit the immune response presumably via immunoreceptor tyrosine-based inhibition motifs (ITIM) (Pillai et al., 2012). In the brains of AD patients, $CD33^{+}$ microglia are enriched relative to age-matched controls and correlate with greater $A\beta_{1-42}$ levels and plaque burden (Griciuc et al., 2013, 2020).

Some of the complement system receptors play a prominent role in the removal of Aβ such as CR3. Thus, CR3 is involved in the uptake and clearance of Aβ *in vivo* and *in vitro* (Maier et al., 2008; Choucair-Jaafar et al., 2011; Fu et al., 2012). Moreover, CR3 acts together with MSR1 in the uptake of Aβ (Fu et al., 2012).

TREM2 is a single pass type I transmembrane protein that is part of the immunoglobulin superfamily. TREM2 mutations have been implicated in increased susceptibility to late-onset AD (Holtzman et al., 2012; Guerreiro et al., 2013). Moreover, TREM2 can interact with fibrillar Aβ, recruiting microglia around plaques, thereby limiting Aβ diffusion and associated toxicity (Wang et al., 2015, 2016b).

Also, adaptor proteins can associate with various receptors and transmit their signals. In particular, Transmembrane Immune Signaling Adaptor (Tyrobp) also called DNAX-activation protein 12 (DAP12) associates with cell membrane receptors such as TREM2 or CR3 (Lowell, 2011). Tyrobp is mainly expressed in microglia (Colonna, 2003), acts as a downstream adaptor of numerous immune receptors and may play a role in pathogenesis of AD since its expression is upregulated in plaques-associated brain regions of APP23 mice (Frank et al., 2008).

Another internalization process is **phagocytosis**, a vesicular engulfment process by which cells internalized large particles (reviewed at Solé-Domènech et al., 2016). Microglia phagocytose fibrillar Aβ (Lee and Landreth, 2010) and interestingly, oligomeric Aβ attenuates the induction of microglial phagocytosis by fibrillar Aβ (Pan et al., 2011).

Principal receptors involved in phagocytosis has been previously mentioned and are SR-A, SR-B, complement receptor such us CR1, CR3 and CR4 and surface receptors CD45, CD11b an CD11c (Solé-Domènech et al., 2016).

- Intracellular Aβ degradation.

Once Aβ is internalized, it can be degraded by lysosomes, the ubiquitin proteasome system (UPS) or by autophagy.

Lysosomes contain more than 60 hydrolytic enzymes involved in the degradation of molecules delivered via endocytic, phagocytic and autophagic pathways (Lübke et al., 2009; Maxfield et al., 2016). Lysosomal hydrolases are expressed by neurons and glia surrounding senile plaques (Cataldo et al., 1991, 1996). In fact, endosomal-lysosomal system is upregulated in AD (Cataldo et al., 1995, 1996, 1997, 2004). The mayor lysosomal proteases are cathepsins. Among the different cathepsins present in microglial lysosomes, cathepsin D and B have shown to cleave soluble Aβ *in vitro* (Cataldo et al., 1995; Mueller-Steiner et al., 2006; Sun et al., 2015; Kim et al., 2021). Cathepsin B is also involved in proteolyzing fibrillar Aβ both *in vivo* and *in vitro* (Mueller-Steiner et al., 2006). Fibrillar Aβ is also degraded by Tripeptidyl peptidase 1 (TPP1) (Solé-Domènech et al., 2018).

UPS is the major protein quality control system and degrades misfolded or abnormally modified proteins. Both inhibition (Oh et al., 2005; Almeida, 2006; Tseng et al., 2008) and increment (Orre et al., 2013) of proteasome activity has been shown in AD. Interestingly, subunits β1i, β2i, β5i of the immunoproteasome, a proteasome variant mediated by pro-inflammatory cytokines and associated with microglia, are increased both AD mice and in *post-mortem* samples of human AD patients (Orre et al., 2013).

Autophagy is another important cellular degradative mechanism involved in Aβ digestion. **Autophagy** is a tightly regulated catabolic pathway for lysosomal degradation of cytoplasmic organelles or cytosolic components and the recycling of the resulting macromolecules (Wong and Cuervo, 2010). Cho et al., (2014) reported increased of both ATG12-ATG5 complex and LC3II autophagic markers in microglia upon fibrillar Aβ treatment, highlighting the contribution of microglial autophagy to Aβ clearance.

Defective autophagy is a common phenomenon in AD mice, and it is believed that such defects are in part caused by lysosomal dysfunction (Wolfe et al., 2013).

- Extracellular Aβ degradation.

Microglia also promotes Aβ clearance by **secreting proteases** like metallopeptidases neprilysin (Wang et al., 2010), insulin degrading enzyme (IDE) (Zhao et al., 2007), plasminogen activators (tissue -type plasminogen activator precursor or PLAT) (Shibata et al., 2007), matrix metalloproteases Metalloproteinases 2 (MMP2) (Wang et al., 2020) and 9 (MMP9) (Gu et al., 2020) among others.

3.3. Lysosomal biogenesis and function in AD.

The lysosome is the terminal degradative organelle of the cell (Bajaj et al., 2019). In recent years, the study of the lysosome and its processes related to late-onset neurodegenerative diseases has gained renewed interest (Sharma et al., 2018).

Lysosomal biogenesis involves the synthesis, targeting, functional residence, and turnover of the proteins that comprise the lysosome (reviewed at Solé-Domènech et al., 2016). Transcription factor EB (TFEB), a master regulator of the lysosomal system, coordinates the expression of lysosomal hydrolases, lysosomal membrane proteins, and autophagy proteins in response to pathways sensing lysosomal stress and the nutritional conditions of the cell among other stimuli. In physiological conditions, TFEB is localized in the cytosol. Under stress or starvation, cytosolic TFEB translocates to the nucleus and promotes transcriptional activity that will lead to the synthesis of lysosomal enzymes, proton pumps and lysosomal structural proteins such as Lysosome-associated proteins (LAMPs) (Sardiello and Ballabio, 2009; Sardiello et al., 2009). The TFEB homologs transcription factor binding to IGHM enhancer 3 (TFE3) and microphthalmia-associated transcription factor (MITF), which belongs to the same subfamily of MiT/TFE transcription factors, also contribute to the transcriptional regulation of the autophagy-lysosome pathway (Martina et al. 2014).

TFEB regulates expression of proteins involved in lysosomal function such as osteopetrosis-associated transmembrane protein 1 (OSTM1) and chloride channel 7 (CLC-7)(Palmieri et al., 2011), which act in cooperation and are essential for regulating

lysosomal pH and Aβ clearance (Lange et al., 2006; Lacombe et al., 2013; Spampanato et al., 2013).

Lysosomal biogenesis may be impaired in the AD brain (Wong and Cuervo, 2010). Studies in primary microglia treated with fibrillar Aβ showed a dose-dependent reduction of nuclear TFEB coinciding with an increase in cytoplasmatic TFEB levels, retaining this transcription factor inactive outside the nucleus, along with a dramatic decrease in OSTM1 levels (Guo et al., 2017). MCSF increases OSTM1 expression, which also increases CLC-7 mobilization to the lysosome. When this happens, the lysosomes become more acidic, and can degrade fibrillar Aβ more efficiently (Majumdar et al., 2007, 2011). Also, TFEB overexpression promoted the clearance of intracellular $A\beta_{1-42}$ mediated by elevated lysosome activity and suppressed oxidative stress and cell apoptosis induced by $A\beta_{1-42}$ in SH-SY5Y cells (Yi-dan Zhang and Zhao 2015).

However, adult APP/PS1 mice and macrophage cell lines exhibited increased levels of LAMP1, cathepsin D and p62, proteins regulated by TFEB (Pastore et al. 2016; Yi-dan Zhang and Zhao 2015). The previously mentioned study in primary microglia treated with fibrillar Aβ that showed a dose-dependent reduction of nuclear TFEB, also showed significant increase levels of LAMP1 lysosomal marker (Guo et al., 2017). Consistent with these findings, LAMP1 mRNA and protein expression are elevated in cerebral cortex of AD cases (Barrachina et al., 2006). Whether this LAMP1 increase is aberrant and/or represents unfunctional lysosomes that will result in a deficient degradation by microglia, has not been clarified.

Overall, scientific evidence indicates that it is crucial to understand the mechanisms behind the degradative capacity of microglia in order to discover new therapeutic targets that contribute to a more efficient lysosomal function in AD.

4. Macrophage colony-stimulating factor (MCSF).

Macrophage colony-stimulating factor (MCSF, also known as CSF1) is a hematopoietic cytokine expressed by a wide range of cells and tissues, namely the kidney, brain, liver, retina, spleen, lung, adipose tissue, skin, and joints (Ryan et al., 2001; Nandi et al., 2006). It stimulates progenitor cells from bone marrow (Stanley et al., 1976)

and has a role in the development, proliferation, and maintenance of mononuclear phagocytes such as monocytes, dendritic cells, microglia, and osteoclasts (Chitu et al., 2016). MCSF is secreted by neurons, astrocytes, and microglia (Nandi et al., 2012).

4.1. MCSF/ CSF-1R signaling.

MCSF signals through a tyrosine kinase family receptor (CSF-1R) also known as cluster of differentiation 115 (CD115) or fms (Ségaliny et al., 2015). CSF-1R is a class III receptor tyrosine kinase activated by two homodimeric glycoprotein ligands, MCSF (Stanley and Heard, 1977) and interleukin 34 (IL-34) (Lin et al., 2008). MCSF signals exclusively through the CSF-1R, while IL-34 interacts with at least one additional receptor known as receptor protein tyrosine phosphatase-ȥ (PTP-ȥ), which is coexpressed with CSF-1R on neuronal progenitor cells (von Holst, 2006). In myeloid cells, activation of the CSF-1R by MCSF and IL-34 leads to comparable biological outcomes (Lin et al., 2008; Wei et al., 2010). Even though CSF-1R is primarily expressed on microglia (Akiyama et al., 1994; Raivich et al., 1998), there are contradictory reports concerning its expression in the neuronal lineage (Chitu et al., 2016).

MCSF binding to CSF-1R leads to rapid dimerization and several waves of tyrosine phosphorylation (Baccarini et al., 1991; Li and Stanley, 1991; Lee, 1999; Wang et al., 1999). The resulting MCSF/CSF-1R complex is internalized by the cell and incorporated into multivesicular bodies, and thereafter into the lysosomal system, in which both ligand (Guilbert and Stanley, 1986) and receptor (Lee, 1999) are degraded.

MCSF/CSF-1R signaling is involved in variety of functions of myeloid cells such as proliferation, inflammation, internalization and clearance mechanisms (Stanley and Chitu, 2014; Nishida et al., 2016).

4.2. Role of MCSF in microglial proliferation.

CSF-1R activates mitogen-activated protein kinase (MAPK) and Akt signaling pathways that contribute to macrophage proliferation (reviewed at Stanley and Chitu, 2014). Additionally, Tyrobp adaptor mediates CSF-1R proliferative signals through a MAPK- and Akt-independent pathway (Otero et al., 2009). MCSF treatment increases microglial proliferation and Tyrobp in primary human microglia (Smith et al., 2013).

4.3. MCSF impact on inflammatory profile of microglia.

MCSF has the ability to polarize microglia towards both pro-inflammatory and anti-inflammatory directions depending on the microenvironment and other inflammatory molecules (Hamilton et al., 2014).

MCSF is a survival and differentiation factor for mononuclear phagocytes. Previous findings demonstrated that IL-1β, at least in part, transcriptionally upregulated MCSF production in human monocytes, a process that can be negatively regulated by both interleukin 4 (IL-4) and IL-10 (Gruber et al., 1994). Moreover, MCSF-induced maturation of human macrophages was accompanied by an increase in CD40, TNFα, IL-6 and TGFβ1 expression compared with other maturation factors (Vogel et al., 2014). In turn, MCSF (as priming or maturation factor), and activation factors like IL-4, IL-10, interleukin 13 (IL-13), or a mixture of these mediators are used for anti-inflammatory induction, towards anti-inflammatory profile by macrophages (Mantovani et al., 2004; Durafourt et al., 2012).

Moreover, decreases the expression of antigen-presenting proteins in human microglia (Smith et al., 2013) and decreases the inflammatory phenotype in mouse macrophages (Caescu et al., 2015), suggesting that MCSF promotes a surveillant phenotype in microglia that may prevent pro-inflammatory activation and neurotoxicity.

4.4. MCSF impact on microglial clearance and internalization functions.

Since most of the work done on MCSF came from studies on monocytes, little is known about MCSF impact on microglia clearance and internalization. Gene expression studies in peripheral monocytes of patients with atherosclerosis showed increased mRNA of scavenger receptors MSR-1 and CD36, elevated serum concentration of MCSF and a positive correlation of MCSF levels with MSR-1 and CD36 expression relative to control individuals (Nishida et al., 2016).

MCSF treatment can modulate microglial clearance function by increasing CD68, MMP2 and MMP9 expression in a monocyte cell line (Mohana et al., 2015), and by rising MMP9 levels in human monocytes (Asakura et al., 1999).

4.5. MCSF impact on lysosomal biogenesis in microglia.

Microglia may respond to MCSF with increased lysosomal function (reviewed at Solé-Domènech et al., 2016). However, little is known about the effects of this cytokine on lysosomal biogenesis in microglia.

TFE3 was identified to bind MITF and has a redundant role in osteoclast (specialized cells differentiated from monocyte/macrophage precursors in the bone tissues) development and function (Steingrimsson et al., 2002; Hershey and Fisher, 2004). MITF and TFE3 become activated by MCSF and receptor activator of NF-kB (RANKL) signaling pathways during osteoclast differentiation. They are essential for osteoclast proliferation and differentiation and regulate a network of genes associated with bone-degrading function of mature osteoclasts (Motyckova et al., 2001; Weilbaecher et al., 2001; Meadows et al., 2007). In addition to MITF and TFE3, TFEB is also activated upon RANKL stimulation and it enhances lysosomal biogenesis in mature osteoclasts (Ferron et al., 2013). Pastore et al. (2016) observed several cytokine expressions such as MCSF were reduced in TFEB deficient macrophages. However, little is known about the link between TFEB and MCSF and how they affect each other in signaling.

5. Role of MCSF-activated microglia in AD.

Patients with presymptomatic AD or MCI exhibited low levels of MCSF as well as low levels of other hematopoietic cytokines, which was predictive of progression toward a dementia diagnosis 2–6 years later (Laske et al., 2010). However, a recent study showed an increased expression of MCSF and CSF-1R mRNAs and reduced expression of IL-34 mRNA in AD samples (Walker et al., 2017). Moreover, human microglia derived from AD patients stimulated with MCSF or IL-34 adopted a pro-inflammatory profile and genes associated with lysosomal biogenesis such as TFEB, LAMP1 or CD68 were downregulated while genes that encoded IDE and TFGβ were upregulated (Walker et al., 2017). In addition, microglia derived from *post-mortem* brain of AD patients expressed higher levels of MCSF than those from non-demented elderly control brains (Lue et al. 2001).

Neurodegenerative diseases are associated with a robust microglial response, which is known to have both beneficial and detrimental properties depending on the disease, animal model, comparing acute versus chronic conditions, and environmental signals (Aguzzi et al., 2013).

Microglia pharmacological ablation with the specific CSF-1R receptor inhibition (PLX5622) prevented microglial association with plaques while improved cognition in aged 3xTg-AD model (Dagher et al., 2015). PLX5622 treatment also led to a marked reduction of brain plaque load in adult 5XFAD mice (Spangenberg et al., 2019). Another approach targeting microglia was by inhibiting its proliferation with the selective inhibitor of CSF-1R tyrosine kinase activity (GW2580) (Olmos-Alonso et al., 2016). GW2580 blocked microglia proliferation and shifted microglia to an anti-inflammatory phenotype (Olmos-Alonso et al., 2016). This treatment also slowed neuronal damage and disease progression in a chronic neurodegeneration mouse model (Gomez-Nicola et al., 2013). These studies highlight the contribution of microglia to disease progression.

However, extracellular supplementation of MCSF have also shown positive results. *In vitro* studies showed that increased expression of CSF-1R or MCSF treatment on cultured murine and human microglia resulted in microglial proliferation, increased pro-inflammatory environment, and enhanced Aβ phagocytosis in part through SR and Fcγ receptor (Mitrasinovic et al., 2001, 2003; Mitrasinovic and Murphy, 2002; Mitrasinovic, 2003). Also, when a co-culture was stablished with microglia overexpressing CSF-1R and in hippocampal organotypic slices treated with NMDA (N-methyl d-aspartate), microglia rescued neurons from excitotoxicity (Mitrasinovic, 2005) or even when microglia and organotypic cultures were treated with MCSF there was no neuronal affection induced by Aβ or NMDA (Vincent, 2002; Vincent et al., 2002).

MCSF promotes Aβ phagocytosis by microglia (Mitrasinovic et al., 2003). MCSF treatment in primary microglia induced lysosomal acidification to levels similar to those measured in J774 macrophage (Majumdar et al., 2007). MCSF treatment led to an increase in OSTM1 expression, the chaperone of CLC-7, which facilitated CLC-7 mobilization to the lysosome leading to full lysosomal acidification and efficient fibrillar Aβ degradation in and by microglia (Majumdar et al., 2011) described in chapter 3.3.

Treatment of APP/PS1 mice with MCSF led to a reduction in brain Aβ load and improved performance in cognitive tests (Boissonneault et al., 2008). In addition, MCSF treatment in young animals without neurological alterations or evident Aβ plaque load prevented AD-like pathology. The main conclusion of this study was that MCSF was able to increase microglial proliferation, microglial association with amyloid deposits, Aβ clearance and led to a reduction in Aβ toxicity to neuronal elements. Moreover, internalized Aβ highly colocalized with microglial late endosomal/lysosomal markers (Boissonneault et al., 2008).

In summary, microglia participate actively in AD, both in a beneficial and detrimental manner. Therefore, a better understanding of the role of MCSF/CSF-1R axis in microglial modulation is crucial to exploit the potential of these cells as targets of therapy in AD. The MCSF/CSF-1R axis is implicated in the regulation of important microglial functions, and it could bring new therapeutic targets for the amelioration of AD progression. This thesis project aims to study MCSF/CSF-1R signaling in order to, in the future, identify similar molecules that could be used to modulate this pathway.

Hypothesis and objectives

Accumulation of soluble, oligomeric Aβ species in the brain is one of the main hallmarks of AD and occurs early during disease pathogenesis. Several studies have shown that microglia are observed surrounding Aβ plaques contributing to the development of the disease. Microglia are inefficient at degrading fibrillar Aβ unless activated by immunotherapy or other methods. There is currently limited knowledge on the effect of MCSF on microglial gene expression, microglial Aβ clearance and synapse pathology. Given the importance of the MCSF/CSF1R signaling axis, we hypothesize that this pathway can be used to enhance microglial degradation of Aβ and therefore in the treatment of AD. In order to investigate this hypothesis, we plan to characterize the effects of MCSF activation of microglia *in vitro* and in mouse models of AD.

To that aim, the following specific objectives were addressed:

Aim 1. To analyze the effect of MCSF on microglial transcriptomics and proteomics in an AD *in vitro* model.

Aim 2. To study the impact of MCSF activation on microglial oAβ clearance and synapse pathology *in vitro*.

Aim 3. To analyze the role of MCSF treatment on microglial dynamics using organotypic brain slices from an AD mouse model.

Aim 4. To characterize the effects of MCSF treatment *in vivo* in the 3xTg-AD mouse model of AD.

Aim 5. To study the MCSF/CSF-1R axis and TFEB transcription factor signaling pathways as potential biomarkers of AD.

Experimental procedures

1. Animals.

All experiments were conducted with the approval and under the supervision of the internal animal ethics committee (University of the Basque Country, UPV/EHU). Animals were handled in accordance with the European Communities Council Directive. All possible efforts were made to minimize animal suffering and the number of animals used.

Animals were housed in standard conditions with 12 h light cycle and with *ad libitum* access to food and water. Experiments were performed in Sprague Dawley rats; in the triple transgenic mouse model of Alzheimer´s disease (3xTg-AD), which harbors the Swedish mutation in the human amyloid precursor protein (APP_{Swe}), presenilin knock-in mutation ($PS1_{M146V}$), and Tau_{P301L} mutant transgene (Tau_{P301L}) (Oddo et al., 2003); in the 5XFAD mouse model of Alzheimer's disease, which overexpresses APP(695) with the Sweedish (K670N, M671L), Florida (I716V) and London (V717I) mutations as well as human PS1 with mutation M146L and L286V (Holly Oakley et al. 2006).

2. Cell cultures.

2.1. Primary cortical neuron culture.

Primary cultures of cerebral cortical neurons were prepared from E18 Sprague-Dawley rats embryos according to previous described procedures (Ruiz et al., 2009). Brain hemispheres were dissected out, meninges and basal nucleus were removed, and cortical lobes were extracted. Selected cortical tissue was enzymatically digested with 0.25% trypsin (Sigma-Aldrich, #T4799) and 0.004% deoxyribonuclease (Sigma-Aldrich, #D5025-15KU) in Hank's balanced salt solution (HBSS, Sigma-Aldrich, #14175-053) for 5 min at 37ºC. Next, the enzymatic reaction was stopped by adding Neurobasal medium (Invitrogen, #21103049) supplemented with 10% Fetal bovine serum (FBS, Gibco, #10270), B27 (Invitrogen, #17504044), 2 mM glutamine (Sigma-Aldrich, #68540) and antibiotic-antimycotic mixture (Gibco, #15140-122), followed by centrifugation at 1,000 rpm for 5 min. The cell pellet was resuspended in 1 ml of the same solution. Mechanical dissociation was performed by using 23-, 25-, and 27G- gauge cutting needles and the resulting cell suspension was filtered through a 40 µm nylon mesh (Millipore,

#NY4104700). 10 µl of filtrate was collected to determine cell number and viability by trypan blue staining (Sigma-Aldrich, #T6146), and all the rest was seeded onto 6/24/48 well plates or glass coverslips (12 mm ø) at 1 x 10^5 or 1 x 10^6 cells per well. Prior to cell culture, the plates and/or glass coverslips were coated with 30 µg/ml Poly-L-ornithine (Sigma-Aldrich, #P4957) for 1 h at room temperature (RT) and washed three times in sterile distilled water.

24 h after seeding cells, culture medium was replaced by supplemented Neurobasal medium without FBS to avoid astroglial growth. Cell cultures were essentially free of astrocytes and microglia and were maintained at 37ºC and 5% CO_2. Cortical neuronal cell cultures were used at 8–10 days *in vitro* (DIV).

2.2. Primary glial cell culture.

Primary cultures of cerebral cortical glial cells were prepared from P0–P2 Sprague Dawley rats as described previously (McCarthy and de Vellis, 1980). Cortical lobes were extracted and enzymatically digested with 400 µl of 2.5% trypsin (Sigma-Aldrich, #T4799) and 40 µl of 0.5% deoxyribonuclease (Sigma-Aldrich, #D5025-15KU) in HBSS (Sigma-Aldrich, #14175-053) for 15 min at 37ºC. The enzymatic reaction was stopped by adding IMDM (Gibco, #42200014) medium supplemented with 10% FBS (Gibco, #10270) and centrifuged at 1,200 rpm for 6 min. The cell pellet was resuspended in 1 ml of the same solution and mechanical dissociation was performed by using 23- and 25G- gauge cutting needles. Resulting cell suspension was centrifuged at 1,200 rpm for 6 min and plated onto 75 cm^2 flasks coated with 30 µg/ml Poly-D-Lysine (PDL, Sigma-Aldrich, #P0899).

After maintaining for 11 DIV, flasks were shaked during 2 h in order to isolate microglia and then microglia were plated onto PDL-coated 6/24/48 well plates or glass coverslips (12 mm ø) at 5 x 10^4 or 1.5 x 10^5 cells per well, depending on the experimental technique.

2.3. Primary neuronal-microglial co-culture.

After maintaining neurons for 7 DIV and glia for 11 DIV, flasks were shaked for 2 h to detach the cells from the bottom of the flasks. Microglia were added to neuronal

primary cultures in a 10:1 ratio. Following addition, the co-culture was stabilized overnight at 37ºC and 5% CO_2.

2.4. Organotypic cerebral cortex and hippocampal slice cultures.

Hippocampal and/or cortical slice cultures were prepared from 5-7 days old mouse pups according to previously described procedures (Stoppini et al., 1991). The brains were extracted and placed on ice in a small petri dishes with HBSS (Sigma-Aldrich, #14175-053) with calcium and magnesium and without phenol red. Brains were then sectioned in 350 µm coronal slices using a vibratome Leica VT 1200S. Intact individual slices of cortex and hippocampus were selected under the microscope and transferred onto membrane inserts (Millipore, #PIHP03050) with fresh culture medium [50% neurobasal medium (Gibco, #21103049), pH 7.2 supplemented with 25% horse serum (Invitrogen, #26050-088), 25% basal medium eagle (Sigma-Aldrich, #M5650), 1.8% glucose (Panreac, #141341.1211), 1% glutamine (Sigma-Aldrich, #68540), 0.5% Penicilin-Streptomicin (Invitrogen, #15240062), 0.5% fungizone (Merck, #1397-89-3) and 21.2% HBSS (Sigma-Aldrich, #14175-053)] (Figure 8).

Cell cultures were maintained at 37ºC and 5% CO_2, and culture media was renewed every 2 days. Experiments were performed after 7 or 11 DIV of incubation, depending on the experiment.

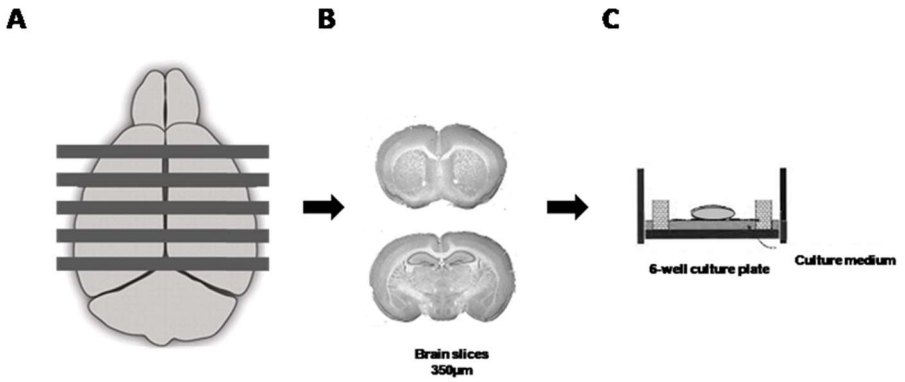

Figure 8. Organotypic culture protocol steps. Representative image of the main steps in the protocol: brain sectioning in 350 µm-thick slices (A), slice selections (B) and slice incubation in 6-well culture plates (C).

3. Human samples.

Patients gave informed consent to all clinical investigations, which were performed in accordance with the principles embodied in the Declaration of Helsinki.

Frozen samples from prefrontal cortex and hippocampus of 53 subject and 34 subjects respectively, were obtained from the Neurological Tissue Bank Hospital Clinic-IDIBAPS Biobank (Table 2). AD samples were sorted according to Braak and Braak staging (Braak and Braak, 1995) into AD-II, AD-III, AD-IV and AD-V, and by CERAD classification (Mirra et al., 1991) into AD-A, AD-B and AD-C.

Table 2. **Characteristics of controls and AD subjects, categorized as stages I to VI of Braak and Braak and A, B or C of CERAD criteria**. *Time (h) elapsed between death and sample extraction. Hp, hippocampus.

Case nº	Ref. nº	Braak stage NFT	CERAD Senile plaque	Gender	Age	Region analyzed	Postmortem delay*
1	1733	-		M	76	Hp	11:30
2	1423	-	A	F	82	Hp	5:00
3	1536	-		M	79	Hp	4:45
4	1878	-	B	M	78	Hp	7:30
5	1357	II		F	79	Hp	10:30
6	1405	II		M	80	Hp	5:30
7	1431	II	-	F	97	Hp	20:00
8	1543	II		M	80	Hp	4:30
9	1687	II		F	69	Hp	12:00
10	1697	II	-	M	78	Hp	6:00
11	1912	II	B	F	72	Hp	13:35
12	1937	II	B	F	83	Hp	7:20
13	0892	III	B	M	76	Hp	16:00
14	1180	III	C	F	86	Hp	14:00
15	1200	III	B	F	89	Hp	16:25
16	1247	III	C	F	80	Hp	8:00
17	1345	III	A	M	78	Hp	8:00
18	1411	III	C	F	74	Hp	13:30
19	1435	III	B	F	93	Hp	5:45
20	1791	III	B	F	75	Hp	21:00
21	0497	IV	B	M	82	Hp	2:30
22	0608	IV	-	M	78	Hp	7:00
23	0806	IV	C	M	67	Hp	6:00
24	1040	IV	C	M	76	Hp	8:25
25	1102	IV	-	F	84	Hp	3:25
26	1417	IV	-	F	79	Hp	4:30
27	1914	IV	-	F	80	Hp	8:30
28	1230	IV	C	M	79	Hp	4:15
29	1286	V	C	M	79	Hp	5:00

30	1392	V	C	M	77	Hp	5:00
31	1445	V	C	F	73	Hp	3:30
32	1456	V	C	F	74	Hp	3:30
33	1585	V	C	F	74	Hp	6:30
34	1622	V	C	M	76	Hp	5:00
35	1637	V	C	M	78	Hp	7:00
36	1645	V	C	F	77	Hp	5:30
37	1198	V	C	F	77	Hp	5:00

4. Preparation of amyloid β-oligomers and fibrils.

$A\beta_{1-42}$ (ABX, Radeberg, Germany) was solubilized in hexafluoroisopropanol (HFIP, Sigma-Aldrich, #105228) to 1 mM and distributed into aliquots in sterile microcentrifuge tubes. Hexafluoroisopropanol was totally removed under vacuum in a speed vac system and the peptide film was stored dried at -80°C. For the aggregation protocol, two procedures were carried out to yield either oligomeric or fibrillar Aβ species. The peptide was first resuspended in anhydrous dimethyl sulfoxide (DMSO) (Sigma-Aldrich, #D12345) to a concentration of 5 mM. For oligomer preparation, the DMSO-resuspended peptide was diluted to a final concentration of 100 µM in Hams F-12 (Biowest, #L0136-500) pH 7.3 and incubated at 4ºC for 24 h. For fibril preparation, the DMSO-resuspended peptide was diluted to a final concentration of 100 µM in 10 mM HCl (Thermo fisher scientific, #15578334) and incubated at 37º for 24 h (Dahlgren et al., 2002).

5. Drugs and treatment.

The following drugs and inhibitors were used: Rat (#40028) and murine (#31502) macrophage colony-stimulating factor (MCSF) (Preprotech).

6. Viability assay.

Calcein-AM (Sigma-Aldrich, #C1354) was used to quantify the number of living cells. Cells were incubated with 1 µM calcein-AM for 30 min followed by 2 washes with Phosphate saline buffer (PBS) (125 mM NaCl (Thermo fisher scientific, #S/3160/65), 19 mM Na_2HPO_4 (Panreac, #141679.1211), 8 mM KH_2PO_4 (Acros organics, #AC205925000)

in ddH_2O, pH 7.4). Fluorescence was measured with a Synergy-HT fluorimeter (Bio-Tek Instruments Inc.).

7. Electron microscopy.

Aβ$_{1-42}$ oligomers were prepared following the protocol described in section 4 (Preparation of Aβ oligomers). After overnight incubation, 5 µl of 100 µM Aβ$_{1-42}$ were incubated on nickel coated grids (EMSdiasum, #G150-Ni) for 1 min. The solution was carefully removed using filter paper 5 µl of filtered 4% uranyl acetate (Merck, #K18237473) were then incubated on top of the grid for 1 min as contrast agent and the solution was dried using filter paper. The grids were allowed to dry for a few mins prior to imaging. Grids were imaged using a Zeiss EM900 electron microscope (Zeiss). Oligomeric Aβ$_{1-42}$ images were taken at 80000x magnification while fibrillar Aβ$_{1-42}$ images were taken at 15000x magnification.

8. Protein extracts preparation and detection by Western blot.

8.1. Total protein preparation.

After treatment, cultured cells were washed twice in cold 1X PBS. Cell lysates were prepared from cultures using a cell scraper (Costar, #3008) and 50-100 µl Pierce™ RIPA buffer (Thermo Fisher Scientific, #89900), with Halt™ Protease & Phosphatase Inhibitor Cocktail (Thermo Fisher Scientific, #1861284) and 0.5 M ethylenediamine tetraacetic acid solution (EDTA, #1861283). All this process was performed on ice to enhance the lysis process and prevent protein degradation. After that, protein concentration of the samples was measured with a detergent-compatible protein assay reagent (DC protein assay reagent A #5000113, DCtm Protein assay reagent S #500-0115, DC Protein assay reagent B #5000114 from Biorad) according to the manufacturer's instructions, then was mixed with sample buffer in a fixed protein concentration and finally boiled at 95ºC for 5 min.

8.2. Western blot.

Equal amounts of protein lysates were separated by SDS-PAGE using Bolt 4-12% Bis-Tris plus gels (Invitrogen, #NW04127BOX). Electrophoresis was conducted in a Bolt

SDS running buffer (Invitrogen, #B000202) using a protein gel electrophoresis chamber system (Invitrogen). Gels were transferred to iBlot PVDF mini stacks (Invitrogen, #IB24002).

For immunoblotting, membranes were blocked in PBST buffer (125 mM NaCl (Thermo fisher scientific, #S/3160/65), 19 mM Na_2HPO_4 (Panreac, #141679.1211), 8 mM KH_2PO_4 (Acros organics, #AC205925000) in dH_2O, pH 7.4, 0.1% Tween-20 (Acros organics, #A0406604) in dH_2O, pH 7.6) in the presence of 5% fat-free milk during 1 h at RT. Membranes were incubated overnight with the specific primary antibodies in the same solution at 4ºC with gentle shaking. Following incubation, membranes were washed three times with PBST and incubated with secondary antibodies in blocking solution for 1 h at RT. Finally, membranes were again washed three times with PBST.

Immunoreactive bands were detected by using enhanced electrochemical luminescence (NZY standard ECL #MB40101 and NZY advanced ECL #MB40201 by Nzytech) and ChemiDoc XRS Imaging System (Bio-Rad). Signals were quantified using Image Lab® software (Bio-Rad) and values were normalized to β-actin or α-tubulin signal and provided as the mean ± S.E.M. of at least three independent experiments.

When needed, membranes were stripped of antibodies using Restore Western Blot Stripping Buffer (Thermo Fisher Scientific, #21059) for 8 min at RT. Membranes were then washed in PBST for three times, blocked and incubated again with other primary antibodies.

8.3. Antibodies for Western blot.

The following antibodies were used for western blot: mouse anti-6E10 (1:1000, Biolegend, #803015), rabbit anti-CSF-1R (1:1000, Cell Signaling, #3152S), rabbit anti-TFEB (1:500, Cell Signaling, #803015), rabbit anti-CD11b (1:1000, Invitrogen, #ab128797), rabbit anti-CD18 (1:1000, Thermo fisher scientific, #PA5-95027), mouse anti-Tyrobp (1:100, Santa Cruz Biotechnology, #sc166084), rabbit anti-MSR1 (1:1000, Invitrogen, #MA1-81060), rabbit anti-CD36 (1:1000, Abcam, #ab252922), mouse anti-AT8 (1:1000, Invitrogen, #44-752G), mouse anti-hT7 (1:1000, Invitrogen, #MN1000), mouse anti-α-tubulin (1:5000, Abcam, #ab7291) and rabbit anti-β-actin (1:5000, Sigma-

Aldrich, #SAB5600088). Secondary antibodies conjugated with horseradish peroxidase (HRP) were purchased from Sigma-Aldrich (1:1000).

9. Immunoprecipitation.

Neuron cultures and neuronal-microglial co-cultures were incubated with 1 µM oAβ for 24 h (Manterola et al., 2013) and Aβ levels in the media were quantified by immunoprecipitation thereafter. Following incubation, media samples were immunoprecipitated overnight at 4ºC with 4G8 antibody (Biolegend, #800701) and rabbit anti-mouse secondary antibody (Invitrogen, #31188) and Protein A sepharose (Abcam, #ab193256) in IP buffer composed of 760 mM NaCl, 200 mM TrisHCl pH8.8, 24 mM EDTA, 10% Triton X-100. Next day, samples were washed with IP buffer B, composed of 150 mM NaCl, 10 mM TrisHCl pH 8.3, 5 mM EDTA, 0.1% Triton X-100 (Sigma-Aldrich, #11332481001). Next, loading buffer was added to the samples, which were then heated at 95ºC for 5 min and thereafter centrifuged at 14000 rpm at 4ºC for 3 min. Aβ species were isolated from media samples using electrophoresis with Mini-PROTEAN Tris-Tricine gel containing 10-20% poliacrilamide (Invitrogen, #EC66252BOX) and later transferred to nitrocellulose membranes (Invitrogen). Membranes were boiled in 1X PBS for 5min and processed by Western blotting using 6E10 primary antibody (1:1000, Biolegend, #803015) and sheep anti-mouse HRP secondary antibody (1:1000, Cell Signaling, #7076) to detect oligomeric Aβ.

10. Intraperitoneal injection in adult mice.

Prior to injection, animals were anesthetized with isoflurane. The animals used in the *in vivo* study of MCSF were all female mice of the 3xTg-AD mouse model starting at 12 months of age and were injected intraperitoneally every week for 4 months. Animals were injected with either 0.9% NaCl (130 µl) (ERN, #999789.2) or a solution containing 10 ng/µl mouse MCSF (Preprotech, #31502) (final injection: 40 µg/kg, 130 µl).

After 4 months of treatment, animals were anesthetized with pentobarbital, followed by CSF extraction from the cisterna magna (Lim et al., 2018) intracardial blood extraction and finally by intracardial perfusion with phosphate buffer (PB). Brain hemispheres were separated during dissection. One hemisphere was snap frozen at -

80ºC and the other hemisphere was post-fixed by overnight incubation in 4% paraformaldehyde (PFA, Panreac, #141451.1211) 4ºC, followed by incubation in 30% sucrose containing 0.1 M PBS pH 7.5 at 4°C overnight. Following sucrose gradient, the hemisphere was stored in cryoprotectant solution (30% ethylene glycol (Merck, #1.09621), 30% glycerol (Acros organics, #410985000) and 10% PB 0.4 M in dH_2O) at -20°C.

11. Immunochemistry.

11.1. Immunofluorescence.

11.1.1. Primary neuronal and microglial cell cultures.

9 DIV neurons and 12 DIV microglia were fixed with methanol or 4% PFA depending on the protein analyzed (PFA in case of presynaptic markers, methanol in case of postsynaptic markers) and rinsed once with 1X PBS. Fixed cells were permeabilized with blocking buffer [2% Normal Goat Serum (NGS, Palex, #S-1000), 1% Bovine Serum Albumin (BSA, Nzytech, #MB04602), containing 0.1% saponin (Sigma-Aldrich, #57900) in 1X PBS] for 1 h at RT followed by incubation in primary antibodies in blocking buffer, overnight at 4ºC. Next, cells were rinsed three times with PBST buffer [0.1 M PBS pH 7.5 containing 0.1% Tween-20 (Acros organics, #233362500)] and incubated with fluorescent secondary antibodies in blocking buffer for 1 h at RT. After incubation, cells were washed three times with PBST for 10 min, the second wash containing 4 µg/ml DAPI (4',6-diamidino-2-phenylindole, Sigma-Aldrich, #10236276001). Finally, coverslips with cells were mounted on glass slides with Fluoromount-G mounting medium (SouthernBiotech, #0100-01). Preparations were kept at 4ºC until examination.

11.1.2. Animal tissue and organotypic slices.

Mice were anesthetized with chloral hydrate and perfused intracardially, first with 30 ml of 0.1 M PB followed by 30 ml of 4% PFA in 0.1 M PB. The brains were extracted and postfixed with the same fixative solution for 4 h at RT, followed by incubation in 30% sucrose in 0.1 M PBS at 4°C. After incubation with sucrose, brains were stored in cryoprotectant solution [30% ethylene glycol (Merck, #1.09621), 30%

glycerol (Acros organics, #410985000) and 10% PB 0.4 M in dH_2O] at -20°C. Tissues were sectioned using a Leica VT 1200S vibratome (Leica microsystems). 40 µm-thick coronal sections were prepared.

In the case of organotypic slices, slices were fixed in 4% PFA for 40 min at RT followed by three washes in 0.1 M PBS, followed by storage in 0.1 M PBS at 4°C. Free-floating vibratome sections were permeabilized and blocked with 0.25% Triton X-100 (Sigma-Aldrich, #1133248100), 3% NGS (Palex, #S-1000) in 0.1 M PB for 1 h at RT and thereafter incubated with primary antibodies overnight at 4ºC with gentle shaking. Followed primary antibody incubation, slices were washed three times in 0.1 M PB and incubated with blocking solution containing fluorescent secondary antibodies at RT for 1 h. After that, slices were washed three times in 0.1 M PB, the second wash containing 4 µg/ml DAPI (Sigma-Aldrich, #10236276001) and were mounted on glass slides with Fluoromount-G mounting medium. In Magdalena Sastre's lab, organotypic slices were permeabilized with 0.5% Triton X-100 (Sigma-Aldrich, #1133248100), 5% NGS (Palex, #S-1000) in 0.1 M PBS for 3 h at RT and washed three times in 0.1 M PBS. After that, tissues were incubated with primary antibodies in a solution containing 0.1% Triton X-100 (Sigma-Aldrich, #1133248100) and 1% NGS (Palex, #S-1000) in 0.1 M PBS, overnight at 4ºC with gentle shaking. Slices were then washed three times in 0.1 M PBS and incubated with fluorescent secondary antibodies in a solution containing 0.1% Triton X-100 (Sigma-Aldrich, #1133248100) and 1% NGS (Palex, #S-1000) in 0.1 M PBS at RT for 1h, followed by three washes in 0.1 M PBS, the second wash containing DAPI 4 µg/ml (Sigma-Aldrich, #10236276001). Slices were finally mounted on glass slides using Fluoromount-G mounting medium (Southern biotech).

11.2. Antibodies for immunofluorescence.

The following antibodies were used for immunofluorescence: mouse anti-Synaptophysin (1:500, Millipore, #101002), rabbit anti-Homer (1:500, Synaptic systems, #160003), guinea pig anti-Iba1 (1:500, Synaptic systems, #234004), rabbit anti-TFEB (1:500, Cell Signaling, #4240), rabbit anti-OSTM1 (1:500, Sigma-Aldrich, #HPA010851), mouse anti-LAMP1 (1:500, Abcam, #ab25630), rabbit anti-Iba1 (1:500, Wako, #019-19741), mouse anti-AT8 (1:1000, Invitrogen, #44-752G), and rat anti-GFAP (1:500,

Invitrogen, #13-0300). For amyloid plaque detection, Thioflavin-S dye was used (1:1000, Sigma-Aldrich, #T1892). Secondary antibodies coupled to Alexa Fluor 488, Alexa Fluor 594, Alexa Fluor 546 were purchased from Invitrogen (1:500).

12. RNA extraction and quantitative PCR.

12.1. RNA isolation.

Cultured microglia were treated with 1 µM oAβ and/or 25 ng/ml MCSF for 24 h. Total RNA was isolated using trizol (300ul per well) (Ambion, #T9424) and stored at -80ºC. The extracted RNA samples were processed by the Gene Expression Unit of the Genomics and Proteomics Service at the University of the Basque Country (UPV/EHU) to carry out large-scale gene expression analysis via the use of high-density microarray.

12.2. Retrotranscription and Real Time-Polymerase Chain Reaction (RT-qPCR).

RNA was reverse transcribed in a 20 µl reaction volume containing 5X reaction buffer (Invitrogen, #p/n y02321), 0.1M DTT (Invitrogen, #p/n y00147), random primers (Promega, #C118A), dNTPs (Invitrogen, #18427-013), RNase OUT and Superscript II retrotranscriptase (Invitrogen, #10777-019) following manufacturer's instructions in a Verity Thermal Cycler (Applied Biosystems). Resulting cDNA samples were diluted in sterile Mili-Q H_2O and stored at 20ºC.

Quantitative Polymerase Chain Reaction (qPCR) was performed in a reaction mixture containing 3.5 µl RNAse-free water (Promega, #P1195), 5 µl Master mix Sybr [30µM] (Bio-Rad, #1725124), 1 µl diluted primers [500 nM] (Integrated DNA technologies, IDT) and 0.5 µl cDNA sample [10ng/µl]. All reactions were performed in triplicates and carried out in cDNA CFX96 Touch Real-Time PCR Detection System (Bio-Rad). Amplification reactions were optimized: 3 min at 95ºC, 40 cycles of 10 sec at 95ºC and 30 sec at 60ºC and finally, 5 sec at 60ºC and 5 sec at 95ºC.

Primers were purchased from Integrated DNA Technologies (IDT) taking the optimal sequence option by PrimerBlast (NIH). PCR product specificity was checked by melting curves. Data were normalized by a normalization factor obtained in geNorm

Software through the analysis of the expression of 4 housekeeping genes. Primer sequences are detailed in the Table 3.

Table 3. Sequences of primers used in the transcriptional analysis grouped in the different categories: housekeeping genes, microglial receptors, inflammation, complement system, lysosomal biogenesis and secreted degrading enzymes.

Category	Gene	Gene bank nº	Sequence
Housekeeping genes	GAPDH	NM_017008	Fwd GAAGGTCGGTGTCAACGGATTT
			Rev CAATGTCCACTTTGTCACAAGAGAA
	HPRT2	NM_012583	Fwd ATGGACTGATTATGGACAGGACTGA
			Rev ACACAGAGGGCCACAATGTG
	BM2	NM_012512.2	Fwd CACCGAGACCGATGTATATGCTT
			Rev TTACATGTCTCGGTCCCAGG
	CICA	NM_017101.1	Fwd CAAAGTTCCAAAGACAGCAGAAAA
			Rev CCACCCTGGCACATGAATC
	UBC	NM_017314.1	Fwd CCTGACAGGCAAGACCATCAC
			Rev ACACCATTGAAAATGTCAAGGCA
Microglial receptors	CSF1R	NM_001029901.1	Fwd GGGCGGTGACCACTGAGATT
			Rev GATGGGGCCATCCCATTCCA
	CD33	NM_001100836.1	Fwd GAGCAGGCGTCACTGTGGAA
			Rev TCAGGAGCTTGACTGCTGCC
	CD36	NM_031561.2	Fwd TGGCTAGCTGATTACTTCTGTGTAG
			Rev TGCAGCAGAATCAAGGAAGAGCA
	CD40	NM_134360.1	Fwd AAGGTGGTCAAGAAACCAAAGGA
			Rev GCTGACACCCATGCAACGTC
	CD74	NM_013069.2	Fwd GGACCCGTGAACTACCCACA
			Rev TGTCCAGTGGCTCTTTAGGTGG
	MRC1	NM_001106123	Fwd AGGTTCCGGTTTGTGGAGCA
			Rev AGAGCCATCCATCTGACCGC
	MSR1	NM_001191939.1	Fwd GACGCACGTTCCATGACAGC
			Rev AGAGCGACGAGGGCAACTTT
	AGER, RAGE	NM_053336.2	Fwd GCTATCGGAATTGTCGATGAGG
			Rev GCTGTGAGTTCAGAGGCAGGAT
	ITGAM	NM_012711.1	Fwd TACTTTGGGCAGTCTCTGAGTG
			Rev ATGGTTGCCTCCAGTCTCAGCA
	ITGB2	NM_001037780.2	Fwd AGTCCCAGTGGAACAACGAC
			Rev AGCACTGGGGCTAGCTGTAA
	TYROBP	NM_212525.1	Fwd TTCCTGTCCTCCTGACTGTGG
			Rev AGGAACATTCGCATCCTGGGTAA
Inflammation	TNFA	NM_012675.3	Fwd GGTGTCTGTGCCTCAGCCTCTT
			Rev GCCATGGAACTGATGAGAGGGAG
	IL1B	NM_031512.2	Fwd TGTCTTGCCCGTGGAGCTT
			Rev AGGTCGTCATCATCCCACGA
	IL6	NM_012589.2	Fwd TACCACTTCACAAGTCGGAGGC
			Rev CTGACAGTGCATCATCGCTGTTC

	STAT1	NM_032612.3	Fwd GGAAGCACCAGAACCGATGGA
			Rev ATGGGAAGCAGGTTTTCTGTGC
	IRF8	NM_001008722.1	Fwd CGTCCCCGAGGAAGAGCAAA
			Rev GCCACACTCCATCTCCGTGA
	MCSF1	NM_023981.4	Fwd CAGGCTCTCCAGCCACTAGC
			Rev GTGGCTACAGTGCTCCGACA
	IL10	NM_012854.2	Fwd CTGCGACGCTGTCATCGATTT
			Rev AGTAGATGCCGGGTGGTTCAA
	TFGB1	NM_021578.2	Fwd TGCCAACTTCTGTCTGGGGC
			Rev TGCGACCCACGTAGTAGACG
	TFGB3	NM_013174.2	Fwd AATCTGTTCCGGGCGGAGTT
			Rev GCGCTGCTTGGCTATGTGTT
Complement system	C1qA	NM_001008515.1	Fwd CAAAGGAGAGAGAGGGGAGCC
			Rev GGTCCCTGATATTGCCCGGAT
	C1qB	NM_019262.2	Fwd AACCAGGCACTCCAGGGATAAA
			Rev TTGTAGTCTCCAGAGCCACCTT
	C1qC	NM_001008524	Fwd GATGGACTTCAGGGGCCCAA
			Rev CATGGGGCCGTTTTTCCCAC
	C2	NM_172222.2	Fwd TGGGCATCAGTCGGAACAGA
			Rev CTCTCGCCGTCCTTCTTGGA
	C3	NM_016994.2	Fwd GAAGATCCTGAGTGCGCCAAG
			Rev CTTTGTCCATCCTCCTTTCCATCA
	C4A	NM_031504.3	Fwd GTCCTGTTGCAAGTTTGCTGAG
			Rev CGCACGAGAATGTCATCTTCATC
Lysosomal biogenesis	LAMP1	NM_012857.2	Fwd GCCTACCTGCCGAGTAGCAA
			Rev GGGTTTGTGGGCACAAGTGG
	OSTM1	NM_001029925.2	Fwd GCCGGATCTGGAGCCTGAAT
			Rev GAGGCGTTCCCGACGTTTC
	TFEB	NM_001025707.1	Fwd TGCTGATCCCCAAGGCCAAT
			Rev TCCAGCTCCTGGATGCGAAG
	MITF	NM_001191089.3	Fwd ATCGGGAATCGTGGCGGATT
			Rev CTGGCGTAGCAAGATGCGTG
Secreted degrading enzymes	IDE	NM_013159.2	Fwd CAAACCTCTCCTTCCAAGTCAGC
			Rev TGTTCTCCGAGGTGCTCTGCAT
	MMP2	NM_031054.2	Fwd ATGCCTTTGCTCGGGCCTTA
			Rev CCGTCCTTGCCGTCAAATGG
	MMP9	NM_031055.2	Fwd AAAGGCCATTCGTTCACCGC
			Rev GCGGCAAGTCTTCGGTGTAG
	PLAT	NM_013151.3	Fwd ATCAGCTCAGCGCCAAGGAGAAG
			Rev TTTTGCTCCCCGTTTCTTCCGT

^Ct value was calculated from the threshold cycle (Ct) of each gene (Table 3), by subtracting the Ct of the housekeeping gene from the Ct of the target gene. Then, ^^Ct was calculated by subtracting ^Ct of a given gene in the condition fixed as the

normalization to the resting conditions ^Ct. Finally, gene expression fold change relative to control was calculated as $2^{-\Delta\Delta Ct}$ for each ^^Ct. Differences in gene expression (fold change data) were assessed by One-way ANOVA test and a following posttest (Bonferroni and Sidak) depending on the sample characteristics.

13. Enzyme-linked immunosorbent assay (ELISA).

The levels of human $A\beta_{1-42}$ were determined in homogenates using the High Sensitivity Human Amyloid Aβ42 ELISA kit (Millipore, #KHB3491). For the analysis of mouse cytokines (IL-1β #900TM73, TNFα #900M95 and MCSF #900M245) in tissue lysates from the cultures we used kits from Preprotech. For the analysis of human MCSF from tissue lysates, we used a kit from Invitrogen #EHCSF1. Concentrations were quantified according to the manufacturer's instructions and normalized to total protein concentration.

Supernatant samples were used undiluted, and tissue homogenates were used diluted to quantify cytokine concentration in a fixed protein sample concentration (in mouse samples, 0.5 µg/µl and in case of human samples, 1 µg/µl). 100 µl of standards solutions and samples were added into a 96-well plate pre-coated for the corresponding cytokine and incubated for 2.5 h at RT with gentle shaking. The plate was washed with washing solution, and 100 µl of biotinylated detection antibody were added to each well. After incubating for 1 h at RT with gentle shaking, the plate was washed again, and 100 µl of HRP-Streptavidin solution were added to each well. The plate was incubated for 45 min at RT with gentle shaking and washed before adding 100 µl of stabilized chromogen, tetramethylbenzidine (TMB) reagent to each well. After a 30 min incubation at RT with gentle shaking in darkness, 50 µl of stop solution were added and the plate was read immediately in a fluorimeter at 450 nm. The standard curve was obtained plotting the standard concentration (pg/ml) on the x-axis and absorbance on the y-axis. All the solutions and the protocol mentioned in this section come in the kit from Preprotech and Invitrogen.

14. Single molecule array (SiMOA).

The levels of human $A\beta_{1-42}$ and $A\beta_{1-40}$ were quantified in CSF using the High Single Molecule Array (SiMOA) Amyloid Tau, Aβ42 and Aβ40 kits from Quanterix called SIMOA Neurology 3-plex advantage kit (#101995). Samples were prepared according to the manufacturer's instructions.

15. Image acquisition and analysis.

15.1. Image acquisition.

15.1.1. Immunofluorescence images.

Images were acquired by Leica TCS STED CW SP8X confocal microscope using a 63X oil-immersion objective. Except in two cases: first, fluorescence immunostaining preparations from *ex vivo* cultures in 5XFAD model were visualized by Leica TCS STED CW SP8X confocal microscopy of Imperial College London microscopy facility using a 20X objective; and second, for the quantification of $Iba1^+$ microglia cell number *in vitro*, 3D Histech Pannoramic MIDI II slide scanner was used to scan of the immunofluorescence coverslips with Iba1 staining.

In experiments with multiple fluorophores, channels were scanned sequentially to avoid crosstalk. The same settings were applied to all images within the same experiment.

When the expression of a protein was analyzed inside the microglia (6E10, OSTM1, TFEB and LAMP1), the image was acquired with zoom 2x, both in case of *in vitro* and *in vivo* experiments.

15.1.2. Two-Photon Time-Lapse Imaging.

Microglia dynamics were imaged via two-photon time-lapse microscopy in organotypic cortical slices from $Cx3Cr1^{+/eGFP}$ mice, where microglia and monocytes display green fluorescence (Jung et al., 2000). Live imaging was performed at a continuous perfusion of medium at 37ºC bubbled with 95% O_2 and 5% CO_2, at a depth of 50-80 μm below the surface of the slice. Laser power was adjusted to 3% of its

maximum power at 920 nm, corresponding to 9 mW, well within the intensities used by others (Pfeiffer et al., 2016; Madry et al., 2018). For imaging of microglial surveillance (baseline surveillance), stacks of 20 slices (z-step 2 μm) were acquired every 60 sec. Images were typically 512 x 512 pixels and covered a square field of view 200 to 250 μm wide.

16. Image analysis.

16.1. Immunofluorescence image analysis.

Most of the image analysis was carried out by Fiji-ImageJ. All the images were background corrected.

Protein (6E10, Synaptophysin, Homer, TFEB, OSTM1 and LAMP1) expression levels were quantified in Iba1$^+$ microglia in microglia and neuronal-microglial cultures. ROIs (region of interest) were created around each Iba1$^+$ cell and fluorescence was measured within these ROI. A threshold was applied to discard background signal. Next, the mean gray value of each target protein was measured inside the ROIs and normalized to the area measured to calculate the average intensity.

In case of LAMP1 analysis, a filter based on the median signal was applied to the signal to discriminate background and all the signal outside the ROI was deleted. Next, default threshold available in Fiji-ImageJ was applied. “Analyze particles” function was used to identify the number, area and size of LAMP1$^+$ signal spots. In this case, this procedure was done due to characteristic and define labelling of LAMP1 to quantify number, area and size.

For TFEB staining analysis, ROIs of Iba1$^+$ and DAPI$^+$ staining were created to dissect cells and TFEB staining intensity was measured in total cell area, nuclear area and cytoplasmatic area. In the case of the cytoplasmatic area, there is an option named XOR in the “ROI manager” of Fiji-ImageJ that selects the area between 2 ROIs, in this case, the Iba1 ROI and the DAPI ROI. Each mean gray value was normalized by its own area value. For the MCSF *in vivo* treatment experiments, for this same analysis, z-stack of 10 slices was needed to reconstruct entire microglia with the Iba1 and DAPI staining maximal projection.

A macro designed by Dr. Jorge Valero was used to quantify synaptic marker staining in distal neuronal processes or neurites in primary neurons as a measure of synaptic damage. 20x4 µm ROIs were fixed in the image with the help of a rotable tool to localize properly the ROI in the corresponding neurite orientation and then, integrated density value was calculated for each ROI.

Iba1$^+$ microglia cell numbers for each coverslip were quantified manually using Case viewer software (3HDHistech Pannoramic MIDI II).

In 5XFAD model *ex vivo* experiments, maximal projection of z-stacks from two channels (on the one hand, IBA1 and DAPI and on the other hand, GFAP and DAPI) was created with a custom-made macro provided by the laboratory of Dr. Magdalena Sastre. Then, the area (µm^2) of both channels was measured using the area quantification FL module in the HALO software (Indico Labs) and finally, a ratio of both areas was calculated as a percentage of the Iba1 or GFAP staining area normalized by the nuclei area.

Iba1 staining was measured in rat cortical organotypic slices, fixing a threshold and calculating the area fraction by Fiji-ImageJ.

Quantification of Iba1 and GFAP staining in the MCSF *in vivo* treatment was based on a previous published quantification protocol (Young and Morrison, 2018). First, z stack of 10 slices were converted to maximum intensity projection by Fiji-ImageJ of Iba1 and GFAP staining independently. In this analysis, 2 different quantification process were carried out: skeleton analysis and Fraclac analysis. For the skeleton analysis, 8-bit binary skeletonized image of individual cells was needed, and the quantification was carried out with the Fiji-ImageJ plugin named “AnalyzeSkeleton (2D/3D)”. In this case we compared the data obtained by Fiji-ImageJ of total length, branches, junctions, and triple points of the skeleton of Iba1$^+$ cells between the analyzed groups. These parameters give information about the spread and process complexity of the cells. For Fraclac analysis, images of individual cells were binarized and converted in outlined form, and the quantification was carried out with the Fiji-ImageJ plugin. In this case we compared density (number of pixels of foreground color divided by the total number of pixels in the convex hull) and span ratio (a measure of shape, as ratio of major and minor

axes for the convex hull) of outlined cells between the analyzed groups (3xTg-AD treated with vehicle and MCSF).

Thioflavin-S staining was measured in tyled scans acquired on organotypic brain slices using an Eclipse E600 Nikon. Then, a ROI of the subiculum area was created in each slice, a threshold of Thioflavin-S staining was fixed and the % area (area of the staining normalized by the total area) was calculated by Fiji-ImageJ.

16.2. Microglia analysis.

For microglia analysis, a maximum intensity projection was generated, and a fluorescence intensity profile was captured by drawing through the longest dimension of the cell body and across a cross-section of the outer most tips of all associated processes (Figure 9). This intensity profile was then used to estimate the soma size as well as the number and area of processes using custom written code in MATLAB currently used in Madgalena Sastre's laboratory at Imperial College London. Soma size was estimated by normalizing the portion of the fluorescence trace corresponding to soma to the background and then calculating the area under the curve for this section by multiplying the fluorescence peak by the width. The number of branch processes was estimated by using a custom written code (MATLAB) to detect peaks that were 25% greater than background (threshold derived from visual inspection). These peaks were then used to estimate the process area, which was calculated by adding the area under each fluorescence peak. Finally, the total process perimeter was calculated by adding the total number of pixels covered by all detected peaks and dividing this number by the scaling factor of the image (pixels/µm).

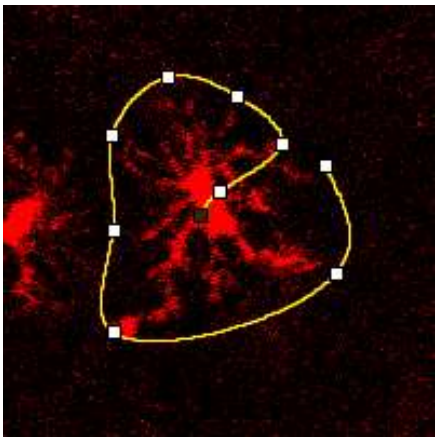

Figure 9. Microglial morphology quantification in organotypic slices. Schematic illustration of an intensity profile drawn through the microglial soma and around the cell perimeter, capturing the number and area of processes along with microglial soma size.

16.3. Image analysis of time-lapse recordings.

Image processing and analysis was performed in Fiji-ImageJ (Schindelin et al., 2012). A pre-processing of images was performed using a series of custom scripts (Nikolic et al., 2018). Time-lapse two-photon microscopy images were captured as individual z-stacks (xyz), concatenated as hyperstacks (xyzt) and registered to minimize drift. Individual cells were then cropped, and background fluorescence was corrected through a difference of Gaussians filter. For motility analysis, a custom macro (Available at https://github.com/SoriaFN/Microglia_tools) was used to binarize the images and quantify the territory surveyed by each microglial cell. Cumulative area was then monitored through at least 20 minutes (t-step = 1 min). To estimate the ratio of change in motility, we quantified the initial slope of the cumulative area curve, i.e. the difference in cumulative territory from the first two frames. We also compared the total cumulative territory surveyed by microglia in each condition.

The binary images obtained from the motility analysis were also used to analyze morphology of GFP^+ microglia. From the hyperstacks, frame number 5 was extracted to analyze as the representative point of each condition. Binary images were skeletonized and analyzed by Sholl analysis using the "Neuroanatomy" plugin in Fiji-ImageJ (starting radius = 5 µm, ending radius 50-100 µm, step size 1 µm). The comparison between conditions was done with the area under curve of the data.

17. Statistical analysis.

Measurements are expressed as mean ± S.E.M (Standard error of the mean) and scaled that the average value for the corresponding control was 100%. Statistical analyses were performed comparing raw data or fold change value between conditions using with GraphPad Prism 8 software (Graph Pad Software). Raw data values were analyzed when data belong to independent experiments performed at the same conditions and the same time, and fold change value were analyzed when data belong to experiments performed at the same conditions but at different time. All data sets were tested for normality and homoscedasticity. Paired or not paired two-tailed Student's t-test or One-way ANOVA test were applied and corrections (Bonferroni and Sidak) were applied depending on the sample characteristics. Statistical significance was represented as $p<0.05$ (*), $p<0.01$ (**), $p<0.001$ (***) and $p<0.0001$ (****).

Results

Soluble forms of Aβ, rather than the large insoluble fibrils localized in plaques, are the main toxic species (Masliah et al., 1991; Cline et al., 2018) and appear soon after the onset of AD (Selkoe, 2002). Moreover, Aβ can activate microglia in early stages of the disease (Lautner et al., 2011), indeed, as the disease progresses microglia surround amyloid plaques (Nicoll et al., 2003). However, microglia are not able to eliminate Aβ unless are activated by immunotherapy (Wilcock, 2004) or the action of cytokines such as MCSF (Majumdar et al., 2007). Thus, it is still in debate which is the role of microglia in AD progression. In this thesis project we will study the role of MCSF-activated microglia in the context of AD.

1. Role of MCSF and oligomeric Aβ on microglial transcriptomic and proteomic profile.

1.1. Characterization of Aβ species and the use of MCSF for *in vitro* experiments.

Experimental models of AD typically use synthetic Aβ peptides. In this thesis project we have used oligomeric forms of Aβ to evaluate early amyloid-related pathology in different *in vitro* and *ex vivo* models. First, we assessed that our protocol was specific for oligomeric, non-fibrillar, Aβ. We prepared both oligomers and fibrils following the protocol detailed in experimental procedures (section 4) (Dahlgren et al., 2002) and visualized them by electron microscopy. Accordingly, we observed Aβ in the oligomeric (Figure 10A) and fibrillar (Figure 10B) forms in these preparations. Then, we evaluated the toxicity of different concentrations (0.5, 1, 2, 3, 5μM) of oAβ applied to both primary neurons and microglia for 24 h. We observed neuronal toxicity at 2 μM of oAβ for 24 h (a viability reduction of 2.6±1.5%, *$p<0.05$) compared with control (Figure 10C); however, there was no viability reduction in neither of the concentrations used on microglia compared with the control condition (Figure 10D). Therefore, we confirm that our preparation contains mainly oligomers and that the optimal concentration for our *in vitro* experiments with neurons and microglia is 1 μM oAβ as the viability of the cell types is not compromised.

Since we are going to study the role of MCSF-activated microglia in the context of AD, we also tested different concentrations of MCSF in neurons and microglia. Previous publications showed that 25 ng/ml of MCSF could activate microglia to

efficiently degrade fibrillar Aβ (Majumdar et al., 2007, 2011). We treated primary neurons and microglia separately with 25, 50 and 100 ng/ml for 24 h and performed a viability assay. According to the results, there is no toxicity induced by MCSF neither in neurons nor in microglia at these conditions (Figures 10E and 10F, respectively).

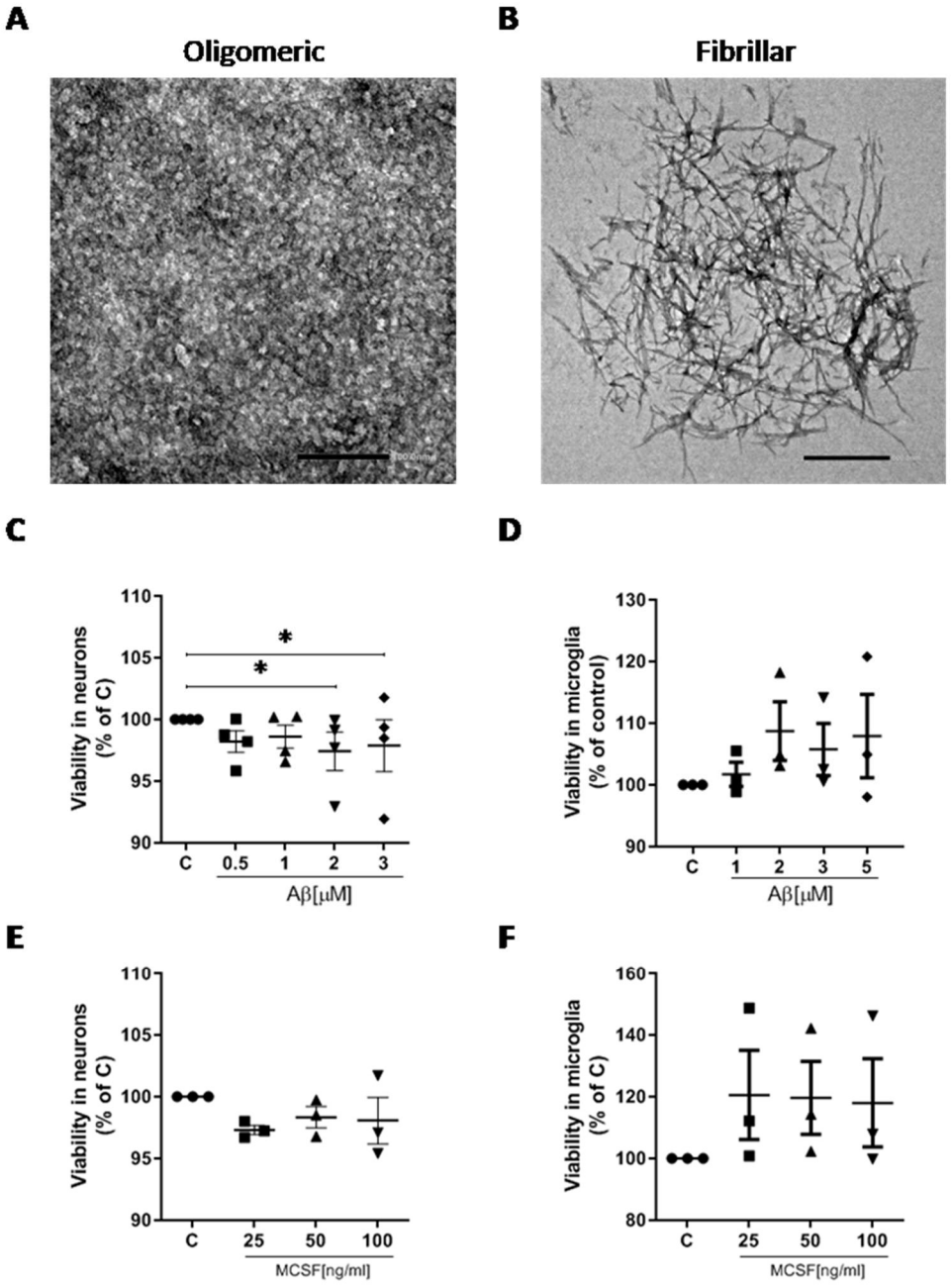

Figure 10. Characterization of Aβ species and the use of oAβ and MCSF for *in vitro* experiments. Representative images of oligomeric (A) and fibrillar (B) forms of synthetic $A\beta_{1-42}$ observed by electron microscopy. Quantification of the viability assay of oAβ at 0.5, 1, 2, 3 and 5 μM for 24 h in neurons (C) and microglia (D) (N=4 and N=3, respectively). Quantification of the viability assay of MCSF at 25, 50 and 100 ng/ml for 24h in neurons (E) and microglia (F) (N=3). Scale bar in A is 100 nm and in B is 500 nm. Bars indicate means ± SEM. Statistical differences between groups were assessed by repeated measures One-way ANOVA with Bonferroni correction. *p<0.05 compared with control cells.

1.2. MCSF promotes the expression of microglial receptor and inflammation associated genes.

Once we established the subtoxic concentrations of both oAβ and MCSF in microglia, we performed a transcriptomic analysis of genes belonging to the categories of microglia receptors, inflammation, complement system, lysosomal biogenesis, and secreted degrading enzymes (Table 4). Microglial expression of these genes is altered in AD (reviewed at the introduction section), and therefore, we studied how oAβ (1 μM) and MCSF (25 ng/ml) modify their expression in microglia cultures.

Table 4. List of the genes included in the transcriptomic analysis in primary microglial cultures.

Category	Gene
Microglial receptors	CSF-1R, CD33, CD36, CD40, CD74, MRC1, MSR1, AGER, ITGAM, ITGB2 and Tyrobp.
Inflammation	TNFα, IL-1β, STAT1, IRF8, MCSF1, IL-10, TGFβ1 and TGFβ3.
Complement system	C1qA, C1qB, C1qC, C2, C3 and C4a.
Lysosomal biogenesis	LAMP1, OSTM1, TFEB and MITF.
Secreted degrading enzymes	IDE, MMP2, MMP9 and PLAT.

First, we analyzed the expression of microglial receptors and adaptor genes in our *in vitro* model, to evaluate microglial activation upon oAβ and/or MCSF administration. We measured the expression of these genes by RT-PCR in isolated murine primary microglia treated with or without 1 μM oAβ and/or 25 ng/ml MCSF during 24 h. The following genes were analyzed: macrophage colony-stimulating factor receptor 1 (CSF-1R); cluster of differentiation 33 (CD33); cluster of differentiation 36 (CD36); cluster of differentiation 40 (CD40); cluster of differentiation 74 (CD74); mannose receptor c type 1 (MRC1), macrophage scavenger receptor 1 (MSR1), advance glycosylation end-product specific receptor (AGER), integrin subunit αM (ITGAM), integrin subunit β2 (ITGB2) and transmembrane immune signaling adaptor (Tyrobp) (Table 4). Our results showed that 1μM oAβ did not modify the expression of these

microglia receptor genes compared with control condition (Figure 11). However, MCSF induced the upregulation of CD36 (17.36±4.27 fold change (fc), **p<0.01), MSR1 (3.94±0.59fc, *p<0.05), ITGAM (1.96±0.19fc, *p<0.05), TYROBP (1.46±0.096fc, *p<0.05) and a tendency to increase of CD40 (3.35±0.90fc, p=0.07) and ITGB2 (1.92±0.19fc, p=0.06) compared with control condition (1fc) (Figure 11). oAβ did not significantly change the effects of MCSF on the expression of these genes. Moreover, there was a significant increase in microglia cotreated with oAβ and MCSF in the case of CD36 (15.56±3.89fc, **p<0.01), CD40 (3.35±0.90fc, *p<0.05), MSR1 (3.14±0.47fc, **p<0.01) and ITGAM (1.81±0.17fc, **p<0.01) compared with oAβ alone [CD36 (1.19±0.14fc), CD40 (1.11±0.13fc), MSR1 (1.05±0.06fc) and ITGAM (0.96±0.05fc), respectively]. CSF-1R, CD33, CD74, MRC1 and AGER genes expression did not change with oAβ and/or MCSF treatment compared with the control condition (Figure 11). These results suggest that MCSF promotes the expression of microglial receptors *in vitro* and that oAβ does not significantly interfere with this effect.

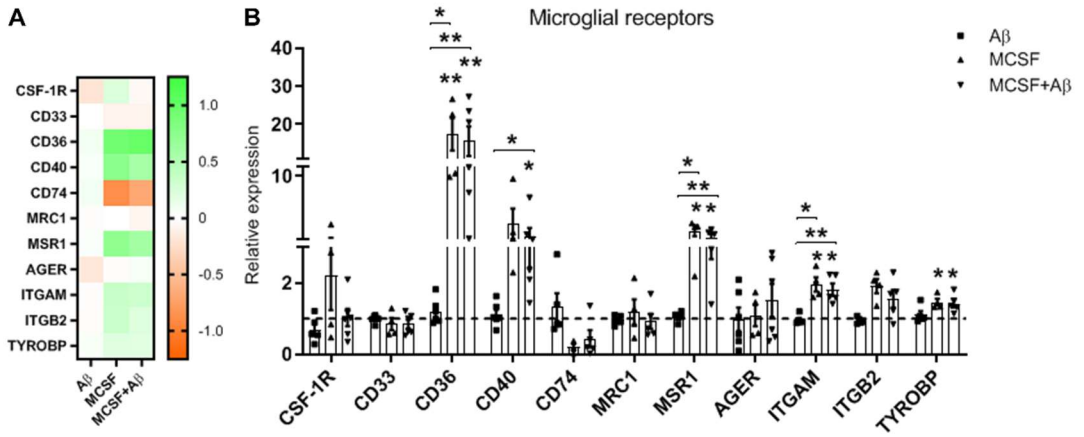

Figure 11. Effect of MCSF and oAβ treatments on microglial receptor genes. (A) Heatmap and (B) quantification of relative expression of CSF-1R, CD33, CD36, CD40, CD74, MRC1, MSR1, AGER, ITGAM, ITGB2 and Tyrobp genes in primary microglia treated with oAβ and/or MCSF during 24h measured by RT-PCR (N=6). Data is represented in heat map (upregulated genes in green and downregulated genes in orange) and in graph indicate means ± SEM. In the graph the control condition is represented as a horizontal dashed line. Statistical differences between groups were assessed by repeated measures One-way ANOVA with Sidak correction. *p<0.05, **p<0.01 compared with control cells.

Next, we measured the expression of downstream genes classified in four categories (Table 4): 1) inflammation (genes that encode tumor necrosis α, TNFα; interleukin 1β, IL-1β; interleukin 6, IL-6; signal transducer and activator of transcription 1, STAT1; interferon regulatory factor 8, IRF8; macrophage colony-stimulating factor 1,

MCSF1; interleukin 10, IL-10; transforming growth factor β1 and β3, TGFβ1 and TFGβ3); 2) complement system (three genes that encode complement factor 1q (C1QA, C1QB, C1QC), and genes that encode complement factor 2, C2; complement factor 3, C3; and complement factor 4, C4A); 3) lysosomal biogenesis (genes that encode lysosomal-associated membrane protein 1, LAMP1; osteopetrosis-associated transmembrane protein 1, OSTM1; transcription factor EB, TFEB; and microphthalmia-associated transcription factor, MITF); and 4) secreted degrading enzymes (genes that encode insulin degrading enzyme, IDE; matrix metallopeptidase 2, MMP2; matrix metallopeptidase 9, MMP9; and plasminogen activator tissue type, PLAT).

As we did for the receptors, we analyzed the expression of inflammatory genes by RT-PCR in isolated primary microglia treated with or without 1 μM oAβ and 25 ng/ml MCSF during 24 h. Results showed that 1μM oAβ treatment caused a reduction of IL-10 gene expression (0.79±0.06fc, *p<0.05) compared with control condition (1fc) (Figure 12). No differences were observed in the expression of TNFα, IL-1β, IL-6, STAT1, IRF8, MCSF1, TGFβ1 and TGFβ3 genes treated with oAβ compared with the control condition (Figure 12). On the other hand, MCSF treatment induced significant upregulation of TNFα (6.24±2.19fc, *p<0.05), IL-6 (3.99±0.81fc, *p<0.05) and TGFβ1 (1.86±0.17fc,*p<0.05) and a trend to increase in case of IL-1β (2.09±0.71, p=0.37) genes compared with the control (1fc), and that the presence of oAβ did not alter significantly this effect (Figure 12). On the contrary, IL-10 gene expression was reduced with MCSF (0.22±0.05fc, *p<0.05) and MCSF+oAβ (0.25±0.04fc, ***p<0.001) treatment compared with control condition (1fc). Besides, there were significant changes in oAβ and MCSF cotreatment for TNFα (5.35±1.22fc), IL-10 (0.25±0.04fc) and TGFβ1 (1.96±0.11fc) relative to oAβ treatment [TNFα (1.17±0.17fc), IL-10 (0.78±0.05fc) and TGFβ1 (1.19±0.17fc), respectively] (Figure 12). These data indicates that MCSF treatment induced changes of microglial inflammatory profile in vitro by upregulating pro-inflammatory and anti-inflammatory cytokines such as TNFα, IL-6 and TGFβ1, and downregulating IL-10 anti-inflammatory cytokine expression and that the presence of oAβ does not interfere significantly with these modifications.

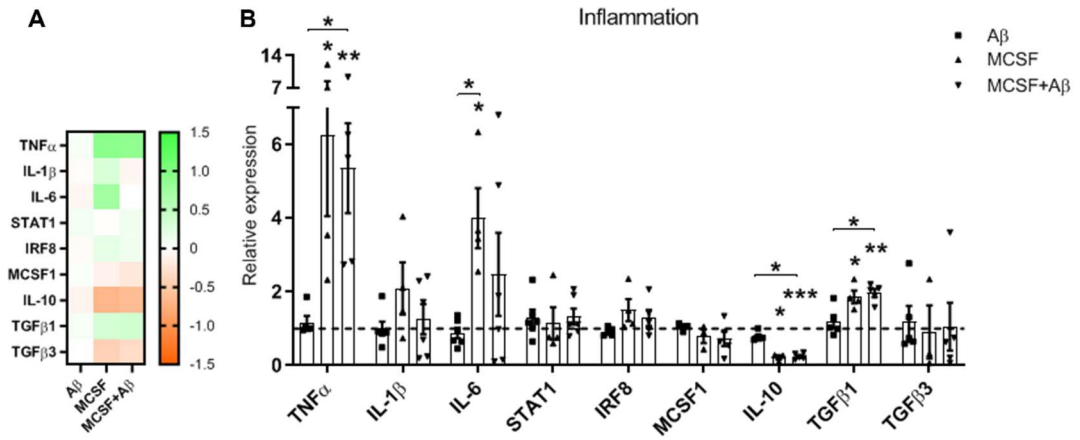

Figure 12. Effect of MCSF and oAβ treatments on inflammatory genes. (A) Heatmap and (B) quantification of relative expression of TNFα, IL-1β, STAT1, IRF8, MCSF1, IL-10, TGFβ1 and TGFβ3 genes in primary microglia treated with oAβ and/or MCSF during 24 h measured by RT-PCR (N=6). Data is represented in heat map (upregulated genes in green and downregulated genes in orange) and in graph indicate means ± SEM. In the graph the control condition is represented as a horizontal dashed line. Statistical differences between groups were assessed by repeated measures One-way ANOVA with Sidak correction. *p<0.05, **p<0.01, ***p<0.001 compared with control cells.

In the case of complement system, oAβ treatment alone did not modify the expression of any of the studied genes. MCSF treatment significantly downregulated C2 expression (0.46±0.06fc, *p<0.05) compared with control condition (1fc) and showed a tendency to reduce in the case of C3 and C4a relative to control condition. Also, there were significant differences in C3 gene expression following oAβ treatment (0.97±0.12fc, *p<0.05) and MCSF+oAβ cotreatment (0.60±0.14fc, p=0.10) (Figure 13). In conclusion, MCSF reduces the expression of C2 and C3, an effect that is not significantly modified by oAβ.

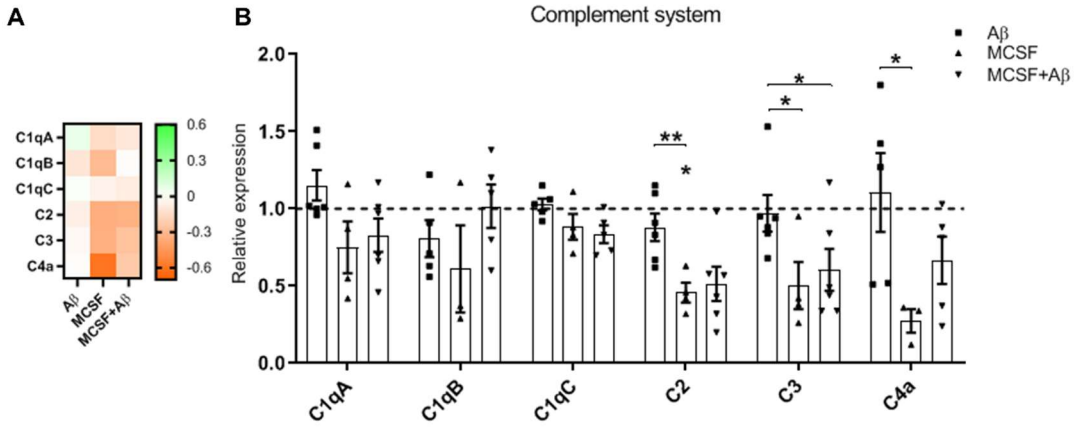

Figure 13. MCSF reduces the expression of C2 and C3, and oAβ does not modify these changes. (A) Heatmap and (B) quantification of relative expression of C1qA, C1qB, C1qC, C2, C3 and C4a genes in primary microglia treated with oAβ and/or MCSF during 24 h measured by RT-PCR (N=6). Data is

represented in heat map (upregulated genes in green and downregulated genes in orange) and in graph indicate means ± SEM. In the graph the control condition is represented as a horizontal dashed line. Statistical differences between groups were assessed by repeated measures One-way ANOVA with Sidak correction. *p<0.05, **p<0.01, ***p<0.001 compared with control cells.

In lysosomal biogenesis category, neither oAβ nor MCSF treatments showed significant modification of the expression of LAMP1, OSTM1, TFEB and MITF. Interestingly, MCSF induced an increase in TFEB gene expression. However, this difference in gene expression relative to control was not statistically significant. LAMP1, OSTM1 and MITF gene expression did not significantly vary among the different conditions (Figure 14).

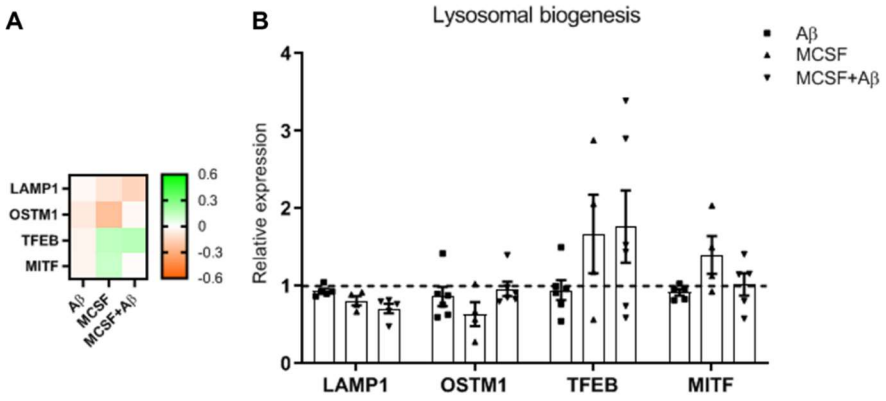

Figure 14. MCSF and oAβ treatments do not modify the expression of genes associated with lysosomal biogenesis. (A) Heatmap and (B) quantification of relative expression of LAMP1, OSTM1, TFEB and MITF genes in primary microglia treated with oAβ and/or MCSF during 24 h measured by RT-PCR (N=6). Data is represented in heat map (upregulated genes in green and downregulated genes in orange) and in graph indicate means ± SEM. In the graph the control condition is represented as a horizontal dashed line. Statistical differences between groups were assessed by repeated measures One-way ANOVA with Sidak correction.

In the group of secreted degrading enzymes, as was the case for genes associated with lysosomal biogenesis, neither oAβ nor MCSF treatments induced any significant changes in gene expression. MCSF induced an increase in the expression of IDE and MMP9 genes, albeit statistically non-significant, relative to control condition (Figures 15). In conclusion, these results show that neither Aβ oligomers nor MCSF treatments were able to modify the expression of genes associated with lysosomal biogenesis or extracellular enzymatic degradation in our *in vitro* microglia model.

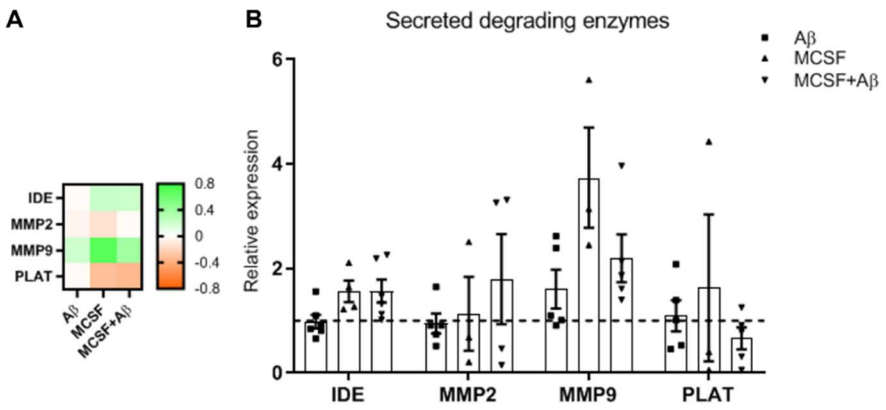

Figure 15. Neither MCSF nor oAβ treatments modified the expression of Aβ-related secreted degrading enzymes. (A) Heatmap and (B) quantification of relative expression of IDE, MMP2, MMP9 and PLAT genes in primary microglia treated with oAβ and/or MCSF during 24 h measured by RT-PCR (N=6). Data is represented in heat map (upregulated genes in green and downregulated genes in orange) and in graph indicate means ± SEM. In the graph the control condition is represented as a horizontal dashed line. Statistical differences between groups were assessed by repeated measures One-way ANOVA with Sidak correction.

Overall, the transcriptomic analysis shows that 1 μM oAβ treatment does not modify the expression of genes related to microglial receptors, inflammation, complement system, lysosomal biogenesis, and secreted degrading enzymes. MCSF does alter the expression of microglial receptors, inflammation and complement systems, oAβ does not significantly alter the effects induced by MCSF treatment.

1.3. Oligomeric Aβ partially reverts the expression of MCSF-promoted microglial receptors.

Following our study on gene expression, we next evaluated the effect of oAβ and/or MCSF treatments on protein levels. To do so, we incubated primary microglia cultures with 1 μM oAβ and/or 25 ng/ml MCSF for 24 h. Following treatment, we prepared cell lysates and measured protein expression levels by Western blot. As per our earlier transcriptomic results, we measured protein expression levels of microglial receptors CD36, MSR1, CD11b (protein encoded by ITGAM gene), CD18 (protein encoded by ITGB2 gene), adaptor protein Tyrobp and CSF-1R. Even though CSF-1R gene expression did not vary upon MCSF and oAβ exposure, we opted for measuring its protein levels too.

We first evaluated the effect of oAβ on the protein expression of CSF-1R, CD36, MSR1, CD11b, CD18 and Tyrobp and we observed that oAβ treatment did not modify the amount of these proteins being produced in the microglia (Figure 16). This result confirmed transcriptomical data, where no significant changes were observed in gene expression following oAβ treatment. When evaluating the effect of MCSF treatment alone, there was a significant reduction in the protein expression of CSF-1R (33.92±10.33%, *p<0.05) and CD36 (26.95±6.13%, ***p<0.001) relative to control condition (100%) (Figure 16A and 16B, respectively). In contrast, MCSF treatment induced an increase in the expression of MSR1 (182.30±20.23%, *p<0.05), CD11b (175.10±22.18%, *p<0.05), Tyrobp (192.7±22.48%, **p<0.01) and CD18, although the latter was not statistically significant (151.9±16.76%, p=0.0503) relative to control condition (100%) (Figures 16C-F). These differences in protein levels were no longer statistically significant when oAβ was added to MCSF during the incubation, specifically for CSF-1R (50.79±20.63%, p=0.32), CD36 (45.91±12.94%, *p<0.05), MSR1 (159.60±18.02%, p=0.10), CD11b (132.90±6.40%,**p<0.01), CD18 (131.80±13.15%, p=0.12) and Tyrobp (159.20±19.73%, p=0.08) relative to control condition (100%), with the exception of CD11b (132.90±6.40%, **p<0.01). Also, there was a significant reduction of CSF-1R protein expression between MCSF+Aβ condition (50.79±20.63%) and Aβ condition (112.0±8.09%, *p<0.05) (Figure 16). These results indicate that MCSF changes protein expression of CSF-1R, CD36, MSR1, CD11b/CD18 (CR3) and Tyrobp and oAβ attenuates this effect.

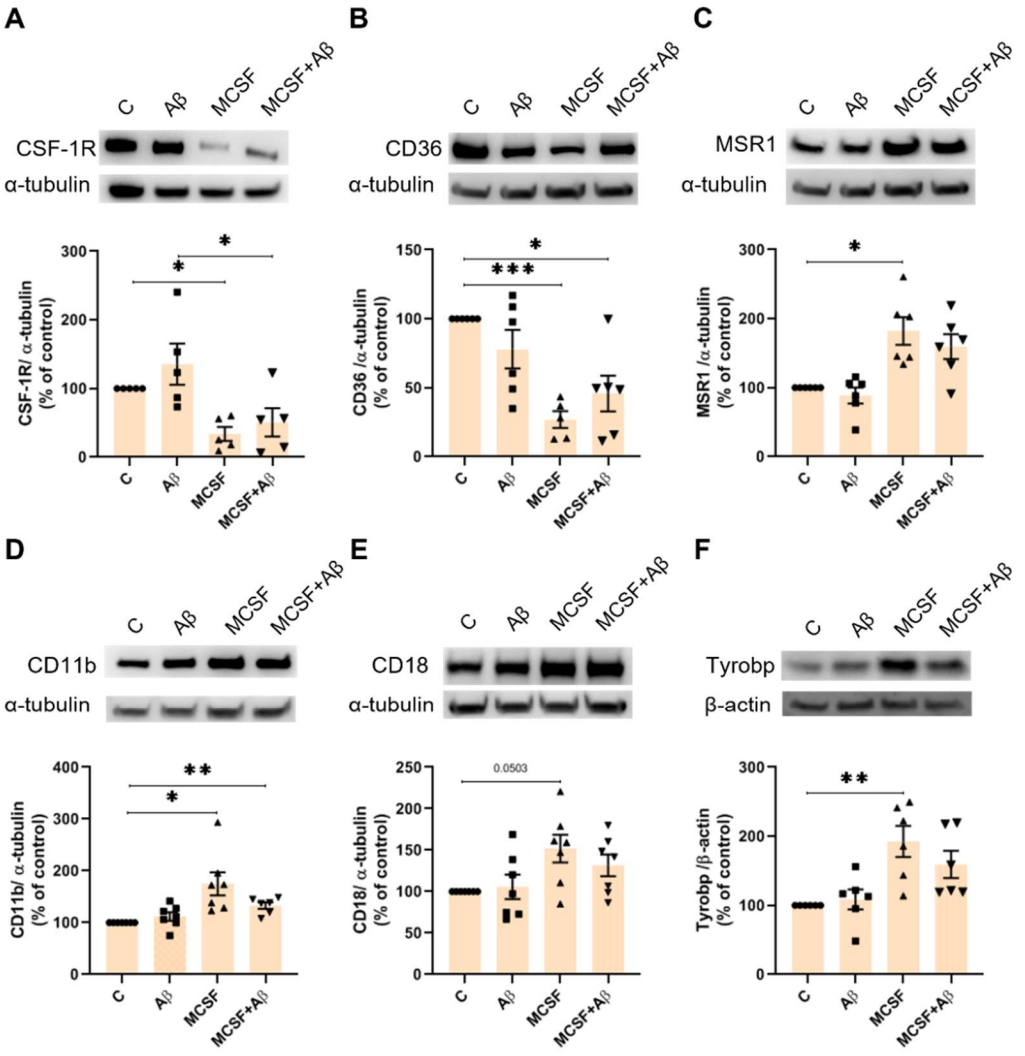

Figure 16. Effect of MCSF and oAβ in the protein expression of microglial receptors and adaptor Tyrobp. Representative image and quantification of protein expression of CSF-1R (A), CD36 (B), MSR1 (C), CD11b (D), CD18 (E) and Tyrobp (F) in primary microglia treated with oAβ and/or MCSF during 24 h measured by Western blot (N=5-7). Bars indicate means ± SEM. Most of the protein levels are normalized by α-tubulin signal except for Tyrobp. Statistical differences between groups were assessed by repeated measures One-way ANOVA with Sidak correction. *p<0.05, **p<0.01, ***p<0.001 compared with control cells.

1.4. MCSF treatment induces CSF-1R downregulation.

Our proteomic study revealed that even though we did not see differences at the transcriptomic level, the expression of the CSF-1R protein level was reduced in microglia upon MCSF treatment. To further characterize MCSF/CSF-1R interaction, we first evaluated whether other cell types expressed CSF-1R. Quantification of the expression of CSF-1R in neurons, microglia, and astrocytes at physiological conditions revealed that only primary microglia expressed CSF-1R in detectable amounts (Figure 17A). We evaluated the expression of CSF-1R both in neuronal-microglial co-cultures and

organotypic cultures in the presence and absence of MCSF and oAβ. We treated neuronal-microglial co-cultures and cortical organotypic cultures with 1 μM oAβ and/or 25 ng/ml MCSF during 24 h. As was the case for microglia primary culture, oAβ did not alter the expression levels of CSF-1R. However, MCSF treatment did decreased CSF-1R expression both in neuronal-microglial co-cultures (24.7±5.28%, ***p<0.001) and in organotypic cultures (54.72±6.52%, *p<0.05) relative to control condition (100%) (Figures 17B and 17C). This effect was preserved, through attenuated, when oAβ was added to MCSF in the incubation media in the neuronal-microglial co-cultures (41.05±12.34%, *p<0.05), but not in the organotypic cultures (76.7±15.37%, p=0.65) (Figures 17B and 17C).

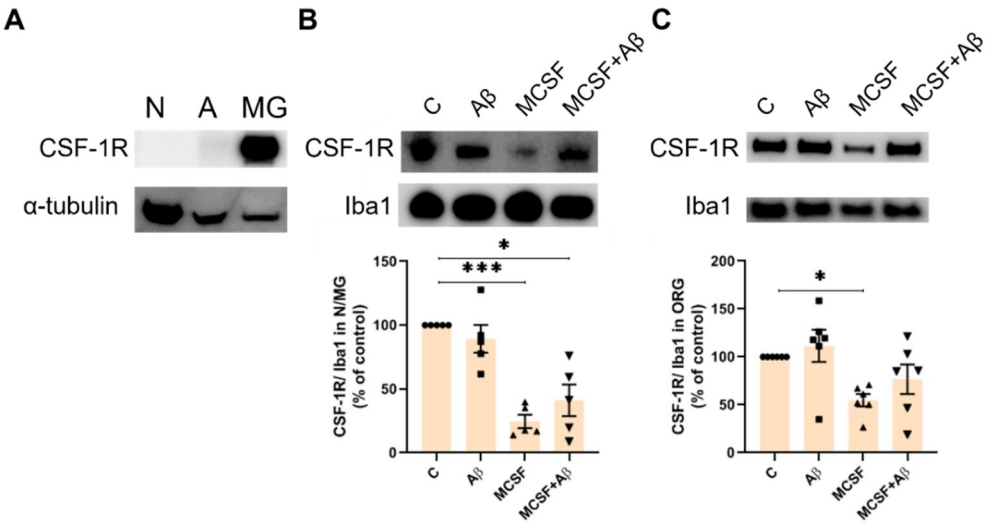

Figure 17. CSF-1R levels decrease in microglia after MCSF treatment in microglia-neuron co-cultures and organotypic cultures. (A) Representative image of CSF-1R expression in neuron, astrocyte and microglia culture in physiological conditions. Representative image and quantification of protein expression of CSF-1R in neuronal-microglial co-culture (B) and organotypic culture (C) treated with oAβ and/or MCSF during 24 h measured by Western blot (N=5-6). Bars indicate means ± SEM. N: neurons, A: astrocyte, MG: microglia. Statistical differences between groups were assessed by repeated measures One-way ANOVA with Sidak correction. *p<0.05, ***p<0.001 compared with control cells.

The MCSF/CSF-1R complex is incorporated into the endosomal system, and eventually reaches late endosomal and lysosomal compartments, in which both ligand and receptor undergo enzymatic degradation (Guilbert and Stanley, 1986; Lee, 1999). To study the MCSF/CSF-1R axis *in vitro*, we incubated primary microglia cultures with 25 ng/ml MCSF for different times (5', 10', 30', 1h, and 24h) (Figures 18). After 30 min incubation, there was an already significant decrease in CSF-1R receptor levels

(59.71±4.51%, **p<0.01) and a 24 h incubation time led to a 50 % decrease in CSF-1R receptor levels (41.71±1.08%, ****p<0.0001) relative to control condition (100%). These data indicates that the presence of MCSF promotes CSF-1R degradation as earliest as 30 minutes after exposure, which is consistent with a rapid and dynamic activation of the of the MCSF/CSF-1R axis.

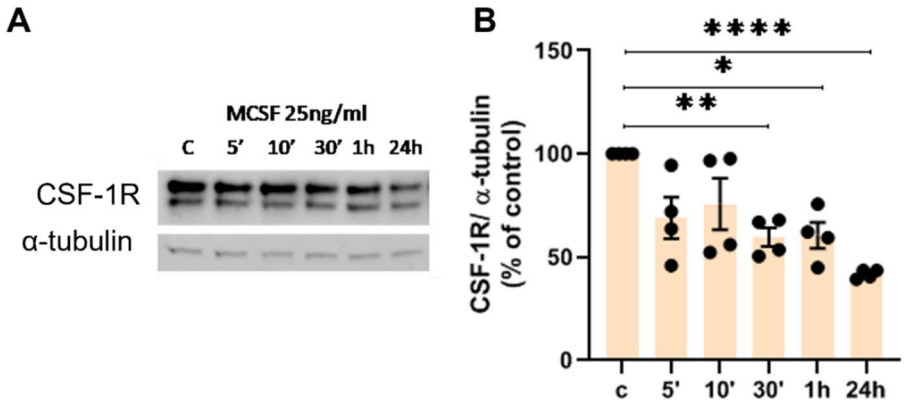

Figure 18. MCSF promotes CSF-1R reduction after 30 minutes. Representative measurement of protein levels (A) and quantification (B) of CSF-1R expression in primary microglia exposed to 25ng/ml MCSF for 5 min, 10 min, 30min, 1 h and 24 h measured by Western blot (N=4). Bars indicate means ± SEM. Statistical differences between groups were assessed by repeated measures One-way ANOVA with Sidak correction. *p<0.05, **p<0.01, ****p<0.0001 compared with control cells.

In summary, transcriptomic and proteomic studies show that incubation of various cellular models with MCSF induces changes in the gene expression and protein levels of CSF-1R, CD36, MSR1, CD11b/CD18 (CR3) and Tyrobp. In addition, MCSF modulates inflammatory cytokine expression towards a pro-inflammatory profile and downregulates genes of classical complement cascade proteins. Interestingly, oAβ alone does not modify the expression of those genes. In turn, in cotreatment with MCSF, oAβ does not alter the microglial response to MCSF.

2. MCSF-activated microglia internalize oAβ and prevent synaptic pathology *in vitro*.

2.1. MCSF promotes oAβ internalization by microglia.

Previous studies reported that MCSF treatment improved fibrillar Aβ degradation (Majumdar et al., 2007; Boissonneault et al., 2008). Whether MCSF modulates oAβ elimination has not yet been determined. Thus, we investigated how MCSF treatment affected internalization of oAβ by microglia in cell culture. To that aim,

we treated microglia primary cultures with 1 µM Aβ and with or without 25 ng/ml MCSF for 24 h and performed immunofluorescence staining with 6E10 antibody (against amino acid residue 1-16 of human Aβ) and Iba1 antibody (microglial marker) thereafter. MCSF treatment significantly increased 6E10 immunoreactivity in Iba1^{+} microglia (11.26±2.16fc, *p<0.05) relative to the unstimulated microglia (6.89±1.86fc) (Figures 19A and 19B). These results indicate that MCSF increases Aβ internalization by microglia.

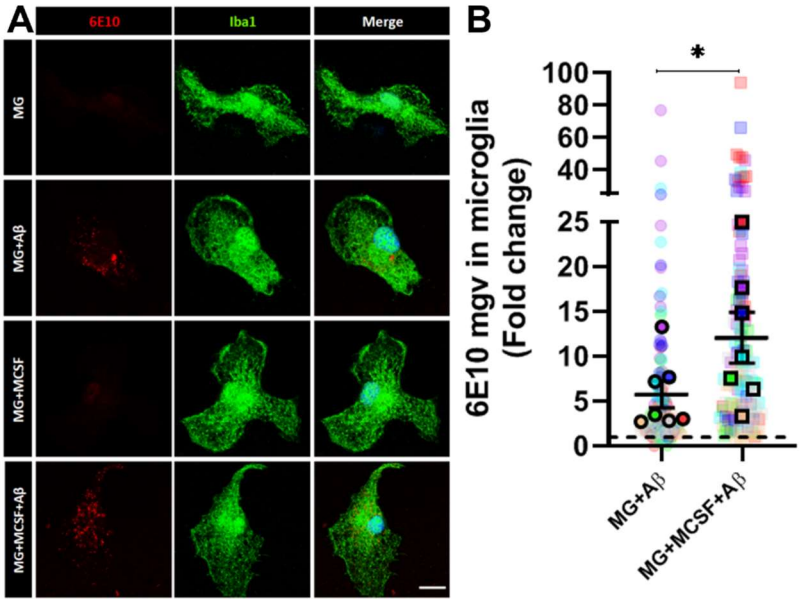

Figure 19. MCSF promotes oAβ internalization in microglia cultures. Representative image (A) and quantification (B) of 6E10 staining (red) inside Iba1^{+} cells (green) in microglia primary culture in presence of Aβ, with or without the addition of 25 ng/ml MCSF for 24h (N=7). Scale bar 10 µm. MG: microglia. Bars indicate means ± SEM and dots represent individual cells. In the graph the control condition is represented as a horizontal dashed line. Statistical differences between groups were assessed by paired repeated measures Student's t-test. *p<0.05, compared with control microglia.

The effect of MCSF treatment on oAβ internalization was also studied in rat neuronal-microglial co-cultures (1:10 ratio). We treated co-cultures with 1 µM Aβ and with or without 25 ng/ml MCSF for 24 h (Figure 20A). Double immunofluorescence staining with 6E10 and Iba1 antibodies showed that in presence of MCSF microglia internalized similar amount of oAβ compared with unstimulated neuronal-microglial co-culture (Figures 20A and 20B). These experiments indicate that microglia internalize Aβ in presence of neurons, but MCSF does not further increase the internalization.

We then examined extracellular oAβ levels in neuronal-microglial co-culture. We treated neuronal and neuronal-microglial co-cultures with oAβ in presence or absence of MCSF and measured oAβ$_{1\text{-}42}$ levels in supernatants by immunoprecipitation.

Measurements indicated that neuronal MCSF treatment did not reduce oAβ levels in neuronal primary cultures (Figures 20D and 20E). However, in neuronal-microglial co-cultures, there was a significant reduction in extracellular oAβ (39.13±4.81%, **p<0.05) compared with neuronal cultures (100%). This reduction was higher in the presence of MCSF (52.13±6.452%, **p<0.01) although not significant. In conclusion, the presence of microglia in the co-culture reduces extracellular Aβ levels and MCSF treatment tends to further reduce extracellular Aβ, although this observation was not statistically significant.

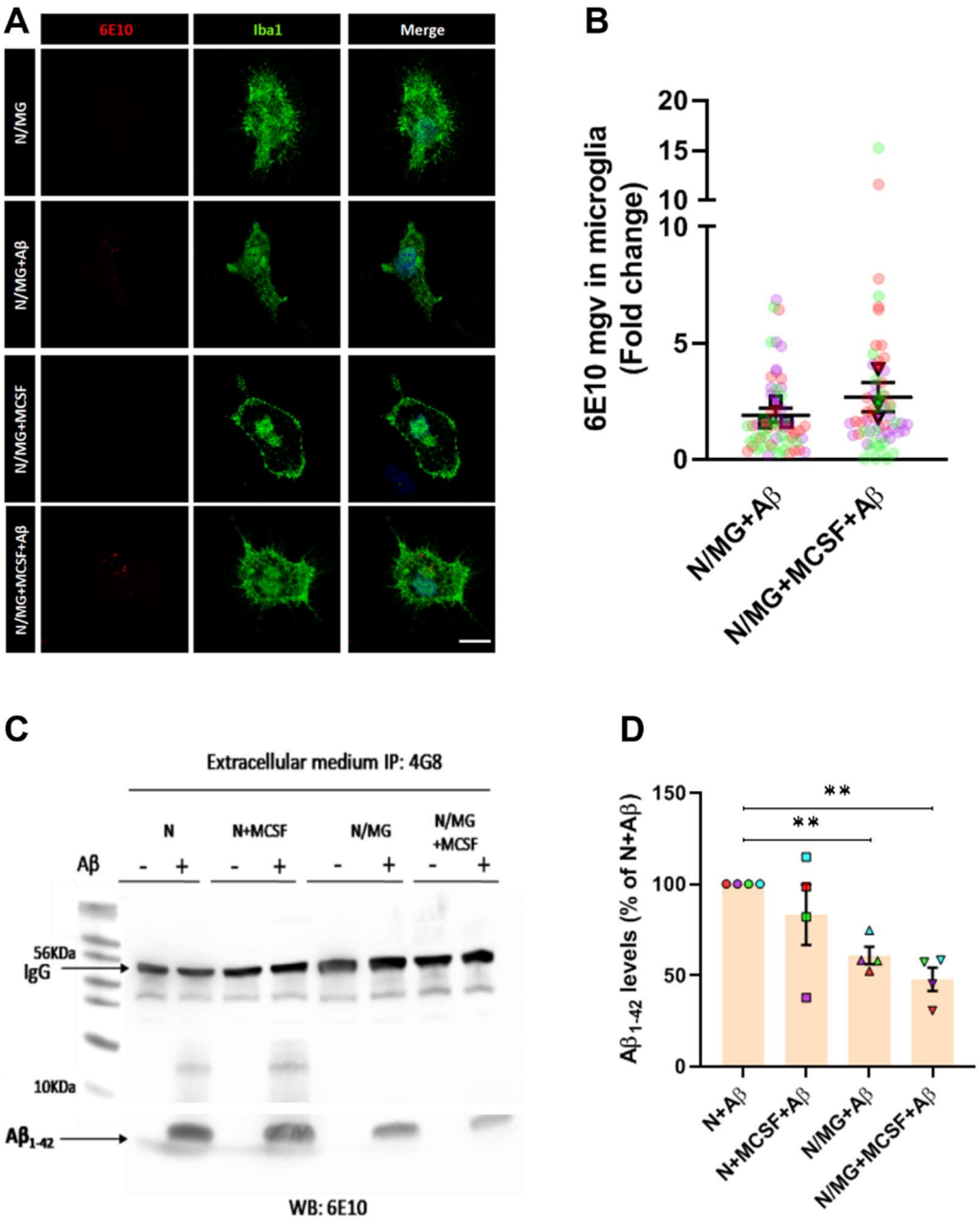

Figure 20. MCSF promotes extracellular Aβ elimination by microglia in neuronal-microglial co-culture. Representative microscopy image of 6E10 immunostaining (red) inside Iba1^{+} cells (green) in neuronal-microglia primary co-culture incubated with or without 25 ng/ml MCSF in presence of 1 µM Aβ (A and B) and extracellular oAβ$_{1-42}$ levels measured in neuronal and neuronal-microglial primary co-culture incubated with 1 µM Aβ and 25 ng/ml MCSF for 24 h determined by immunoprecipitation (N=4) (D and E). Scale bar 10 µm. N: neuron; N/MG: neuronal-microglial co-culture. Bars indicate means ± SEM and dots represent individual cells (B) and individual experiments (D). Statistical differences between groups were assessed by repeated measures One-way ANOVA with Bonferroni correction and Students's t-test. **p<0.01, compared with control cells.

As Smith et al. (2013) described, MCSF promotes microglial proliferation in adult human microglia. Thus, we evaluated the effect of MCSF on microglial proliferation in neuronal-microglial co-culture. We treated co-cultures with 25 ng/ml MCSF for 24 h and

measured Iba1^{+} immunoreactivity thereafter. Our data showed an increase in the number of Iba1^{+} cells per field following MCSF treatment (220.8±33.91%, *p<0.05) relative to control (100%) (Figures 21). Our data supports the proliferative effect of MCSF on microglia in neuronal-microglial co-culture.

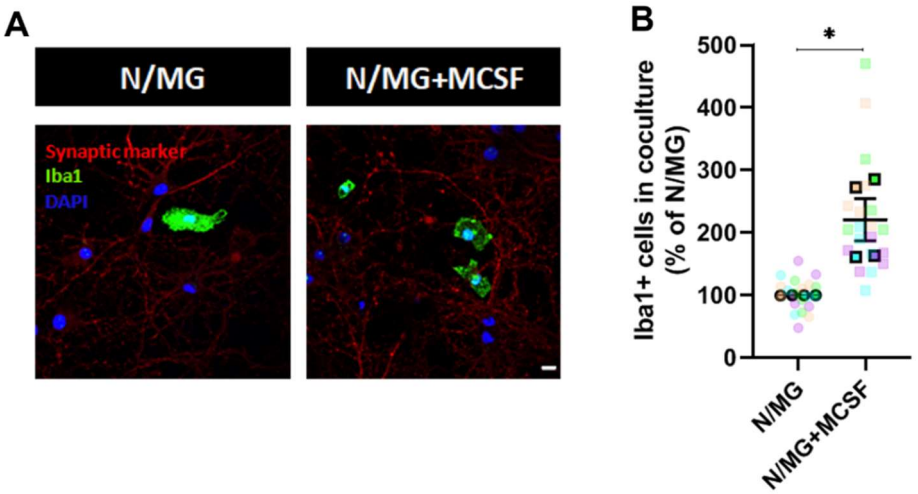

Figure 21. MCSF promotes microglial proliferation in neuronal-microglial co-culture. Representative image and quantification of Iba1^{+} (green) cells in neuronal-microglial primary co-culture treated with 25 ng/ml MCSF for 24 h relative to control (MCSF absence) (N=4). Scale bar 10 µm. N/MG: neuron/microglia co-culture. Bars indicate means ± SEM and dots represent individual fields. Statistical differences between groups were assessed by repeated measures Student's t-test. *p<0.05, compared with control cells.

In sum, microglia internalize synthetic oAβ both in primary cell cultures and in co-culture with neurons. Furthermore, MCSF treatment promotes microglial oAβ internalization and induces microglial proliferation in neuronal-microglial co-culture.

2.2. MCSF-activated microglia prevent oAβ-induced synaptic pathology *in vitro*.

MCSF treatment increases oAβ internalization and reduces extracellular oAβ. Next, we examined whether the reduction in extracellular oAβ ameliorates oAβ-induced synaptic pathology. For this purpose, we treated neuronal primary cultures with oAβ and/or MCSF and measured synaptophysin as presynaptic marker and homer as postsynaptic marker thereafter by immunofluorescence staining. Synaptophysin and homer immunofluorescence were specifically measured in neurites using a digital image analysis procedure developed for Fiji-ImageJ by Dr. Jorge Valero. This analysis is described in detail in the experimental procedures (subsection 16.1).

First, we confirmed, using our primary neuronal culture model, previous findings reporting that 1 µM oAβ-induced synaptic damage in primary neuronal cultures (Almeida et al., 2005). We observed that 1 µM Aβ treatment for 24 h significantly reduced synaptophysin (68.24±6.18%, **p<0.01) and homer (66.61±6.12%, *p<0.05) immunostaining in neurites relative to control (100%) (Figures 22). Thus, oAβ induces pre- and postsynaptic damage in our neuronal primary cultures.

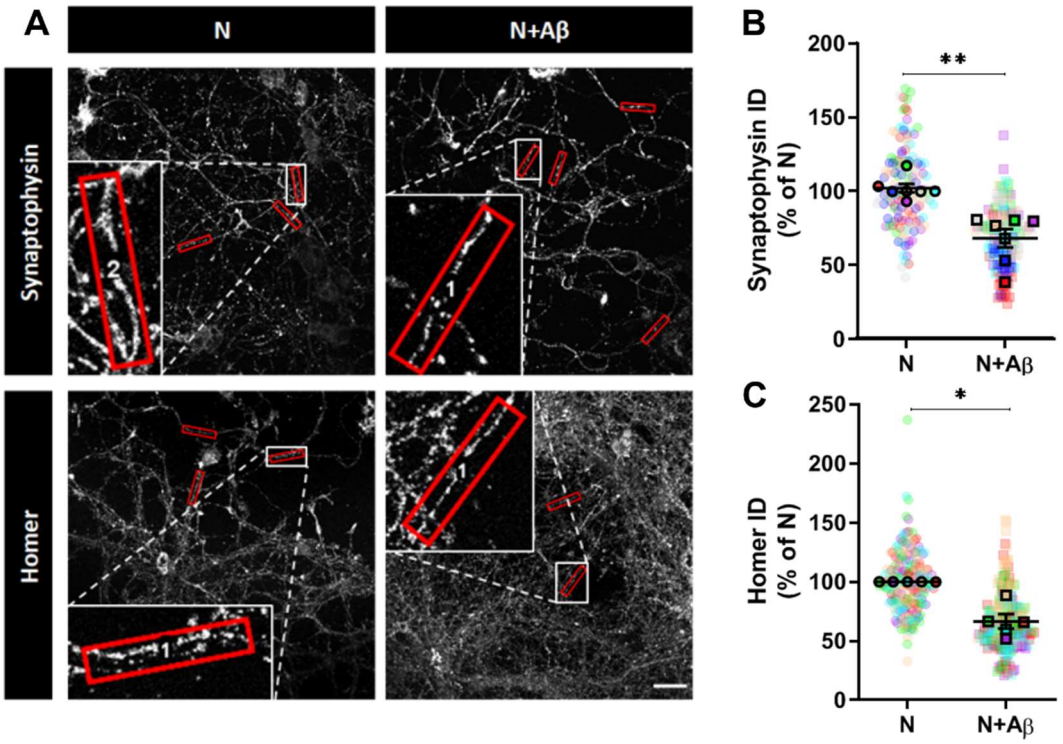

Figure 22. Aβ induces synaptic damage in neurons. Representative immunofluorescence image (A) and quantification (B-C) of synaptophysin and homer immune-staining of neurites in primary neuronal cultures incubated with 1 µM Aβ for 24 h (N=5 and N=7, respectively). Scale bar 20µm. N: neuron. Bars indicate means ± SEM and dots represent individual neurites (red region of interest). Statistical differences between groups were assessed by repeated measures Student's t-test. *p<0.05, **p<0.01, compared with control cells.

Next, we determined whether these synaptic alterations were also present in neuronal-microglial co-cultures at 10:1 proportion with the purpose of studying the role of microglia in this synaptic dysfunction induced by Aβ. As previously described in the experimental section (subsection 2.3), we added 12 DIV primary microglia to a 7 DIV neuron primary cultures. The presence of microglia without Aβ did neither alter the expression of synaptophysin nor homer (Figures 23).

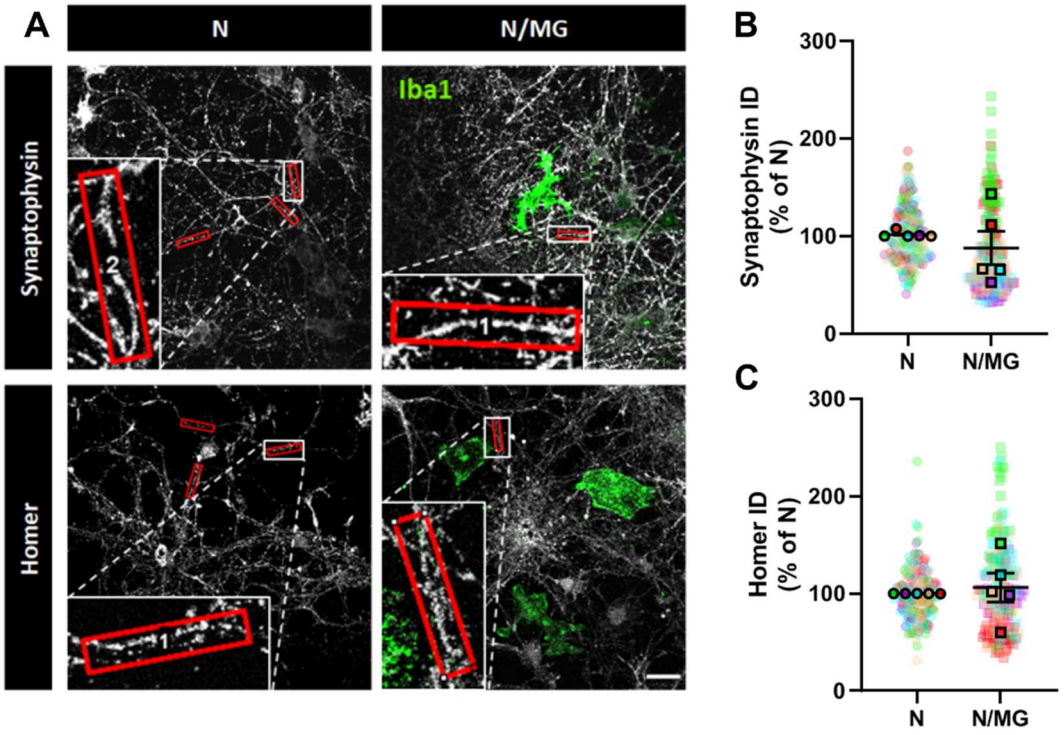

Figure 23. Coculturing microglia with neurons does not change the number of synapses in neurons. Representative image and quantification of synaptophysin (A, B) and homer (A, C) staining (gray scale) on neuronal-microglial primary co-cultures in physiological conditions for 24h measured by immunofluorescence (N=5-7). Scale bar 20 µm. N: neuron. Bars indicate means ± SEM and dots represent individual neurites (red region of interest). Statistical differences between groups were assessed by repeated measures Student's t- test. *p<0.05, **p<0.01, compared with control cells.

Next, to study the role of microglia on oAβ-induced synaptic pathology *in vitro*, neuronal-microglial co-cultures were treated with oAβ (1 µM for 24 h) and synaptic markers were measured by immunostaining. oAβ treatment significantly reduced presynaptic marker synaptophysin (76.33±3.15%, *p<0.05) immunostaining in neurites compared with control condition (N/MG, 100%) (Figures 24A and 24B). In case of homer marker (77.1±8.15%), the reduction was no significant (N/MG, 100%) (Figures 24A and 24C).

Overall, these results demonstrate that the presence of microglia in the neuronal-microglial co-culture is not able to recover presynaptic pathology induced by oAβ and oAβ does not cause significant synaptic damage in the postsynaptic compartment.

Next, we evaluated the impact of MCSF-activated microglia on synaptic damage induced by oAβ. To do so, neuronal-microglial co-cultures were treated with 1 µM oAβ in presence or absence of 25 ng/ml MCSF for 24 h. Results showed no differences in

synaptophysin and homer immunostaining intensity in neurites in the co-cultures treated with or without MCSF in presence of Aβ (Figures 24A-D). Moreover, there was a significant increase of homer staining in MCSF-activated microglia (99.58±13.58%) compared with unstimulated microglia in presence of Aβ (77.1±8.14%) (Figures 24A-D). These results suggest that MCSF treatment attenuated synaptic damage induced by oAβ in presynaptic compartment and improved postsynaptic compartment in neuronal-microglial co-cultures.

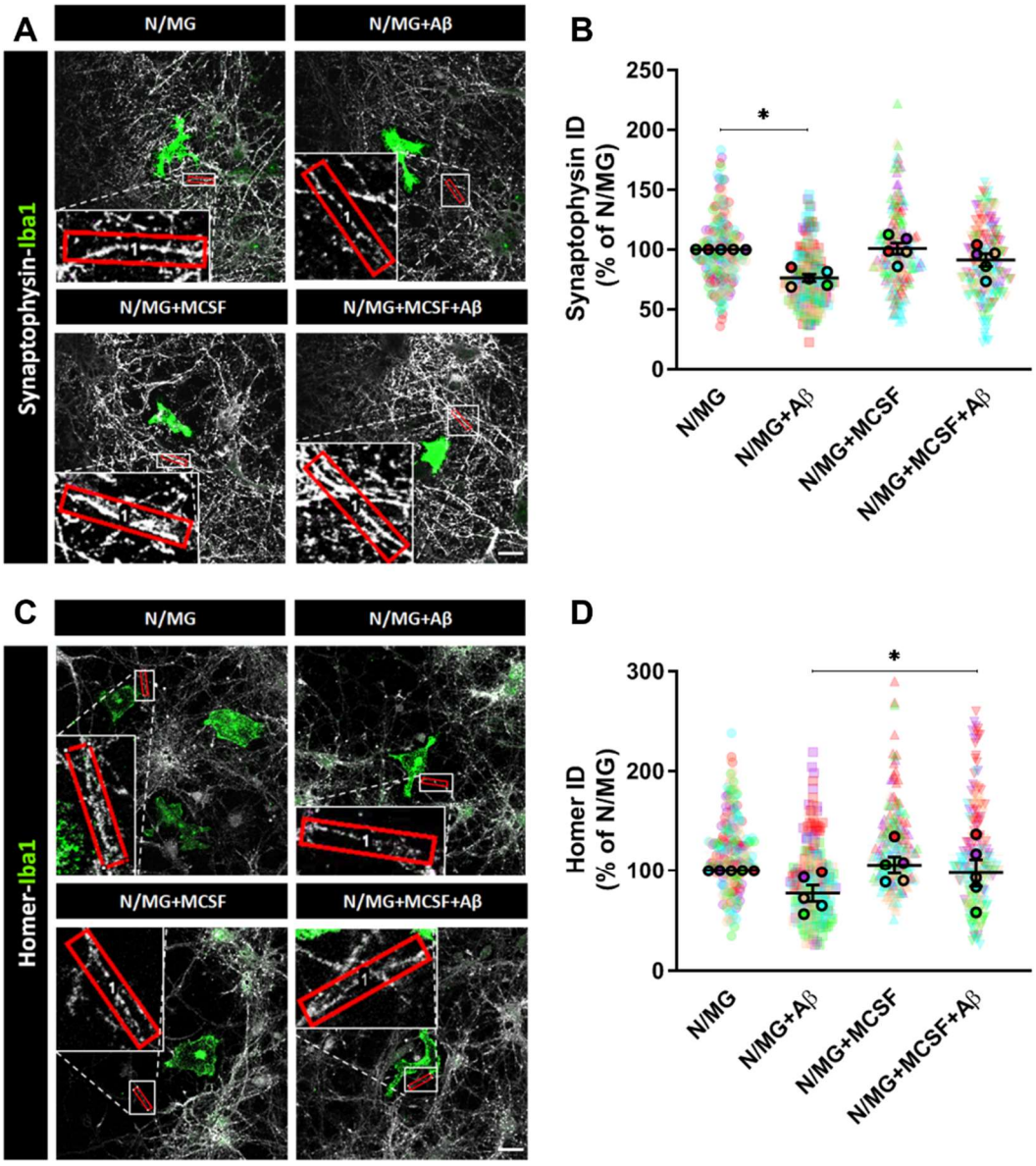

Figure 24. MCSF prevents synaptic damage induced by oAβ in neuronal-microglial co-cultures. Representative immunofluorescence image and quantification of synaptophysin (A and B) and homer (C and D) in neurites in neuronal-microglial primary co-cultures incubated with 1 µM oAβ and/or 25 ng/ml MCSF for 24 h (N=5). Scale bar 20µm. N/MG: neuronal-microglial co-culture Bars indicate means ± SEM and dots represent individual neurites (red region of interest). Statistical differences between groups were assessed by repeated measures Student's t-test. *p<0.05, compared with control cells.

Synaptic pruning is a physiological process that occurs mainly during development to eliminate excessive production of synapses. In AD, synaptic pruning contributes to synaptic loss and disease progression (Hong et al., 2016). To determine whether microglia engage in synaptic pruning when co-cultured with neurons and the effect of oAβ and MCSF on this process, we measured synaptic markers inside microglia in primary co-cultures treated with 1 µM oAβ and/or 25 ng/ml MCSF for 24 h. Treated co-cultures were immunostained with synaptophysin and Iba1 as well as homer and Iba1 antibodies and synaptophysin and homer immunostaining intensities were measured inside $Iba1^{+}$ microglia. We did not observe any changes in any synaptic markers inside the microglia in presence and absence of oAβ and/or MCSF relative to control condition (Figures 25A-D). According to these results, there is no evidence of oAβ-induced synaptic pruning in our AD *in vitro* model.

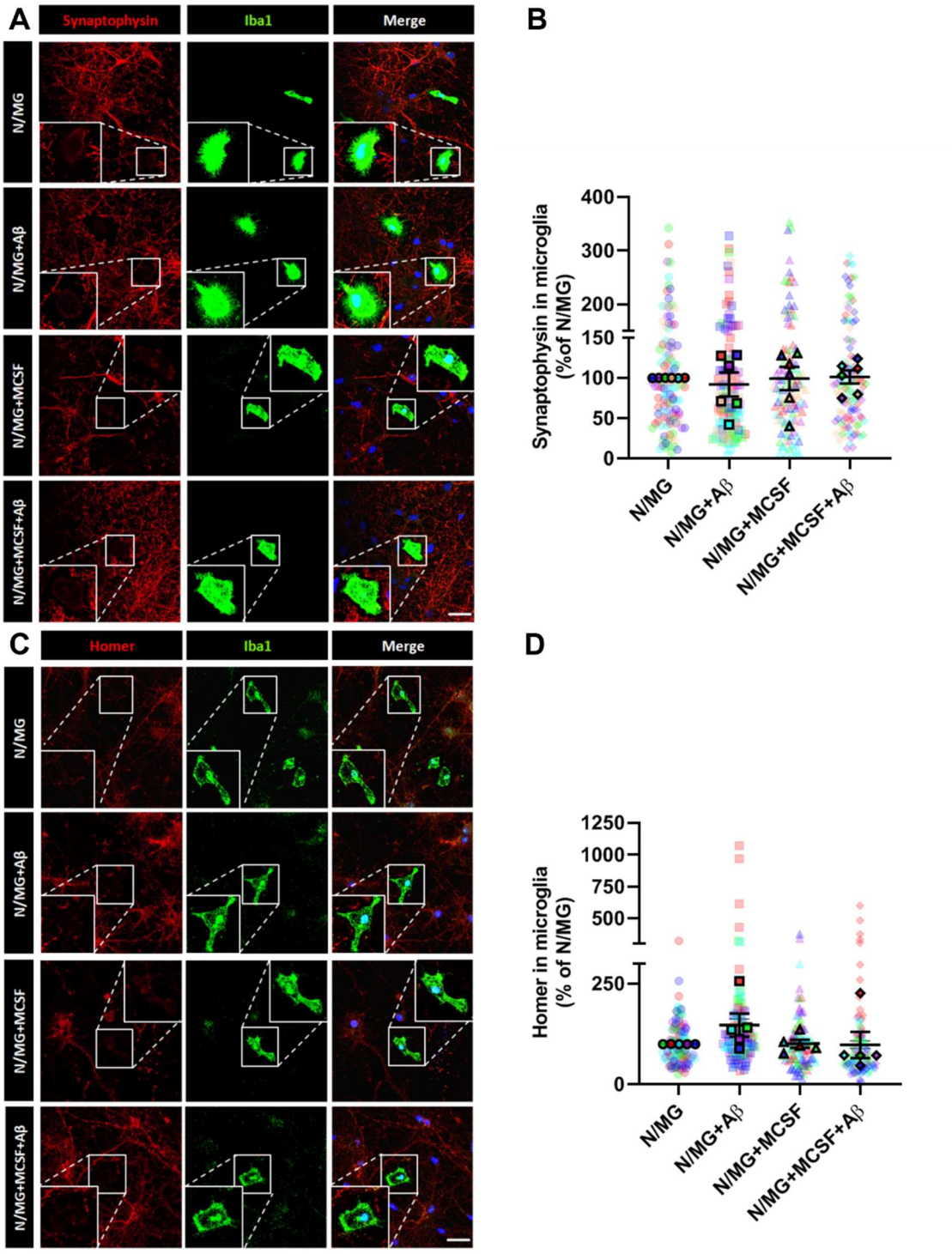

Figure 25. No evidence of synaptic pruning in neuronal-microglial co-culture. Representative immunofluorescence images (A, C) and quantification of synaptophysin (B) and homer (D) staining (red) inside Iba1^{+} microglia (green) in neuronal-microglial primary co-cultures incubated with 1 µM Aβ and/or 25 ng/ml MCSF for 24 h (N=5). Scale bar 30µm. N/MG: neuronal-microglial co-culture. Bars indicate means ± SEM and dots represent individual cells. Statistical differences between groups were assessed by repeated measures One-way ANOVA with Bonferroni correction.

2.3. Effect of oAβ and MCSF on the lysosomal degradation machinery in microglia.

The lysosome is the degradative endpoint of the cell, in which misfolded proteins and other resistant substrates undergo enzymatic degradation (Nixon et al., 2008; Majumdar et al., 2011). Once internalized by microglia, fibrillar Aβ species reach lysosomal compartments for degradation (Paresce et al., 1996; Majumdar et al., 2011). However, little is known regarding the effects of soluble Aβ species on microglial endolysosomal system integrity. Lysosomal function is compromised in AD (reviewed by Orr and Oddo 2013). Lysosomal LAMP1 mRNA and protein expression is upregulated in cerebral cortex of AD cases (Barrachina et al., 2006). Also, 10 µM fibrillar Aβ treatment increases LAMP1 expression in primary microglia (Guo et al., 2017).

In order to determine the effects, if any, of oAβ on the lysosomal degradation machinery in microglia, we treated primary microglia cultures with 1 µM oAβ in presence or absence of 25 ng/ml MCSF for 24 h and measured LAMP1 in $Iba1^+$ microglia by double immunofluorescence staining thereafter. We quantified LAMP1 immunostaining intensity, number of puncta and their size. The resulting data indicated that neither 1 µM oAβ nor treatment with MCSF alone induced any changes in LAMP1 intensity, number of puncta or puncta size. Nor cotreatment with oAβ and MCSF did not led to any changes in LAMP1 measurements either, relative to control (Figure 26). oAβ treatment induced an increase in the number of LAMP1 puncta in microglia but such increase did not statistically differ relative to control (521.2±172.3% versus 100%, p=0.33). According to these results, 1 µM oAβ and/or MCSF do not alter the expression of microglial LAMP1 protein expression *in vitro*.

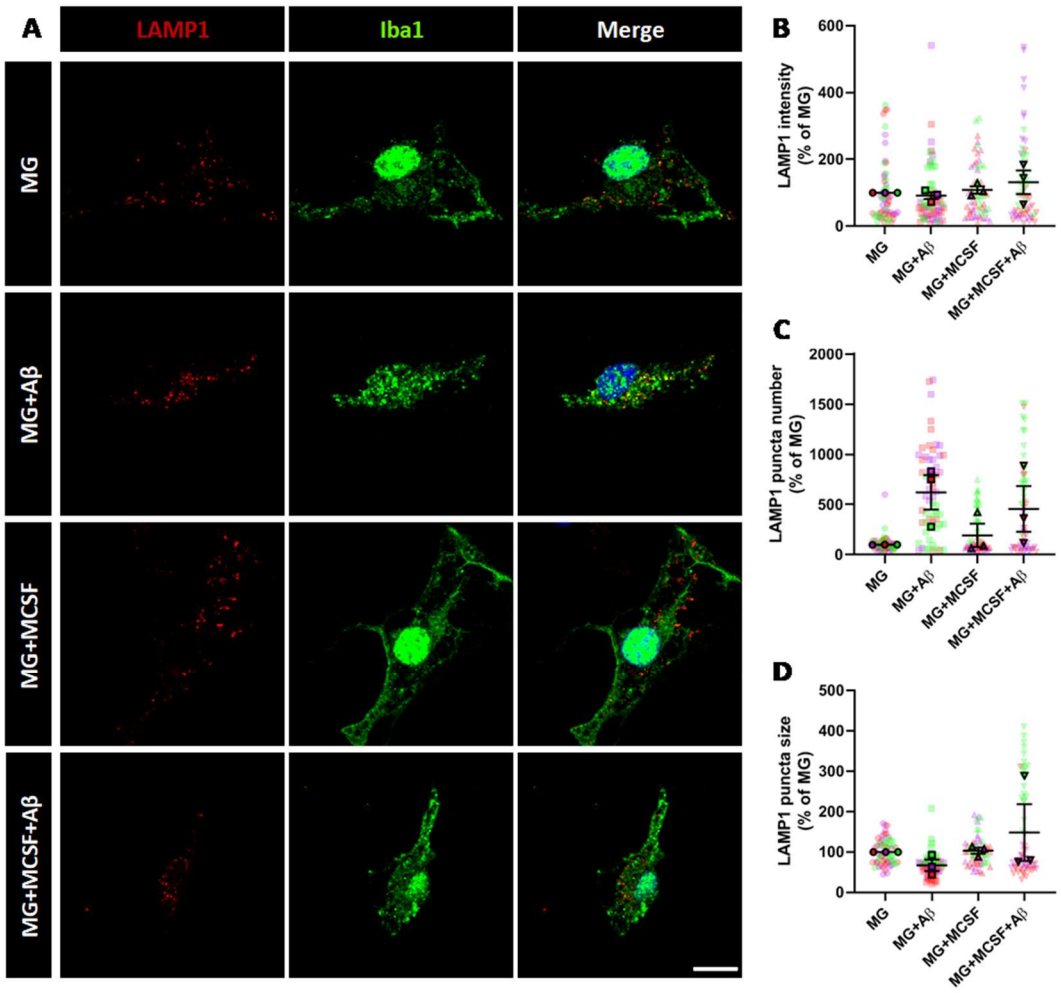

Figure 26. LAMP1 intensity, puncta number and puncta size do not change in presence of oAβ and/or MCSF in microglia. Representative immunofluorescence images of LAMP1 and Iba1 (A) and quantification of LAMP1 (red) staining intensity (B), puncta number (C) and puncta size (D) inside Iba1$^+$ (green) microglia primary cultures incubated with 1 µM Aβ and/or 25 ng/ml MCSF for 24 h (N=3). Scale bar 10 µm. MG: microglia. Bars indicate means ± SEM and dots represent individual cells. Statistical differences between groups were assessed by repeated measures One-way ANOVA with Dunnett correction, compared with control cells

LAMP1 protein expression is regulated by the action of TFEB, the master regulator of lysosomal biogenesis (Zhang and Zhao, 2015). Treatment of microglia with 10 µM fibrillar Aβ during 24 h, inhibits TFEB translocation from the cytoplasm to the nucleus, retaining this transcription factor in the cytoplasm and reducing the expression of genes associated with lysosomal biogenesis (Guo et al., 2017; Napolitano et al., 2018). To investigate whether MCSF or oAβ alter TFEB expression in microglia, we measured TFEB levels in Iba1$^+$ microglia using double immunofluorescence. TFEB immunostaining was quantified in both nucleus and cytoplasm to evaluate its activation state. No changes were seen in nuclear TFEB expression in microglia treated with 1 µM Aβ relative

to the untreated condition. However, significant increase in nuclear TFEB localization was seen following MCSF treatment compared with control condition (196.5±23.99% versus 100%, *p<0.05). Cotreatment with oAβ and MCSF attenuated this effect (Figures 27A and 27B). There were no differences in cytoplasmic TFEB expression (Figures 27A and 27C).

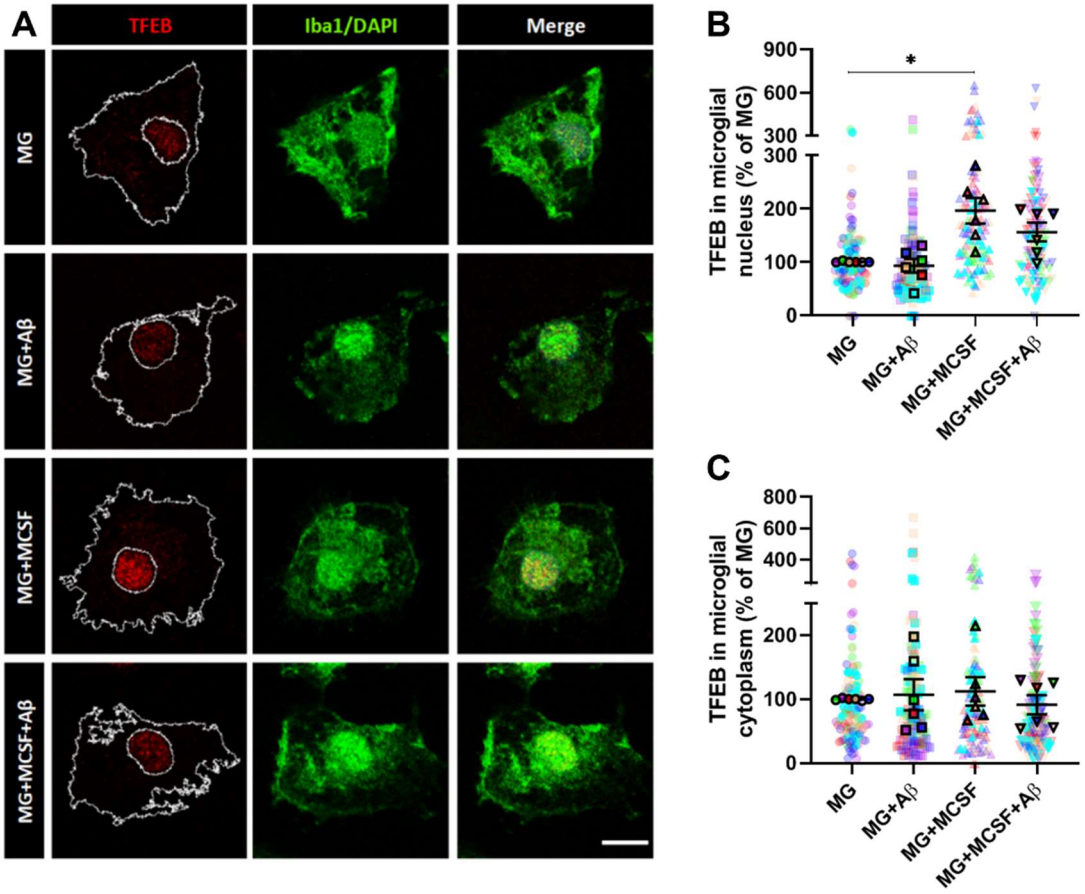

Figure 27. MCSF augments TFEB nuclear expression in microglia. Representative immunofluorescence images of TFEB (red) and Iba1 (green) (A) and quantification of nuclear (B) and cytoplasmic (C) TFEB levels quantified in areas delineated with white ROIs (A) in primary microglia incubated with 1 µM oAβ and/or 25 ng/ml MCSF for 24 h (N=6). Scale bar 10 µm. MG: microglia. Bars indicate means ± SEM and dots represent individual cells. Statistical differences between groups were assessed by repeated measures One-way ANOVA with Dunnett correction. *p<0.05 compared with control cells.

TFEB belongs to the MiTF/TFE family of transcription factors regulating the expression of several proteins implicated in lysosomal biogenesis, such as OSTM1 (Hershey and Fisher, 2004; Meadows et al., 2007). OSTM1 scaffold protein was described as a chaperone for CLC-7, a chloride antiporter that facilitates full lysosomal acidification. OSTM1 plays a key role in the mobilization of CLC-7 to the lysosome (Majumdar et al., 2011). MCSF treatment upregulates CLC-7 and OSTM1 proteins, thus

promoting optimal lysosomal acidification, which in turn allow microglia to degrade fibrillar Aβ more efficiently (Majumdar et al., 2011). 10 µM fibrillar Aβ treatment for 24 h resulted in a significant reduction in OSTM1 expression (Guo et al., 2017). To determine the effect of oAβ in OSTM1 expression, primary microglia were treated with 1 µM oAβ and/or 25 ng/ml MCSF for 24 h and OSTM1 was measured by immunofluorescence in Iba1+ microglia thereafter. No changes were seen in OSTM1 expression following treatments (Figures 28). In conclusion, our results suggest that, as opposed to 10 µM fibrillar Aβ, 1 µM oAβ does not alter OSTM1 expression in primary microglia.

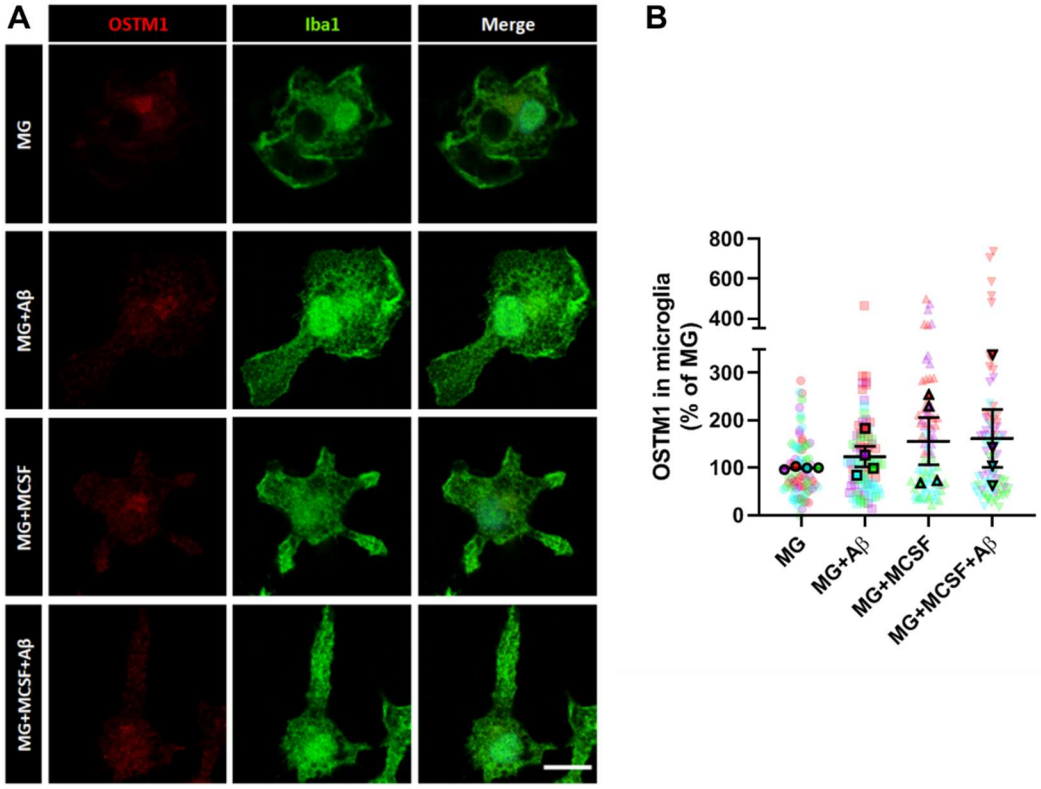

Figure 28. Neither MCSF nor oAβ changes OSTM1 expression in microglia. Representative images of OSTM1 and Iba1 immunostaining (A) and OSTM1 (red) quantification (B) inside Iba1^{+} (green) cells in primary microglia cultures incubated with 1 µM oAβ and/or 25 ng/ml MCSF for 24 h (N=4). Scale bar 10 µm. MG: microglia. Bars indicate means ± SEM and dots represent individual cells. Statistical differences between groups were assessed by repeated measures One-way ANOVA with Dunnett correction, compared with control cells.

Overall, 1 µM oAβ treatment did not induce any significant changes in the expression of LAMP1, OSTM1 or TFEB. However, MCSF treatment induced an increase in TFEB nuclear levels in microglia, which should promote lysosomal biogenesis.

3. MCSF treatment reverts Aβ-induced alterations in microglia dynamics in an *ex vivo* model of AD.

3.1. MCSF reverts Aβ-induced microglial morphological alterations.

When microglia sense different stimuli such as external agents, inflammatory signals, and misfolded proteins, the cells adopt a pro-inflammatory state, change their morphological features (shortening their processes and enlarging their somas), proliferate, and migrate (Nimmerjahn, 2005; Tremblay et al., 2011). To study the impact of MCSF on microglial dynamics, we took advantage of two organotypic AD ex vivo models; cortical organotypic rat cultures treated with oAβ and organotypic cultures from the 5XFAD model of AD.

First, we evaluated the pro-inflammatory state of microglia in the presence of oAβ in cortical rat organotypic cultures. To do so, 13 DIV organotypic slices were incubated with 3 μM oAβ in presence or absence of 25 ng/ml MCSF for 24h, and Iba1 immunoreactivity was measured thereafter by immunofluorescence. oAβ treatment induced an increase in $Iba1^{+}$ area (159.3±15.2%, *$p<0.05$) relative to the control condition (100%), and MCSF addition reduced Iba1 area levels (84.91±14.4%), but this change was not significant relative to Aβ condition (Figures 29A-B).

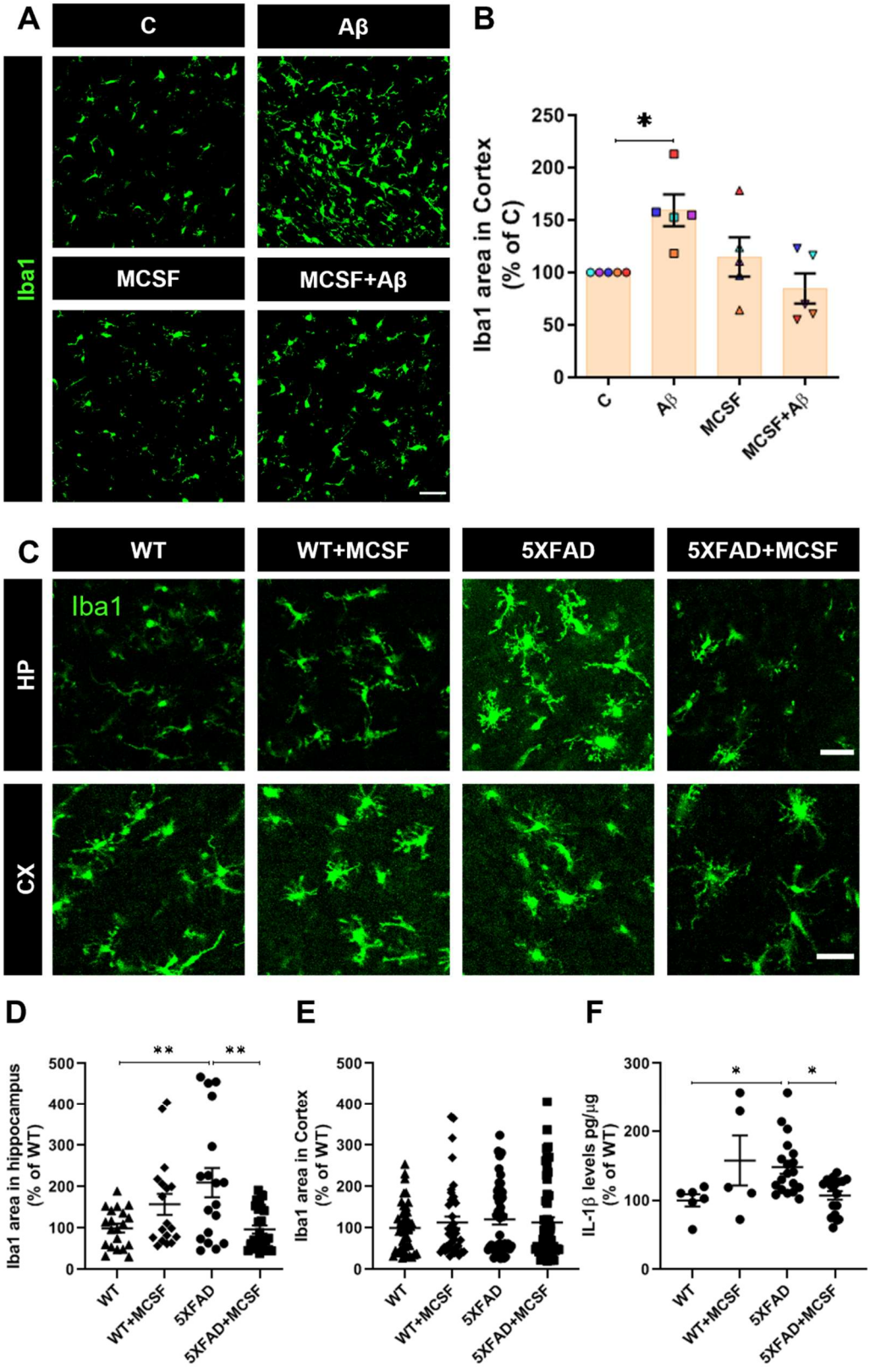

Figure 29. MCSF reverts Iba1 area increase both in oAβ-treated rat cerebral cortex in the hippocampus of 5XFAD mice organotypic cultures. (A and B) Representative images and quantification of Iba1 immunofluorescence (green) area in organotypic cultures from rat cerebral cortex incubated with 3 μM Aβ and/or 25 ng/ml MCSF for 24 h (N=5). (C-F) Representative images of Iba1 and quantification of Iba1 area by immunofluorescence in hippocampus (D) and cerebral cortex (E). IL-1β cytokine quantification in

the extracellular media used to maintain organotypic cultures, by ELISA assay (F) in 5XFAD and wild type mice (N=18-28). Scale bar 40 µm. WT: wild type. Bars indicate means ± SEM and dots represent individual fields. Statistical differences between groups were assessed by not-pairing measures One-way ANOVA with Sidak correction. *p<0.05, **<0.01 compared with control cells.

A number of additional experiments devoted to further study microglial dynamics in the context of AD were completed at the laboratory of Dr. Magdalena Sastre (Imperial College London, London, England). The Sastre laboratory previously showed that microglial morphology and its inflammatory state were altered in organotypic slices from 5XFAD mice (Davis et al., 2021). We aimed to determine whether MCSF was able to revert the morphological alterations seen in microglia following oAβ treatment, using the 5XFAD mouse model available and well stablished at the Sastre laboratory. The 5XFAD mouse model of AD is characterized by high levels of intracellular and extracellular Aβ, gliosis and synapse degeneration (Oakley et al., 2006; Jawhar et al., 2012; Richard et al., 2015) and it is a very robust model to study amyloidosis-associated AD pathology. Organotypic slices of 5XFAD mice were treated with 25 ng/ml MCSF for 24 h followed by Iba1 immunostaining for microglial area detection via immunofluorescence. $Iba1^+$ area was quantified in both hippocampal and cortical regions of the organotypic slices. Results show that $Iba1^+$ total area was increased in hippocampal regions (210.1±35.25%, *p<0.05) when compared with wild type (WT) (100±10.45%) (Figure 29D). This increase was abrogated in the presence of MCSF (96.77±9.61%, *p<0.05). No changes were seen in cortical Iba1 area occupancy between 5xFAD and WT slices (Figure 29E). Quantification of IL-1β levels by ELISA in conditioned media of organotypic cultures revealed a significant increase in the levels of the cytokine in 5XFAD (148.1±9.51%, *p<0.05) when compared with WT (100±8.99%). Again, this effect was reverted in the presence of MCSF (107.2±6.14%, *p<0.05) (Figure 29F). These data confirm a pro-inflammatory profile in 5XFAD mice when compared with WT, as shown by Iba1 and IL-1β measurements. MCSF treatment reverts this pro-inflammatory profile. Moreover, the results in both organotypic models show that presence of Aβ causes inflammation represented by microglial area increase and increment of IL-1β, and MCSF treatment reverts it.

Since results on $Iba1^+$ areas measured in the cortex of 5XFAD mice were very variable, a detailed microglial morphological analysis was performed using MATLAB

following a protocol designed by the Sastre Laboratory (Davis et al., 2021) and described in detail in the Experimental section 16.2.

This analysis revealed a significant increase in the number of processes (150.0±4.97%, ****p<0.0001), process area (155.6±5.43%, ****p<0.0001) and process perimeter (128.8±2.87%, ****p<0.0001) in microglia from 5XFAD relative to WT [number of processes (100±3.43%), process area (100±4.17%) and process perimeter (100±2.14%), respectively] (Figure 30). In contrast, microglial soma size was reduced in 5XFAD (28.35±3.43%, ****p<0.0001) relative to WT mice (100±5.29%). MCSF treatment induced a reduction in the number of processes (123.6±4.39%, ***p<0.001), process area (128.4±4.59%, **p<0.01) and process perimeter (109.4±2.67%, ****p<0.0001) and an increase in soma size (48.58±5.33%) when compared with untreated 5XFAD mice [number of processes (150.0±4.97%), process area (155.6±5.43%), process perimeter (128.8±2.87%) and soma size (28.35±3.43%), respectively].

Interestingly, MCSF induced the opposite effect in WT mice. Following the treatment, there was an increment in number of processes (126.7±5.05%, ***p<0.001), process area (160.1±7.76%, ****p<0.0001) and a reduction in soma size (55.21±6.58%, ****p<0.0001) when compared with untreated WT [number of processes (100±3.43%), process area (100±4.17%) and soma size (100±5.29%), respectively] (Figures 30).

Taken together, these results show that MCSF treatment partially reverts microglial morphological changes in the 5XFAD mice towards a WT phenotype.

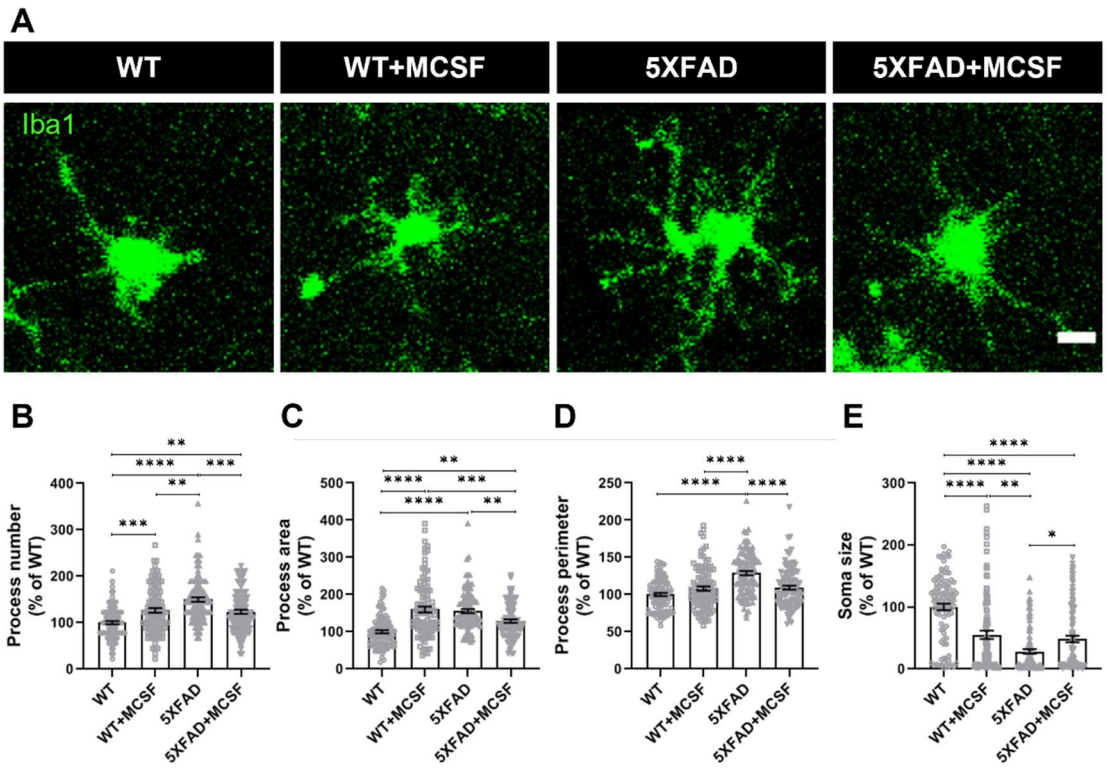

Figure 30. Microglial morphology changes in the cerebral cortex of 5XFAD mice are partially reverted by MCSF. Quantification of the number of processes (A), process area (B), process perimeter (C) and soma sizes (D) in Iba1^{+} microglia in cortex of organotypic cultures from 5XFAD and WT mice, incubated with 25 ng/ml MCSF for 24h and measured by immunofluorescence (N=100). Scale bar 10 µm. WT: wild type. Bars indicate means ± SEM. Statistical differences between groups were assessed by not-pairing measures One-way ANOVA with Sidak correction. *p<0.05, **p<0.01, ***p<0.001, ****p<0.0001 compared with control cells.

3.2. MCSF reverts Aβ-induced astrocytic morphological alterations.

To broaden our analysis on inflammation, we measured astrogliosis in organotypic brain sections. Astrocytic area was measured by immunofluorescence using a GFAP antibody in brain slices from 5XFAD and WT, previously treated with MCSF or control vehicle. We noted an increase in the area occupied by GFAP^{+} astrocytes in the hippocampus of 5XFAD mice (264.9±49.22%, *p<0.05) relative to WT (100±10.45%). MCSF treatment reduced the area occupied by GFAP+ astrocytes in 5XFAD mice (93.39±9.99%, *p<0.05). Similar to the previous study on microglia, no differences were seen in cortical GFAP levels between 5XFAD and WT mice, irrespective of MCSF treatment (Figures 31).

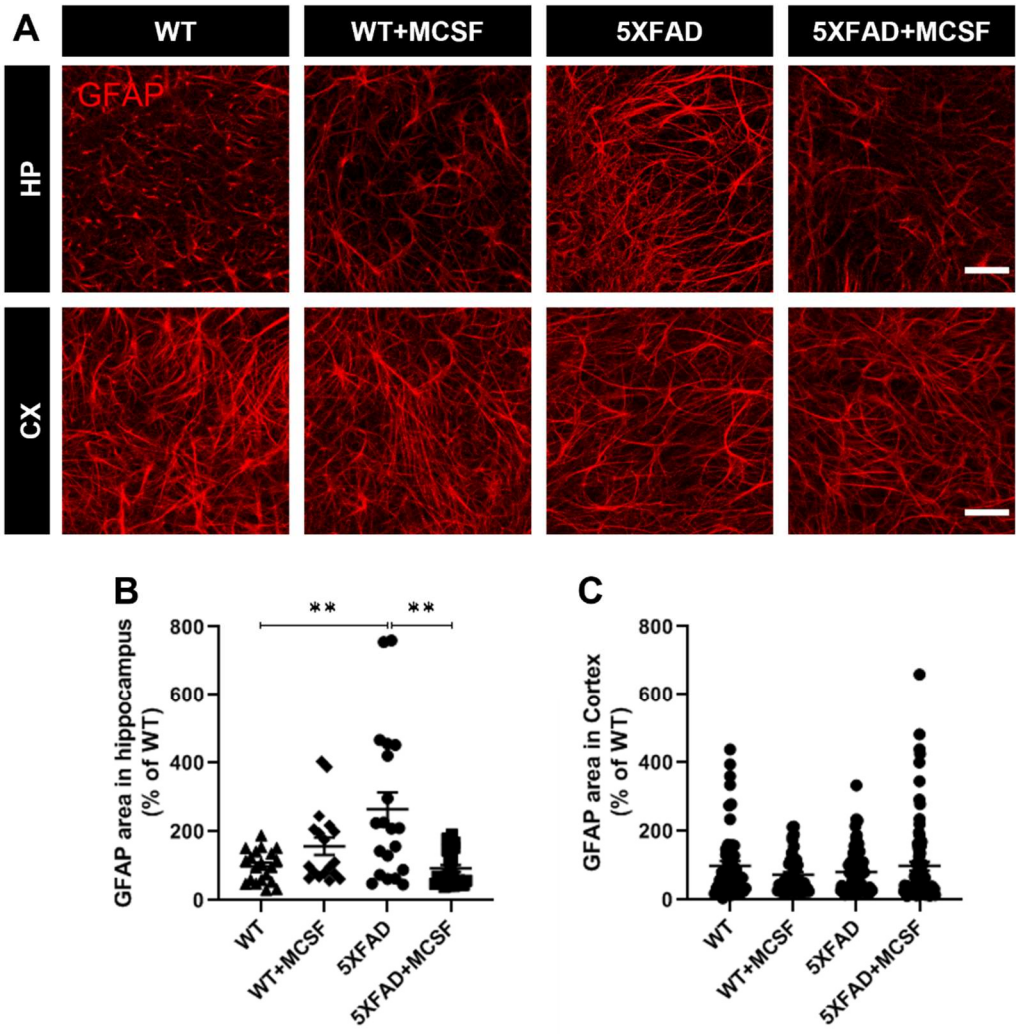

Figure 31. MCSF reduces astrogliosis in 5XFAD organotypic brain slices. Representative image of GFAP immunofluorescence (red) (A) and quantification of the area occupied by the staining in hippocampus (B) and cerebral cortex (C) of organotypic cultures from 5XFAD and WT mice incubated with 25 ng/ml MCSF for 24 h (N=18-27). Scale bar 40 µm. WT: wild type. Bars indicate means ± SEM and dots represent individual fields. Statistical differences between groups were assessed by not pairing-measures One-way ANOVA with Sidak correction. **<0.01 compared with control cells.

3.3. MCSF reverts Aβ-associated alterations in microglial surveillance activity and motility.

Microglia motility and surveillant activity are altered during AD (Gyoneva et al., 2016), and we hypothesized whether MCSF could mitigated these alterations. In collaboration with Dr. Federico N. Soria, we used two-photon microscopy to measure microglial surveillant activity in organotypic brain slices. We used the Cx3Cr1$^{+/eGFP}$ mouse model, where myeloid cells express the GFP fluorescent reporter driven by the CX3CR1 promoter (Jung et al., 2000). eGFP^{+} microglia from organotypic brain slices were visualized by two-photon time-lapse microscopy imaging. GFP^{+} microglia were imaged

for no longer than 20 minutes to avoid tissue toxicity. The qualitative live-imaging evaluation of microglia in 14 DIV organotypic cultures showed separated cell bodies as sign of less integrated tissue derived from cell death and changes in extracellular space during culture, presenting ameboid-like morphology with recurrent phagocytic patches (red arrows) formation indicating an over-reactive phenotype (Figure 32A). To reduce activation as much as possible and to test microglial motility in the best of homeostatic conditions, we decided to study microglial dynamics in 7 DIV organotypic cultures instead of 14 DIV cultures. At 14 DIV, microglia showed a more distended ameboid-shaped with increased phagocytic patches and at 7 DIV, microglial morphology changed into an integrated, more interactive, elongated and more ramified cell shape with smaller patches (Figure 32B).

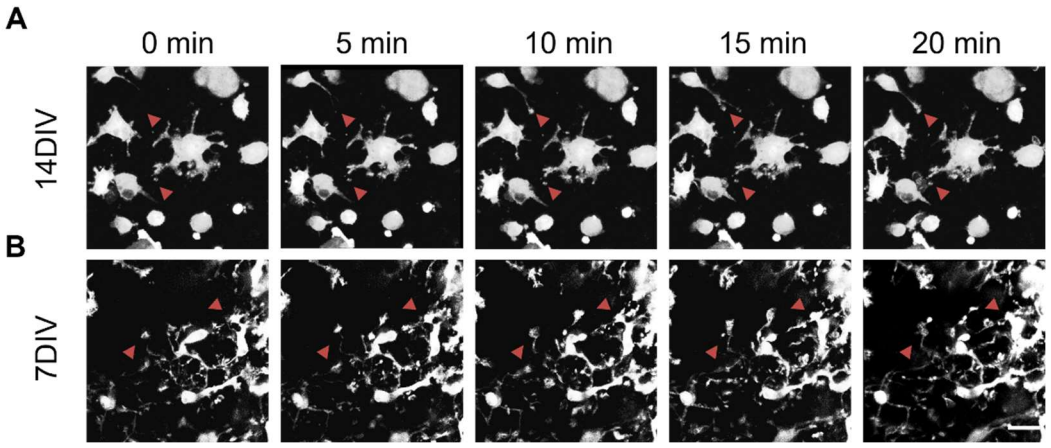

Figure 32. Microglial morphological difference between 14 and 7 DIV organotypic cultures. Representative image of eGFP$^+$ (gray) microglia of organotypic cultures from Cx3Cr1$^+$/eGFP mice in control conditions cultured for 14DIV (A) or 7DIV (B). (A) At 14DIV, microglia showed ameboid shaped with increased phagocytic patches indicated with red arrows. (B) At 7DIV microglial morphology showed more integrated, elongated, and ramified cell shape with smaller patches indicated with red arrows. Scale bar 20µm.

Seven DIV cortical organotypic slices were incubated with 3 µM Aβ in presence or absence of 25 ng/ml MCSF treatment for 24 h. Microglial motility was evaluated by quantifying the area surveyed by the eGFP$^+$ signal per unit of time. This measure depends both on the number of cell processes present in the cell and on their speed and range of movement. oAβ treatment reduced the area surveilled by microglia and MCSF treatment increased it (Figure 33B). The comparison of the area under the curve measured for the various conditions revealed a significant reduction in surveillant activity following oAβ treatment (67.18±6.06 %, **p<0.01) compared with control

(100±13.74%). Also, there was a significant increase in surveillant activity when MCSF was added to the oAβ incubation relative to oAβ (121.5±13.68 versus 67.18±6.06%, respectively, **p<0.01) (Figure 33C). The rate of variation in microglial motility was estimated by calculating the initial slope of the surveyed area per unit of time in the first minute. Indeed, there was a significant reduction in the rate following treatment with oAβ (44.6±4.90%, **p<0.01) relative to control (100±10.99%, **p<0.01) and a significant increase of the initial slope between Aβ condition (44.6±4.90%, **p<0.01) and MCSF+Aβ condition (97.49±16.94%) (Figure 33D). These results indicate that oAβ induces a reduction in microglia surveillant activity, and this reduction can be rescued by MCSF treatment.

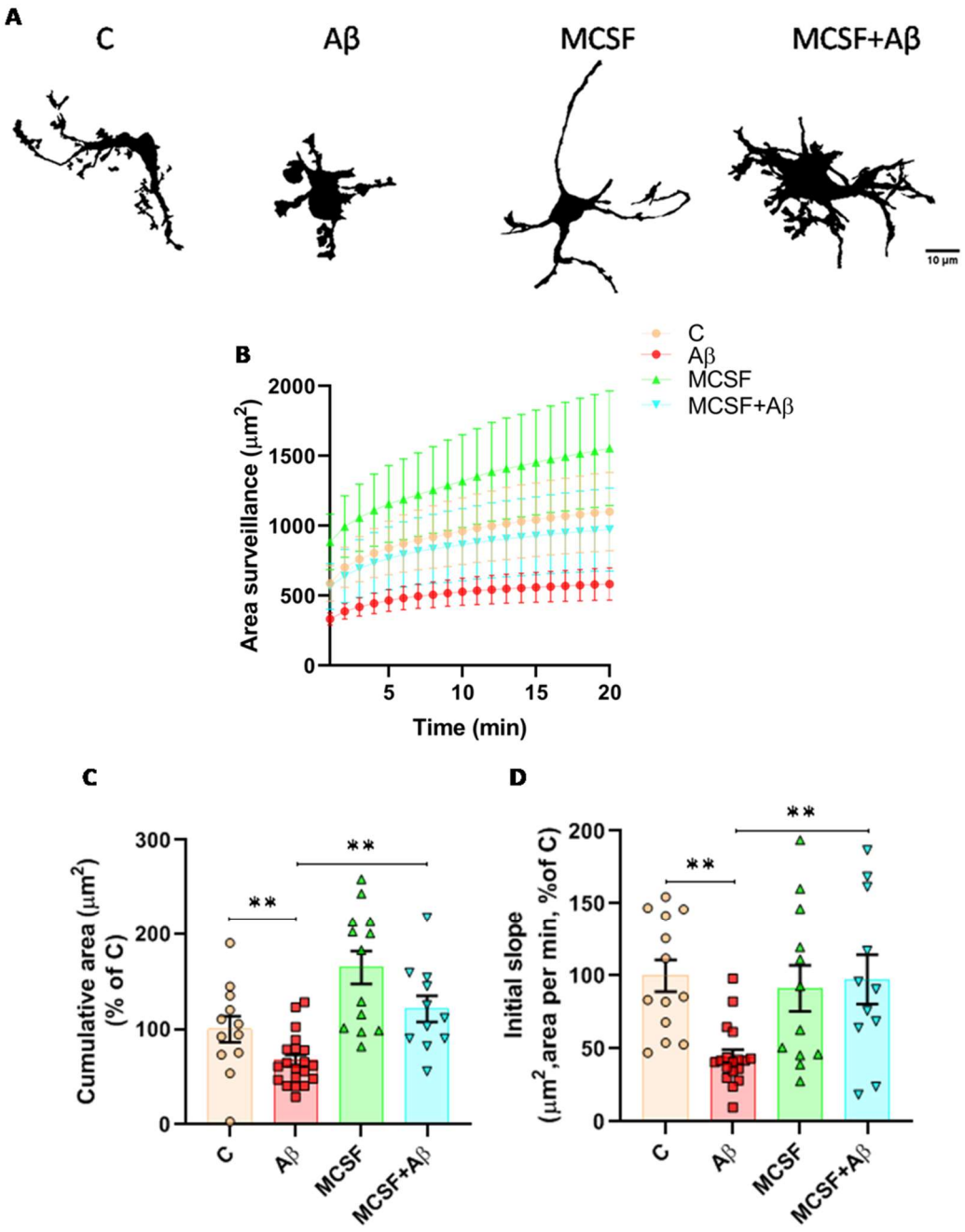

Figure 33. MCSF reverts the reduction in microglial surveilled area and motility induced by oAβ in organotypic cultures visualized by two-photon time-lapse microscopy. Representative image of eGFP$^+$ (black) microglia in the various conditions studied in this experiment (A). Quantification of eGFP$^+$ surveyed area during 20 min recordings (B). Integrated area surveilled during 20 min recordings (C) and initial slope, or rate of variation, of area surveillance (D) in organotypic cultures from Cx3Cr1$^+$/eGFP mouse model incubated with 3 µM Aβ and/or 25 ng/ml MCSF for 24 h (N=11-20). Scale bar 10 µm. Bars indicate means ± SEM and dots represent individual cells. Statistical differences between groups were assessed by not pairing-measures One-way ANOVA with Sidak correction. **<0.01 compared with control cells.

Additionally, we took advantage of this model to investigate microglial morphology and if/how MCSF altered it. Microglia processes were quantified by Sholl analysis. Sholl analysis is a quantitative analysis of cell morphology. A significant

decrease (52.4±4.77%, *p<0.05) in the number of Sholl ring crossings were seen in oAβ-treated microglia relative to control (100±16.8%), indicative of a decrease in both process branching and extensions from the cell body (Figure 34). MCSF treatment prevented the oAβ-induced reduction in the branching and extensions in the MCSF+Aβ (111.0±15.53%, **p<0.01). These results indicate that oAβ reduces complexity of microglial morphology and that MCSF rescues this effect.

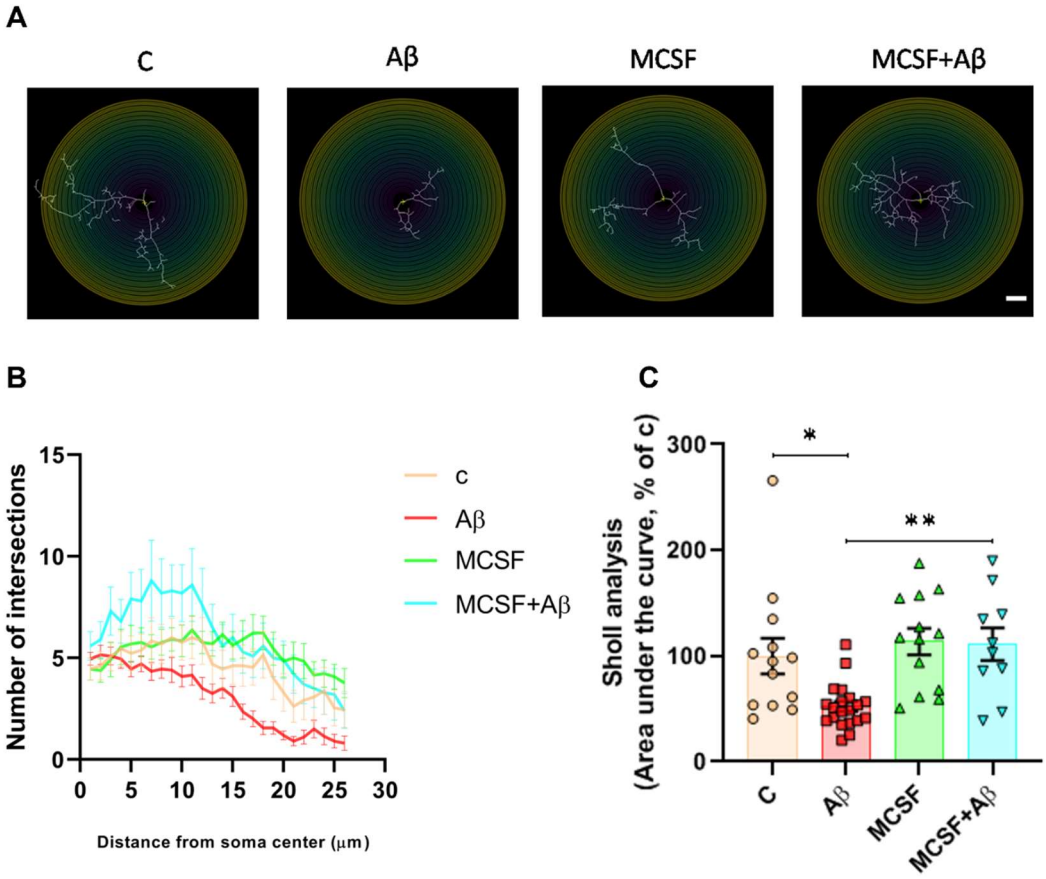

Figure 34. MCSF reverts the reduction of microglial morphological complexity induced by oAβ in organotypic culture visualized by two-photon time-lapse microscopy. Representative image of Sholl analysis (A), quantification of 20 min recordings (B) and quantification of area under curve (C) in organotypic cultures from Cx3Cr1^{+}/eGFP mouse model incubated with 3 μM Aβ and/or 25 ng/ml MCSF for 24 h (N=11-20). Scale bar 10 μm. Bars indicate means ± SEM and dots represent individual cells. Statistical differences between groups were assessed by not pairing-measures One-way ANOVA with Sidak correction. p*<0.05, p**<0.01 compared with control cells.

Overall, the presence of oAβ induces an increase in the area occupied by microglia in organotypic cultures from rat cerebral cortex. Organotypic brain cultures from 5XFAD also show an increase in the area occupied by microglia when compared with WT mice, presumably due to the presence of high levels of endogenous Aβ in the tissues. This is consistent with a pro-inflammatory state. These observations are further

supported by the increased area occupied by GFAP$^+$ astrocytes in 5XFAD. Moreover, microglial surveilled area, motility and morphological complexity are reduced in Cx3Cr1$^+$/eGFP mice following treatment with oAβ. Remarkably, MCSF treatment reverts these alterations.

4. Preclinical study of MCSF treatment in the 3xTg-AD mouse model of AD.

A previous study reported the capacity of MCSF treatment to prevent cognitive decline associated with Aβ burden in young APP/PS1 mice (Boissonneault et al., 2008). Based on this study, we examined amyloid and tau pathology, synaptic pathology and inflammation in adult 3xTg-AD mice subjected to MCSF treatment. The 3xTg-AD mouse model of AD is characterized by age-related, progressive neuropathology including Aβ plaques and neurofibrillary tangles. Extracellular Aβ deposits are described as early as 6 months of age and tau pathology is evident at 12 months. Also, synaptic dysfunction, including LTP deficits, prior to plaques and tangles has been reported (Oddo et al., 2003; Billings et al., 2005; Rodríguez et al., 2008). The animals used in this study were all female, 12-month-old 3xTg-AD mice. The animals were injected weekly with either MCSF or vehicle control (saline) for 4 months (Figure 35). A detailed description of the treatment protocols is included in the experimental procedures (section 10).

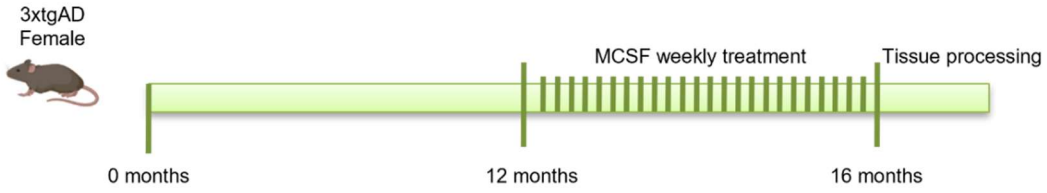

Figure 35. Timeline of MCSF *in vivo* treatment of the 3xTg-AD female mice.

4.1. Effect of MCSF treatment in amyloid and tau pathology

3xTg-AD coronal brain sections were stained with Thioflavin-S dye, which binds to fibrillar Aβ (Xinze et al., 2018). The area occupied by the staining was quantified as a measure of plaque load (Figure 36A). A significant reduction in Thioflavin-S$^+$ area was observed in animals treated with MCSF (48.56±13.35%, *p<0.05) relative to the vehicle group (100±14.28%) (Figures 36B and 36C). $A\beta_{1\text{-}42}$ levels in cortical brain homogenates were also measured, by ELISA. No differences were found in Aβ brain levels between

animals treated with MCSF or vehicle control (76.07±20.8% and 100±30.75%, respectively p=0.54) (Figure 36D). $A\beta_{42/40}$ ratio was measured in CSF extracted from the mice by Single Molecule Assay (SIMOA). No differences were observed in the ratio in animals treated with MCSF relative to vehicle group (114.4±12.67% and 100±10.74%, respectively p=0.41) (Figure 36E). According to these results, MCSF treatment reduces fibrillar plaque load in the 3xTg-AD mice.

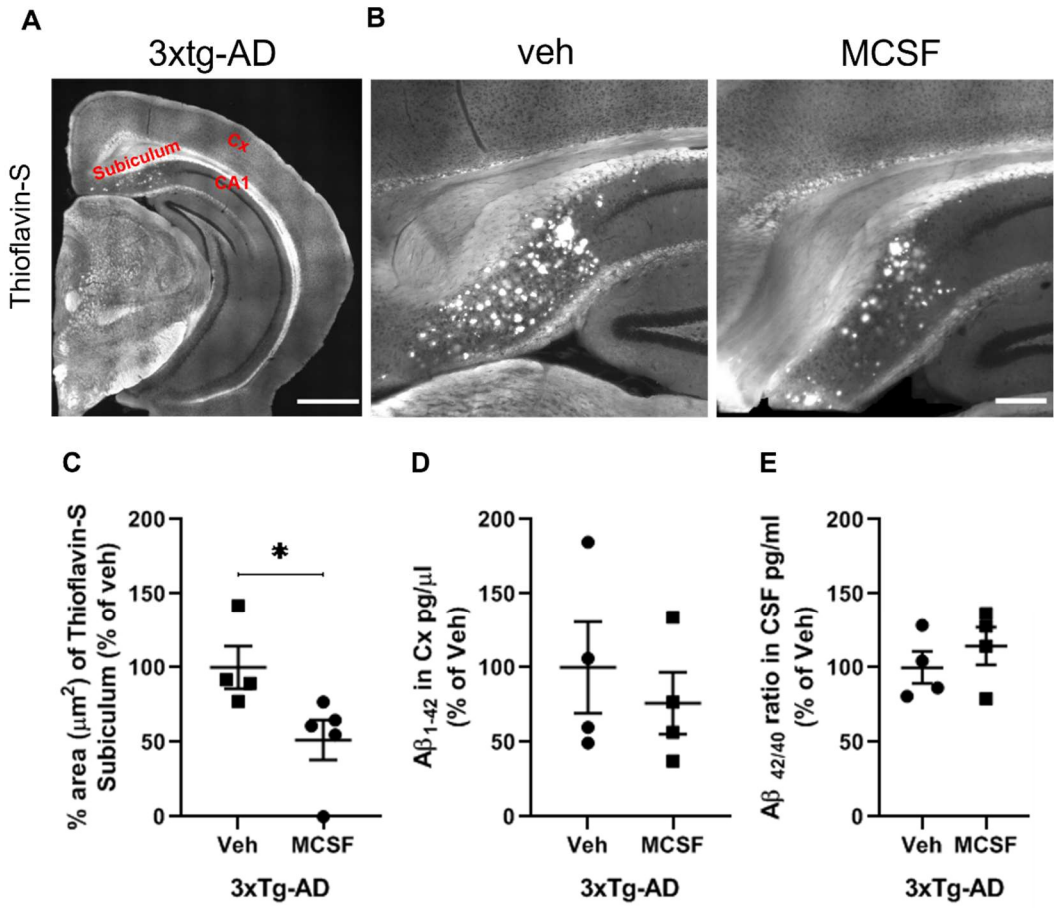

Figure 36. MCSF treatment reduces Aβ plaque load in the 3xTg-AD model of AD. (A) Representative images of Thioflavin-S (gray) staining on a half coronal brain section. The areas of subiculum, CA1 and cortex (Cx) are indicated. (B) Representative images of subiculum and (C) quantification of Thioflavin-S staining in the subiculum of the 3xTg-AD mice treated with MCSF or vehicle control for 4 months (D) Quantification of cortical (Cx) $A\beta_{1-42}$ levels by ELISA in animals treated with MCSF or vehicle control. (C) Quantification of the Aβ42/40 ratio in CSF extracted from mice treated with MCSF or vehicle control. Vehicle N=4, and MCSF treatment N=5. Scale bar 1000 µm (A) and 250 µm (B). Veh: vehicle. Bars indicate means ± SEM and dots represent individual animals. Statistical differences between groups were assessed by not pairing-measures Student's t-test. P*<0.05 compared with vehicle group.

Next, the effect of MCSF treatment on tau pathology was assessed. To do so, hyperphosphorylated tau levels were measured by Western blot in cortical brain homogenates and by immunofluorescence on brain slices prepared from 3xTg-AD mice

treated with MCSF or vehicle control. For both techniques, we used an AT8 antibody. AT8 is a phosphorylation-tau-specific monoclonal antibody that is a commonly used as marker of tauopathy. AT8 is reactive towards phosphorylation sites at pSerine202 and pThreonine205 (Goedert et al., 1995; Malia et al., 2016). Western blot analysis showed a decrease in hyperphosphorylated tau (measured using AT8 antibody immunoreactivity) levels normalized to total tau (measured using hT7 antibody immunoreactivity), in mice treated with MCSF relative to vehicle group. However, this difference was not statistically significant (64.44±8.89% versus 100±19.77%, p=0.12) (Figures 37A and 37B). The tissues were immunostained with AT8 and immunofluorescence was measured in the CA1 hippocampal region. The area occupied by the immunostaining and its mean gray value were quantified. No differences in hyperphosphorylated tau load were seen between mice treated with MCSF or vehicle control (Figures 37D-F). These results indicate that MCSF treatment of adult 3xTg-AD mice does not reduce tau pathology.

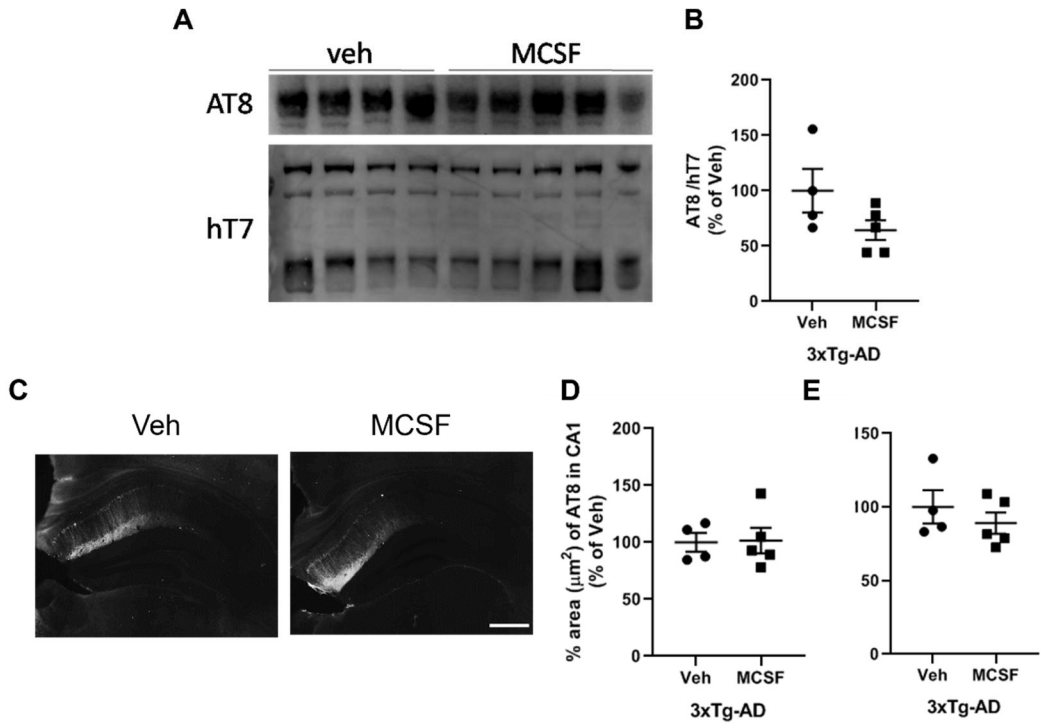

Figure 37. MCSF treatment in adult 3xTg-AD mice does not reduce tauopathy. Representative image of a Western blot using AT8 immunoreactivity to detect hyperphosphorylated tau(A) and quantification of AT8 signal normalized to hT7 total tau levels (B) in cortex tissue homogenates from 3xTg-AD mice treated with either MCSF or vehicle control. Representative images of AT8 immunofluorescence (C) and fluorescence quantification indicating hyperphosphorylated tau area (D) and mean gray value (E) in CA1 hippocampal region from mice treated with MCSF or vehicle control. Vehicle N=4, and MCSF treatment N=5. Scale bar 250 µm. Veh: vehicle. Bars indicate means ± SEM and dots represent individual animals.

Statistical differences between groups were assessed by not pairing-measures Student's t-test, compared with vehicle group.

In summary, MCSF treatment in the 3xTg-AD model of AD reduces Aβ brain plaque load but does not reduce hyperphosphorylated tau.

4.2. MCSF treatment does not modify TFEB expression in the 3xTg-AD mouse model of AD.

MCSF reduced Aβ plaque burden in the 3xTg-AD mouse model of AD and promoted nuclear localization of the lysosomal master regulator TFEB. Next, we evaluated the effect of MCSF treatment on TFEB expression in 3xTg-AD mice *in vivo*. TFEB and Iba1 double immunofluorescence staining was performed on mouse brain coronal tissue sections. As per our previous findings, the study focused on TFEB expression in microglia on the CA1 region of the hippocampus. TFEB immunofluorescence intensity was measured both in the nucleus and cytoplasm of $Iba1^{+}$ microglia. Both compartments were created based on Iba1 and DAPI staining, as explained in experimental procedures (subsection 16.1). No differences were seen in hippocampal microglial nuclear or cytosolic TFEB levels between animals treated with MCSF and vehicle control (Figure 38A and 38B). According to these results, MCSF treatment in adult 3xTg-AD mice does not modify TFEB activation state in hippocampal microglia.

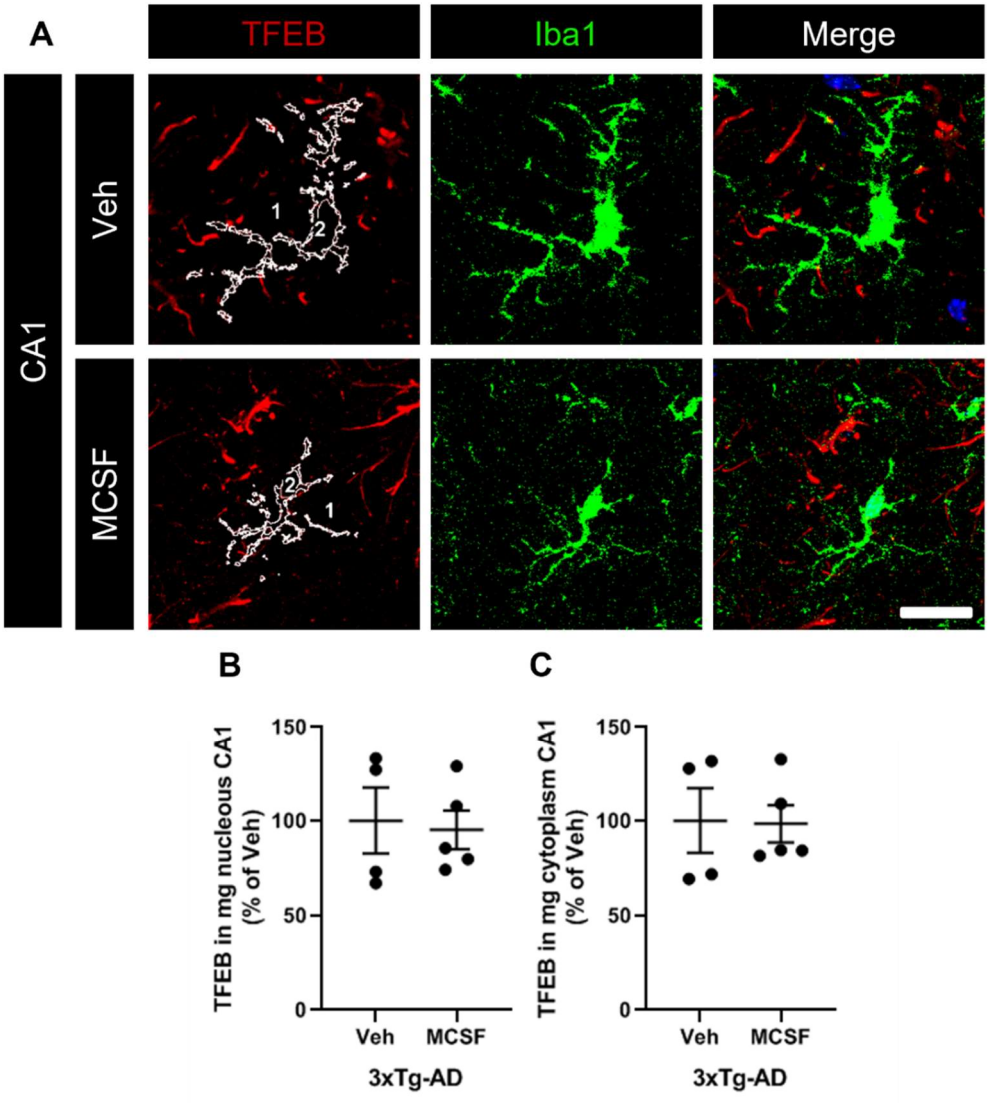

Figure 38. MCSF treatment does not change TFEB expression in CA1 microglia in the 3xTg-AD mouse model of AD. Representative image of TFEB and Iba1 immunofluorescence (A) and quantification of TFEB staining in microglial nucleus (B) and cytoplasm (C) in the CA1 hippocampal region in 3xTg-AD mice treated with MCSF or vehicle control. Vehicle (N=4), and MCSF treatment (N=5). Scale bar 10 µm. Veh: vehicle. In the image, nuclear (2) and cytoplasmatic (1) compartment are indicated in white ROIs. Bars indicate means ± SEM and dots represent individual animals. Statistical differences between groups were assessed by not pairing-measures Student's t-test, compared with vehicle group.

4.3. MCSF treatment elevates hippocampal postsynaptic markers in the 3xTg-AD mouse model of AD.

To evaluate the effect of MCSF on synaptic pathology in the 3xTg-AD model of AD, tissue sections from mice treated with MCSF or vehicle control were immunoreacted against synaptophysin and homer and immunofluorescence was measured in the CA1 hippocampal region. Data showed a significant increase in the levels of homer postsynaptic marker in MCSF-treated mice (153.5±9.864%, **p<0.01)

relative to vehicle group (100±3.73%) (Figure 39A and 39B). However, there were no changes in synaptophysin levels in MCSF-treated mice compared with vehicle group (Figure 39C and 39D).

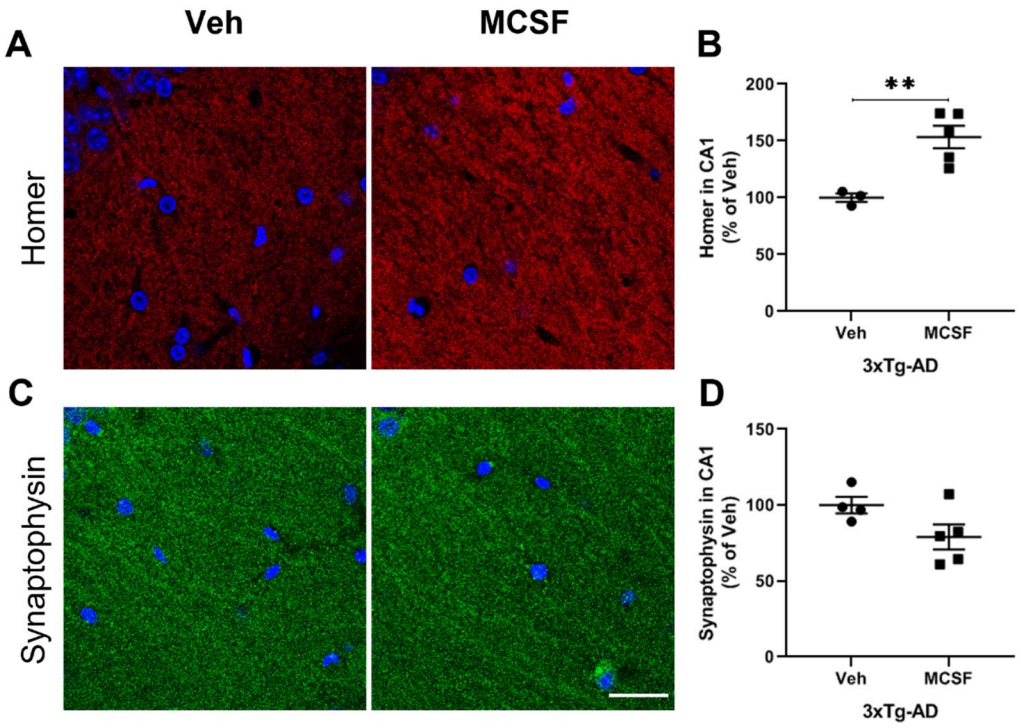

Figure 39. MCSF treatment increases homer protein levels in the CA1 area of hippocampus in the 3xTg-AD mouse model of AD. Representative images of homer and synaptophysin immunoreactivity (A, C) and quantification of homer (A and B) and synaptophysin (C and D) immunofluorescence in the CA1 area of hippocampus in mice treated with MCSF or vehicle control Vehicle (N=4), and MCSF (N=5). Scale bar 35 µm. Veh: vehicle. Bars indicate means ± SEM and dots represent individual animals. Statistical differences between groups were assessed by not pairing-measures Student's t-test. P**<0.01 compared with vehicle group.

Overall, MCSF treatment improves postsynaptic pathology in the CA1 region of the hippocampus in the 3xTg-AD model mice.

4.4. MCSF treatment reduces inflammation in the 3xTg-AD mouse model of AD.

Finally, we studied the impact of MCSF treatment on inflammation in the 3xTg-AD mouse model of AD. To do so, we first measured baseline microgliosis in the CA1 area of the hippocampus as a relative measure of inflammation. Mouse brain sections were immunoreacted against Iba1 antibody and immunofluorescence was used to assess microglial morphological alterations in 3xTg-AD mice and WT mice. A significant increase in the area occupied by Iba1 staining was observed in 3xTg-AD mice

(208.8±18.8%, **p<0.01), relative to WT mice (100±12.65%, **p<0.01) (Figures 40A and 40B).

Microglial morphology was also evaluated, using FIJI plugins -AnalyzeSkeleton (2D/3D) and Fraclac, as described in the experimental section (subsection 16.1). Briefly, AnalyzeSkeleton (2D/3D) plugin generates skeletonized images that dissect microglial processes and examines the complexity and spread of the cells, whereas the Fraclac plugin uses outlined images to examine the morphology and spread of cells. Digital image analysis using these approaches revealed a significant increase of Iba1 total length (214.2±19.24%, **p<0.01), branches (405.5±29.55%, ****p<0.0001), junctions (435.4±45.76%, ***p<0.001), and triple points (440.5±51.89%, ***p<0.001) and a significant reduction in density (48.32±0.92%, ***p<0.001) in 3xTg-AD mice relative to WT [total length (100±14.68%), branches (100±12.3%), junctions (100±18.93%), triple points (100±17.09%) and density (100±5.85%), respectively]. However, microglial process span ratio did not differ between 3xTg-AD and WT (Figures 40C-J). These parameters give information about cell spread, complexity and shape, as described in experimental procedures (subsection 16.1). According to these results, 3xTg-AD microglia show increased overall lengths and morphological complexity when compared with WT mice.

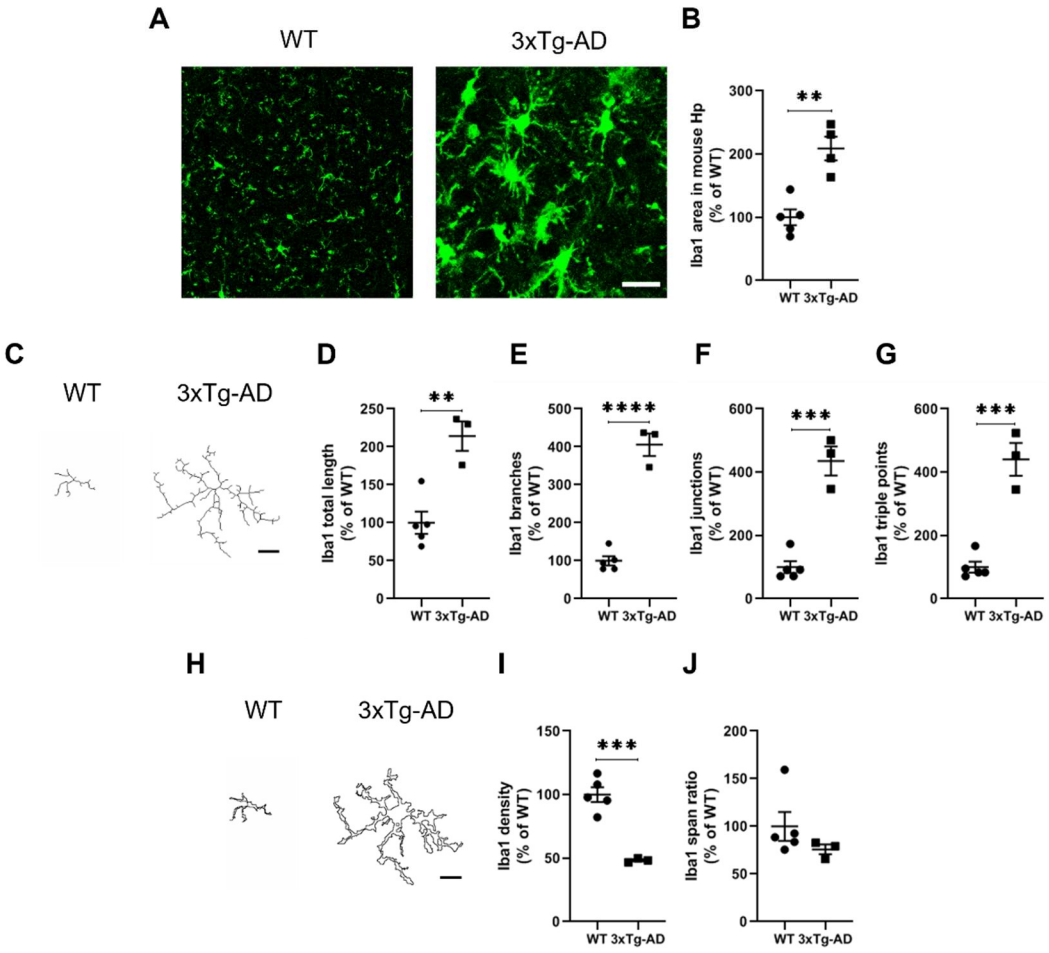

Figure 40. Microglia morphology is more complex in the 3xTg-AD model of AD when compared with WT mice. Representative images of Iba1 immunofluorescence (green) (A) and quantitative analysis (B) in the CA1 hippocampal region in 3xTg-AD mice and WT mice. Representative image of Iba1$^+$ microglia converted to skeletonized (C) and outlined (H) forms and quantification of total length (D), branches (E), junctions (F), triple points (G), density (I) and span ratio (J) in the CA1 area of hippocampus in 3xTg-AD and WT mice. WT N=5 and 3xTg-AD N=4 Scale bar 40 µm (A) and 10 µm (C and H). WT: wild type. Bars indicate means ± SEM and dots represent individual animals. Statistical differences between groups were assessed by not pairing-measures Student's t-test. **p<0.01, ***p<0.001, ****p<0.0001 compared with WT group.

Next, we evaluated baseline astrogliosis in 3xTg-AD brain and compared it with WT. To do so, brain tissue sections were immunoreacted against immune GFAP antibody and morphological alterations in astrocytes were measured GFAP$^+$ astrocytes changed remarkably in 3xTg-AD brain tissue when compared with WT. First, a significant increase in GFAP staining area was seen in 3xTg-AD brain (693.5±68.32%, ****p<0.0001) relative to WT (100±7.73%) (Figures 41A and 41B). Moreover, Fraclac analysis revealed a significant decrease in the density (57.75±2.55%, ***p<0.001) and span ratio (63.1±1.61%, **p<0.01) of astrocytes in 3xTg-AD relative to WT [density (100±5.39%) and span ratio (100±6.55%), respectively]. (Figures 41C-E). These results suggest that

astrocytes became hypertrophic and develop a more complex morphology in 3xTg-AD mouse brain when compared with WT.

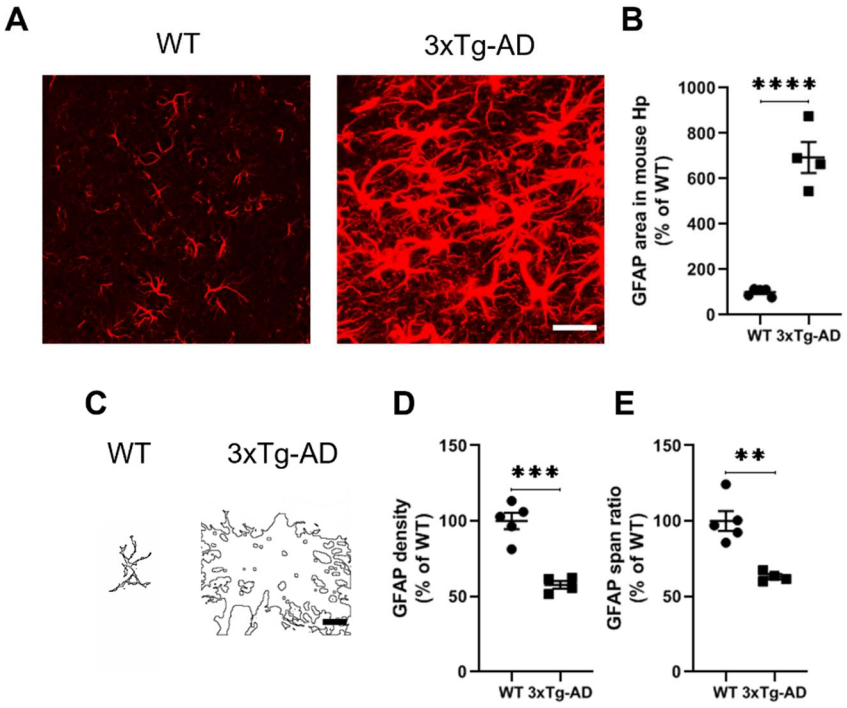

Figure 41. Astroglial area and morphology changes in the 3xTg-AD mice compared with WT. Representative images of GFAP immunoreactivity (red) (A) and quantitative analysis (B) of GFAP immunofluorescence area in the CA1 area of hippocampus in 3xTg-AD and WT Representative outlined images of GFAP staining (C) and quantification of density (D) and span ratio (E) in the CA1 area of hippocampus in the 3xTg-AD and WT mice. WT (N=5) and 3xTg-AD (N=4). Scale bar 40 µm (A) and 10 µm (I). WT: wild type. Bars indicate means ± SEM and dots represent individual animals. Statistical differences between groups were assessed by not pairing-measures Student's t-test. **p<0.01, ***p<0.001, ****p<0.0001 compared with WT group.

After establishing baseline micro- and astrogliosis in 3xTg-AD and WT mouse hippocampus, we studied these observables in mice treated with MCSF or vehicle control using Iba1 and GFAP immunoreactivity. Iba1^{+} microglia area was significantly decreased in 3xTg-AD mice treated with MCSF (72.78±5.41%, *p<0.05) relative to vehicle group (100±9.01%) (Figures 42A and 42B). Skeletal and Fraclac analysis revealed a significant reduction in the number of branches (72.82±5.41%, *p<0.05), junctions (69.38±5.96%, *p<0.05) and triple points (70.81±5.36%, *p<0.05) as well as in the total length of processes (77.42±5.46%, p=0.06), although the latter was not statistically significant compared with vehicle group [branches (100±12.3%), junctions (100±10.51%), triple points (100±11.78%) and total length (100±8.98%), respectively] (Figures 42C-G). Density and span ratio did not differ between 3xTg-AD mice treated

with MCSF or vehicle (Figures 42I-J). According to these results, microglia occupied less area and became morphologically less complex after MCSF treatment in the 3xTg-AD mice, which is indicative of a reduction in microgliosis.

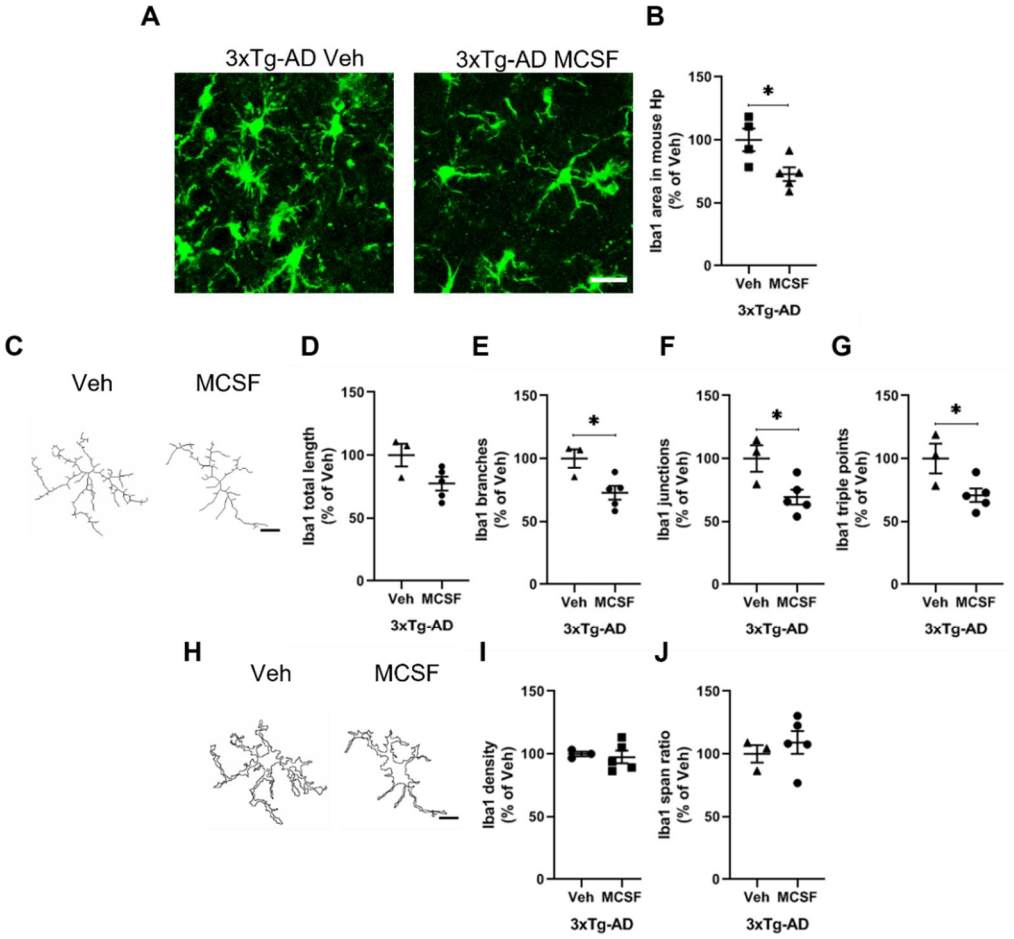

MCSF treatment reduces microgliosis in the 3xTg-AD mouse model of AD. Representative images of Iba1 immunoreactivity (green) (A) and quantitative analysis (B) of Iba1 immunofluorescence area (green) in the CA1 area of hippocampus in 3xTg-AD mice treated with MCSF or vehicle group. Representative image of $Iba1^{+}$ microglia converted to skeletonized (C) and outlined (H) forms and quantification of total length (D), branches (E), junctions (F), triple points (G), density (I) and span ratio (J). Vehicle (N=4) and MCSF (N=5). Scale bar 40 µm (A) and 10 µm (C and H). Veh: vehicle. Bars indicate means ± SEM and dots represent individual animals. Statistical differences between groups were assessed by not pairing-measures Student's t-test. *p<0.05 compared with vehicle group.

GFAP staining in the CA1 area of hippocampus revealed a significant reduction in immunoreactive area in 3xTg-AD mice treated with MCSF (67.25±6.41%, *p<0.05) relative to vehicle (100±9.85%) (Figures 43A and 43B). Moreover, Fraclac analysis showed a significant reduction in density (69.78±7.29%, *p<0.05) and a significant increase in span ratio (130.9±8.03%, *p<0.05) in MCSF treated mice compared with vehicle [density (100±4.4%) and span ratio (100±2.55%), respectively] (Figures 43C-E).

According to these results, both the total area occupied by astrocytes and their size are reduced in 3xTg-AD mice following MCSF treatment.

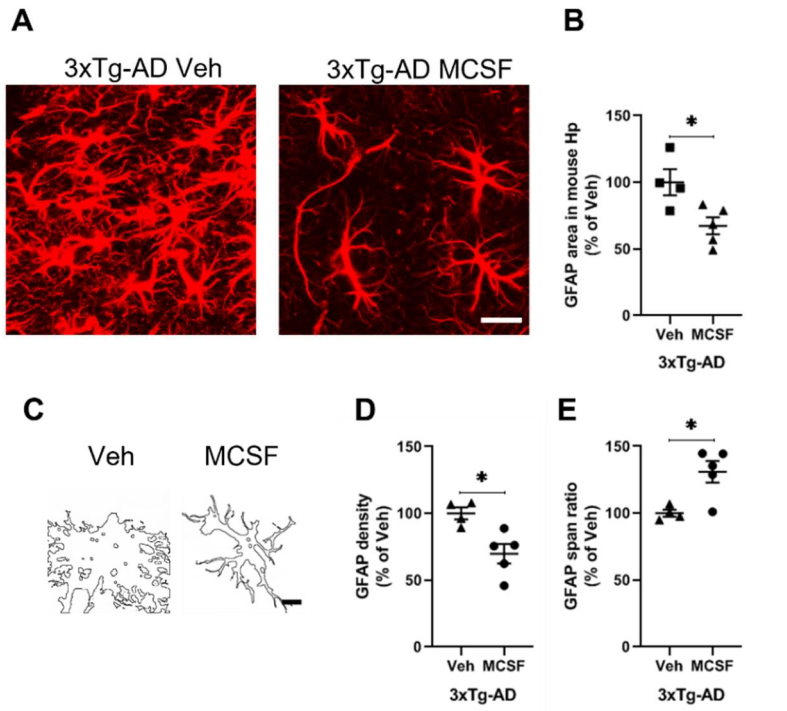

Figure 43. MCSF treatment reduces astrogliosis in the 3xTg-AD model of AD. Representative images of GFAP immunoreactivity (A) and quantitative analysis (B) of GFAP immunofluorescence (red) in the CA1 area of hippocampus in 3xTg-AD mice treated with MCSF or vehicle. Representative image of $GFAP^{+}$ astrocytes converted to outlined (C) forms and quantification of density (D) and span ratio (E) Vehicle (N=4) and MCSF (N=5). Scale bar 40 µm (A) and 10 µm (C). Veh: vehicle Bars indicate means ± SEM and dots represent individual animals. Statistical differences between groups were assessed by not pairing-measures Student's t-test. *p<0.05 compared with vehicle group.

In summary, microglia and astrocytes appear enlarged and higher number of processes in 3xTg-AD hippocampus when compared with WT, consistent with increased micro- and astrogliosis. Remarkably, MCSF treatment reduced gliosis towards a phenotype resembling that of WT mouse brain. These results suggest that MCSF helps reducing inflammation in the brains of 3xTg-AD mice.

Next, MCSF and TNFα cytokine levels were quantified by ELISA in cortical homogenates prepared from 3xTg-AD mice treated with MCSF or vehicle. MCSF levels were increased (153.6±18.56%, p=0.18) and TNFα levels were decreased, (67.54±22.02%, p=0.29) in 3xTg-AD mice treated with MCSF, but these differences were not statistically significant compared with the vehicle [MCSF (100±33.79%) and TNFα (100±16.91%), respectively] (Figures 44A and 44B, respectively).

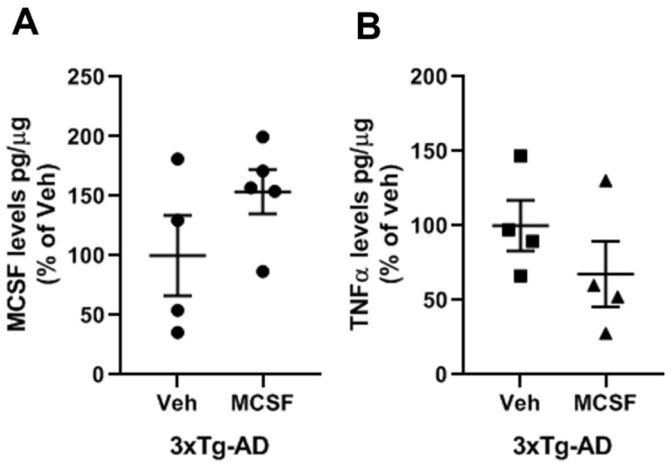

Figure 44. MCSF treatment does not alter MCSF or TNFα levels in the 3xTg-AD mouse model of AD. Quantification of MCSF (A) and TNFα (B) levels in cortical brain homogenates in 3xTg-AD mice treated with MCSF or vehicle quantified by ELISA immunoassay. Vehicle N=4 and MCSF N=5. Veh: vehicle Bars indicate means ± SEM and dots represent individual animals. Statistical differences between groups were assessed by not pairing-measures Student's t-test, compared with vehicle group.

In summary, MCSF treatment *in vivo* reduces Aβ brain plaque load, helps mitigating microgliosis and astrogliosis and increases postsynaptic markers in the CA1 region of the hippocampus in the 3xTg-AD model of AD.

5. Study of MCSF/CSF-1R axis and TFEB as biomarkers in the *post-mortem* hippocampus of AD.

We proceeded to evaluate whether our findings in our *in vitro*, *ex vivo* and *in vivo* AD models translated into human AD *post-mortem* brain samples. For that purpose, we quantified the proteins of interest in *post-mortem* hippocampal tissue from AD patients and compared it to those of age-matched healthy subjects. AD cases were classified according to Braak stages II, III, IV and V (Braak and Braak, 1991). Cases are described in detail at the experimental procedures (Table 2).

MCSF levels were measured by ELISA in hippocampal brain homogenates from tissues classified as Braak stages II, III, IV and V and compared with control. MCSF levels tended to decrease as disease progressed from Braak stages II to V relative to control cases (Figure 45A). Student's t-test analysis revealed a statistically significant difference

between MCSF levels in tissues classified as Braak V stage (48.29±7.29 %, *p<0.05) relative to control condition (100±10.17) (Figure 45B).

Our proteomic results indicated that MCSF lowers CSF-1R expression, which is indicative of MCSF/CSF-1R axis activation (Figure 18). Accordingly, we investigated whether the reduction in MCSF observed during AD pathogenesis could affect CSF-1R expression. Interestingly, our results showed an increase in CSF-1R protein expression with disease progression from Braak stage II to V relative to age-matched healthy subjects, although these differences were not statistically significant, as determined by One-way ANOVA (Figure 45C and 45D). However, a significant increase in CSF-1R protein expression was observed in Braak V stage (170.2±20.42 %, *p<0.05) relative to control cases by Student's t-test analysis (87.88±32.04) (Figure 45C and 45E). A reduction in MCSF expression at late stages of the disease could reflect an alteration of the activation of MCSF/CSF-1R axis.

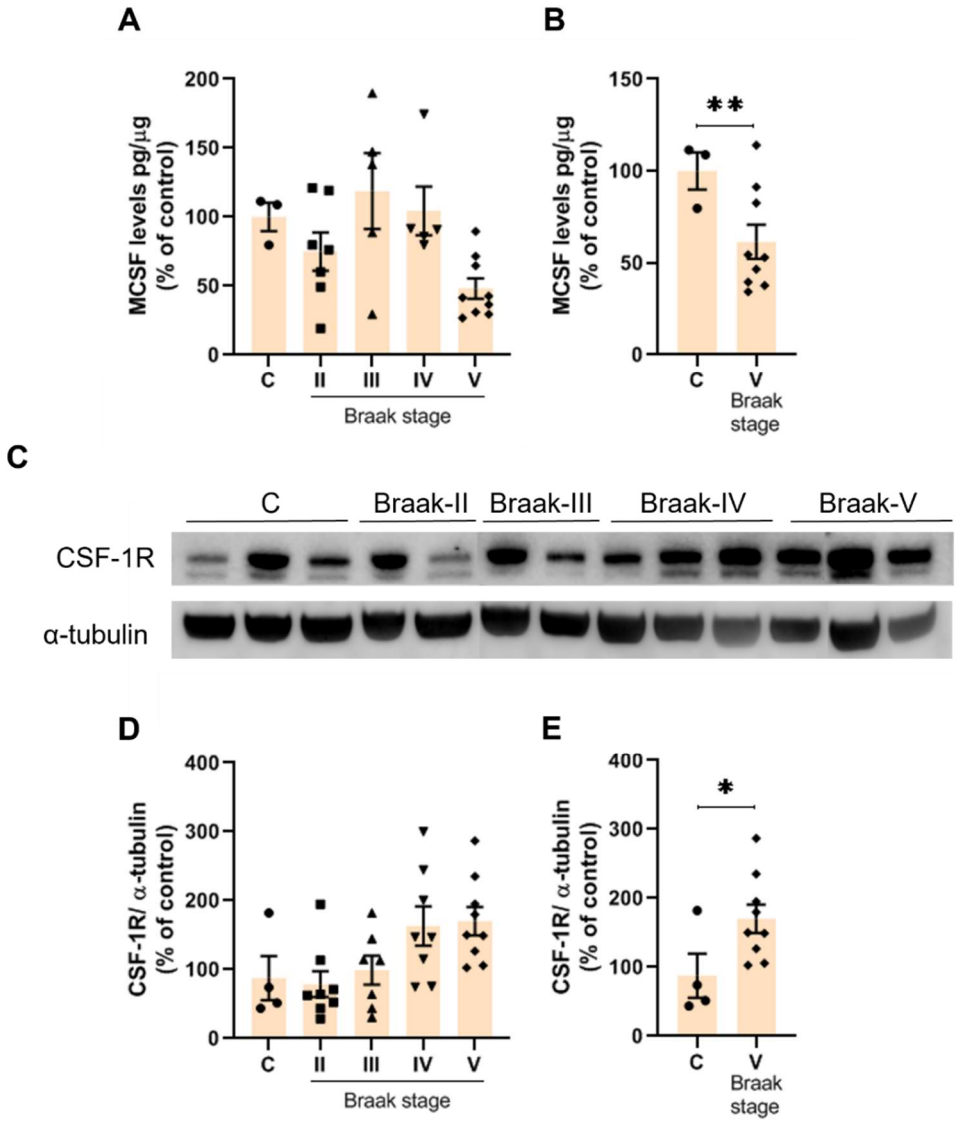

Figure 45. MCSF and CSF-1R levels are altered in hippocampus of AD patients. (A-B) Quantification of MCSF levels by ELISA immunoassay in hippocampal tissue homogenates (C-E) Representative image of a Western blot and quantifications of CSF-1R expression in hippocampal tissue from AD cases and healthy subjects MCSF levels were measured in control, n=3; Braak II, n=7; Braak III, n=5; Braak IV, n=4; and Braak V, n=9. In turn, CSF-1R levels were evaluated in control N=4, Braak II N=8, Braak III N=7, Braak IV N=8 and Braak V N=9. Bars indicate means ± SEM and dots represent individual cases. Statistical differences between groups were assessed by not pairing-measures One-way ANOVA with Dunnett correction on A and D, and not pairing-measures Students t-test on B and D. *p<0.05, **p<0.01. compared with control group.

Finally, we evaluated TFEB expression in human brain samples and a significant increase in TFEB protein levels was found in the hippocampus of AD patients at Braak III (239.4±31.57%, *p<0.05) and Braak V stages (244.2±28.48%, *p<0.05) relative to age-matched control cases (100±15.02) (Figure 46A-C). In conclusion, TFEB expression increases in the hippocampus as early as Braak stage III in AD.

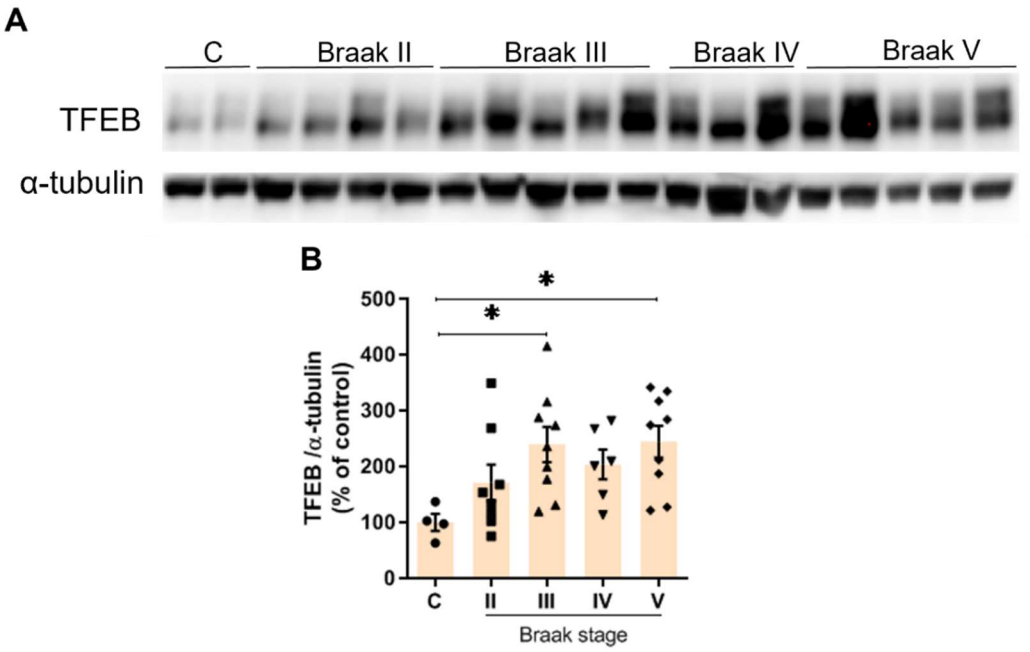

Figure 46. TFEB expression is increased in the hippocampus of AD patients at Braak stages III and V. (A) Representative image of a Western blot and (B) quantification of TFEB expression in hippocampus of AD and healthy subjects Braak II N=4, Braak III N=8, Braak IV N=8 and Braak V N=9. Bars indicate means ± SEM and dots represent individual cases. Statistical differences between groups were assessed by not pairing-measures One-way ANOVA with Sidak correction. *p<0.05, **p<0.01 compared with control group.

Taken together, in the results obtained using *post-mortem* tissue suggest that TFEB expression and the MCSF/CSF-1R axis are altered in the hippocampus of AD patients.

Discussion

Several studies reported that microglia modulation can play a beneficial role in the progression of AD. In this study, we proposed MCSF/CSF-1R signaling as a target to promote microglial functions that act beneficially against the amyloid-related pathology in AD.

We first reported that MCSF treatment potentiates receptor density and cytokine expression, downregulates complement cascade factors and increases TFEB nuclear translocation in microglia. Interestingly, oAβ disrupts the expression of some of the MCSF-promoted microglial receptors and TFEB nuclear localization. Also, MCSF promoted oAβ internalization and attenuated oAβ-associated synaptic damage *in vitro*. Two-photon time-lapse imaging of organotypic brain cultures from the 5xFAD model of AD revealed a reduction in oAβ-associated microglial morphology and motility alterations following MCSF treatment. MCSF improves microglial surveillant activity and promotes a more ramified cellular morphology. This effect on surveillance was corroborated in an additional *ex vivo* model. Both in the rat organotypic culture treated with oAβ and in 5XFAD organotypic cultures, we observed that the area occupied by microglia increased, and MCSF reverted this effect. This effect was also observed in 5XFAD astrocytes (Figure 47).

Adult 3xTg-AD mice treated with MCSF showed decreased Aβ brain plaque load. Synaptic pathology was also improved, and astrogliosis and microgliosis was drastically reduced in the CA1 region of the hippocampus. Remarkably, MCSF treatment in 3xTg-AD mice mitigated the increase in cellular complexity and area occupied by microglia and astrocytes relative to WT animals, which is indicative of a reduction in gliosis (Figure 45).

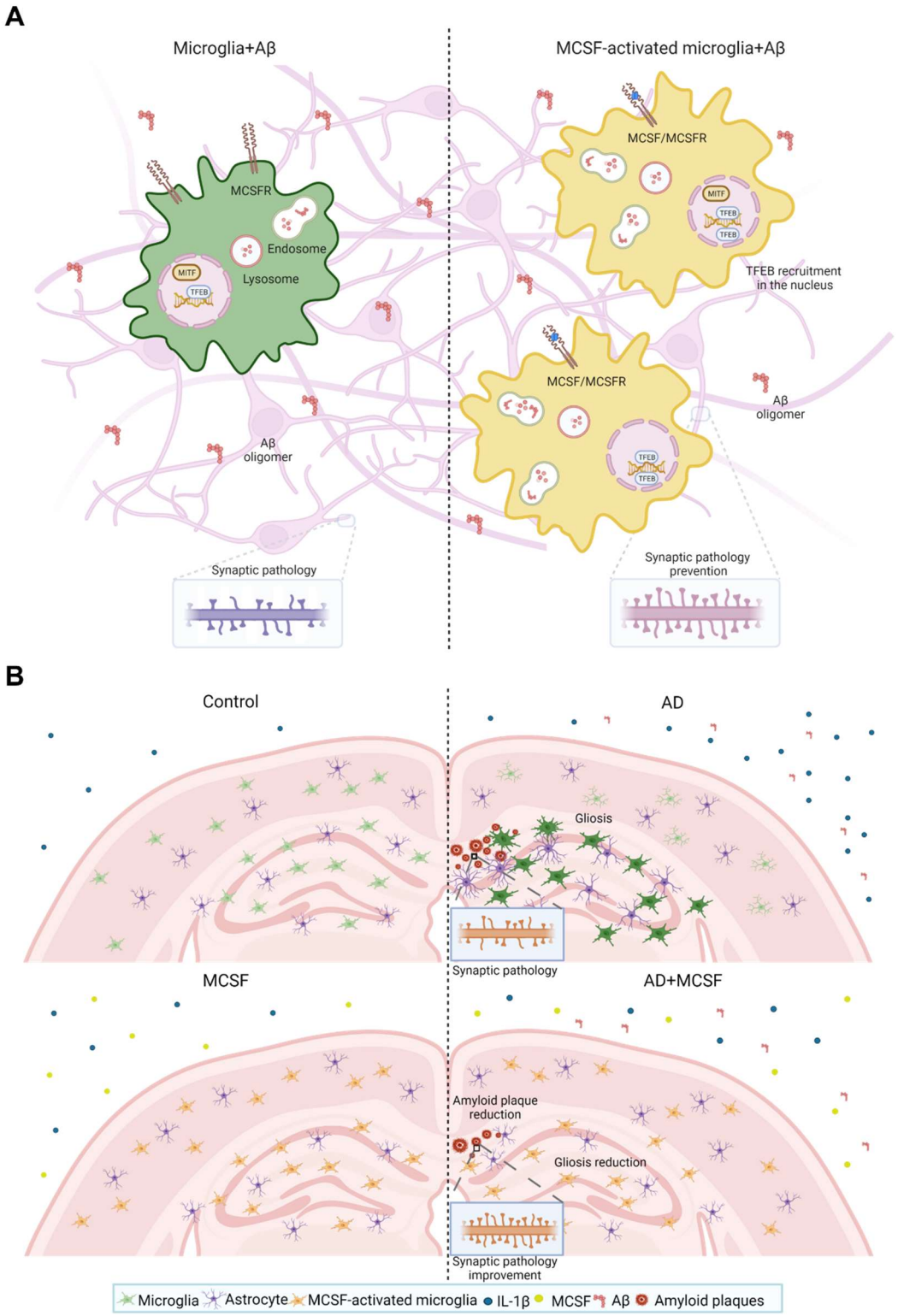

Figure 47. Diagram of *in vitro*, *ex vivo* and *in vivo* effects of MCSF treatment in AD models. (A) MCSF-treated microglia show increased proliferation, oAβ internalization and nuclear TFEB expression, thus promoting oAβ elimination, and improving synaptic pathology induced by oAβ in neuron-microglia co-culture. (B) *Ex vivo* and *in vivo* AD models show gliosis, synaptic pathology, and Aβ plaque deposition whereas MCSF treatment reduces gliosis and IL-1β levels, Aβ plaque deposition and synaptic pathology.

Finally, we observed that MCSF levels were reduced whereas CSF-1R levels were increased in the *post-mortem* hippocampus of AD patients relative to age-matched healthy subjects, suggesting an alteration in the MCSF/CSF-1R axis. Furthermore, TFEB levels were increased in the hippocampus of AD patients relative to age-matched healthy subjects, which may lead to an imbalance in TFEB signaling and lysosomal biogenesis.

1. MCSF activation potentiates microglial Aβ clearance.

Aβ monomers aggregates into oligomers that will lead to protofibers and fibrils, and eventually generate senile plaques. Oligomeric Aβ represents the predominant neurotoxic Aβ species in AD (Klein, 2002; Glabe, 2005) and the Amyloid Cascade Hypothesis postulates that Aβ triggers synaptotoxicity, chronic inflammation and tauopathy, leading to a progressive cognitive decline (Jack et al. 2013; Haass and Selkoe 2007; J. Hardy 2002). Thus, the development of strategies to remove Aβ is crucial to fight AD.

Microglia are involved in different mechanisms to clear Aβ (Ries and Sastre 2016). However, as disease progresses, microglia efficiency to eliminate Aβ is compromised, which might exacerbate disease progression. As Majumdar et al. (2007) described, surveillant microglia are not efficient at degrading fibrillar Aβ aggregates unless they were activated by cytokines such as MCSF. In primary microglial cultures, MCSF speeds up microglial Aβ internalization contributing to the reduction of extracellular Aβ levels.

Additional to Aβ internalization, microglia can also secrete enzymes involved in the extracellular degradation of proteins. MCSF can promote the expression of secreted degrading enzymes such as IDE and MMP9 that have been implicated in AD degrading Aβ extracellular species (Zhao et al., 2007; Gu et al., 2020). To study whether MCSF was also involved in extracellular degradation of Aβ in primary microglia cultures, we evaluated the expression of IDE, MMP2, MMP9 and plasminogen. However, neither the presence of Aβ nor MCSF modified the expression of those genes, indicating that MCSF was mainly involved in promoting microglial internalization of Aβ but not its extracellular degradation.

In a previous study, Boissonneault et al. (2008) reported that MCSF treatment *in vivo* reduced Aβ brain plaque load, via increased Aβ internalization and degradation by microglial cells and even improving cognitive decline at 2-6 months old APP/PS1 male mice. To further evaluate the impact of MCSF on Aβ and tau pathology *in vivo*, we treated 3xTg-AD female mice with MCSF. The 3xTg-AD mouse harbors the Swedish mutation in the human amyloid precursor protein (APPSwe), presenilin knock-in mutation (PS1M146V), and TauP301L mutant transgene (TauP301L) and is characterized by age-related, progressive neuropathology including Aβ plaques neurofibrillary tangles and inflammation (Oddo et al., 2003). It was previously reported that Aβ-immunoreactive plaque deposition occurs earlier in females that males (Oh et al., 2010; Perez et al., 2011) and we studied the effect of MCSF treatment in female mice only, due to animal availability. MCSF treatment in 3xTg-AD female mice led to a reduction in Thioflavin-S^{+} fibrillar Aβ plaques, but there was no change in hyperphosphorylated tau brain levels. Further research is necessary to evaluate the effect of MCSF in tau pathology.

Thus, MCSF treatment promoted clearance of fibrillar and soluble forms of Aβ by microglia, leading to the reduction of amyloid both *in vitro* and *in vivo* models. MCSF treatment not only reduced acute $A\beta_{1-42}$ exposure *in vitro* but also, reduces already established Aβ plaques of the 3xTg-AD adult mice.

Considering our results as well as previously published, we can conclude that MCSF treatment reduces oligomeric and fibrillar Aβ brain load, both *in vitro* and *in vivo* male and female AD mice.

2. MCSF improves synaptic pathology.

Synaptic dysfunction is reported as an early manifestation of AD and correlates best with cognitive decline (Selkoe, 2002). Soluble forms of Aβ, rather than the large insoluble fibrils, are toxic to synapses (Masliah et al. 1991; Cline et al. 2018). Thus, exogenous addition of synthetic oAβ to WT neurons reduces postsynaptic markers and alterations in postsynaptic markers are blocked by γ-secretase inhibition in APP mutant neurons (Almeida et al., 2005).

Since MCSF treatment contributed to a reduction in Aβ levels *in vitro* and Aβ plaque load *in vivo*, we studied whether this could benefit Aβ-related synaptic pathology in our AD models. We first confirmed that 1 μM oAβ induced pre- and postsynaptic alterations in neuronal primary cultures and presynaptic alterations in neuronal-microglial co-cultures. In our neuronal-microglial co-cultures, the presence of MCSF attenuated presynaptic damage induced by oAβ, suggesting that oAβ removal by MCSF-activated microglia restores synapses. Moreover, post synapses increased in MCSF-treated 3xTg-AD mice relative to vehicle. These results suggest a role played by MCSF in ameliorating Aβ-induced synaptic pathology, consistent with previously reported data indicating that MCSF treatment *in vivo* mitigated cognitive decline in APP/PS1 mice (Boissonneault et al., 2008).

3. Role of oAβ and MCSF in microglial degradation machinery.

Previous work showed that MCSF treatment made microglia more efficient at degrading fibrillar forms of Aβ. Microglial lysosomal degradation of Aβ was in part dependent on efficient mobilization of CLC-7, a chloride antiporter, to the lysosome. In turn, CLC-7 mobilization to the lysosome depends on OSTM1 protein, its chaperone, which is responsible for CLC-7 transport to the organelle. In MCSF-activated microglia, OSTM1 associates with CLC-7 at higher rates, rescues CLC-7 from endoplasmic reticulum-associated degradation, and helps translocate it to the lysosomes, which results in increased lysosomal acidification and efficient degradation of fibrillar Aβ (Majumdar et al., 2011).

As per these findings, we wanted to further study the mechanisms modulating lysosomal degradation in the context of Aβ pathology. We first investigated the effect of oAβ and MCSF on transcription of genes related to lysosomal biogenesis. Overall, neither oAβ nor MCSF altered the expression of LAMP1, OSTM1, TFEB and MITF. MCSF treatment of primary microglia led to a minor increase in TFEB gene expression and a significant increase in TFEB nuclear translocation. As reported for the expression of some microglial receptors, the presence of oAβ abrogated this effect. However, we did not see differences in TFEB expression following MCSF treatment *in vivo*. Interestingly, TFEB expression is increased in AD patients at late stages. These findings *in vitro* an in

post-mortem tissue warrant further experiments to clarify the role of TFEB in lysosomal function in AD. Also, TFEB activation by MCSF as shown *in vitro*, needs further research to establish a connection between these two factors.

Previous studies reported that high concentrations of fibrillar Aβ (5 and 10 μM) caused a reduction in the expression of OSTM1, promoted the cytoplasmic localization of TFEB and increased LAMP1 expression, indicating lysosomal dysfunction (Guo et al., 2017). Regarding that TFEB regulates LAMP1 expression, the recruitment of TFEB in the cytoplasm theoretically should not induce the expression of LAMP1 and also, the Aβ concentration used might be too high. However, in our hands, neither LAMP1 nor OSTM1 levels changed following 1μM oAβ treatment in microglia *in vitro*.

When compared with previous studies, our working oAβ concentration was significantly lower (1μM versus 10μM). Also, we used oligomeric Aβ instead of fibrillar. Thus, our *in vitro* conditions do not seem to be detrimental for microglial lysosomal degradation machinery.

Further experimental work is needed to clarify whether higher concentrations of oAβ are detrimental for the lysosomal degradation machinery. Also, it is not yet clear which form of Aβ (fibrillar or soluble) is most detrimental towards the proper functioning of the lysosomal degradation machinery in microglia.

4. MCSF reverts surveillance and motility alterations induced by oAβ in microglia.

In the presence of an insult, microglia adopt a pro-inflammatory stage, change their morphology (shortening their processes and enlarging their soma), proliferate, and migrate towards the injury site, thereby accumulating around the damaged areas. In their highest activation state, microglia adopt a severe amoeboid morphology resembling that of macrophages (Fernandez-Albarral et al., 2022).

We first evaluated whether, the area occupied by microglia and astrocytes was increased in our *ex vivo* and *in vivo* AD models, which could be used as an indication of reactive, pro-inflammatory status. Both in the two *ex vivo* models studied, oAβ-treated WT slices and 5xFAD brain slices, the area occupied by microglia and astrocytes was increased in the hippocampus. This observation was corroborated *in vivo* in 3xTg-AD

model mice. Also, morphological analysis of cortical microglia revealed an increase in the number of processes and their spread as well as a reduction in microglial soma size in 5XFAD *ex vivo* model relative to WT.

It has been reported that MCSF triggers a rapid membrane response followed by cell spreading and polarization (Boocock et al., 1989; Webb et al., 1996; Chitu et al., 2005). Accordingly, we evaluated the effect of MCSF treatment on Aβ-related glial morphological changes.

The presence of MCSF in 5XFAD *ex vivo* slices or coincubated with oAβ in rat organotypic cultures, mitigated oAβ-induced glial morphological alterations. As seen in *ex vivo* experiments, MCSF treatment in 3xTg-AD mice also reverted the increase in Iba1 and GFAP area and complexity, indicative of gliosis, towards a WT phenotype.

Previous studies using two-photon microscopy to visualize cerebral slice preparations revealed that microglial motility was reduced in AD mouse models (Krabbe et al., 2013). Also, impaired baseline dynamics in plaque-associated microglia was described (Koenigsknecht-Talboo et al., 2008). Thus, we first evaluated whether oAβ altered microglial dynamics by *in vivo* time-lapse imaging in organotypic cultures. Our results indicate that microglial surveillance is altered in the presence of extracellular oAβ and MCSF treatment reverts these effects, highlighting the beneficial role of MCSF in promoting microglia surveillance.

Our experiments in microglial morphology and surveillance indicate that oAβ alters microglial motility, and this effect can be rescued by MCSF. Surprisingly, we obtained somewhat opposite result depending on the experimental technical approach. Immunofluorescence staining with Iba1 and GFAP labeling shows a more expanded and complex microglia and astrocytes in the fixed *ex vivo* and *in vivo* AD models, whereas in the live time-lapse imaging experiments using GFP^+ microglia from the $Cx3Cr1^{+/eGFP}$ model, microglia are less expanded and complex in presence of oAβ. However, in both cases MCSF reverts the effect induced by oAβ towards a WT phenotype. Further research is needed to clarify such opposed observations on glial status associated with different AD models.

Interestingly, MCSF also modulates astrocytic responses to Aβ, suggesting an involvement of additional mechanisms independent of microglial CSF-1R signaling cascade.

5. Pro- and anti-inflammatory microglial phenotype following MCSF treatment.

Post-mortem brains from AD patients and APP transgenic animals exhibit increased levels of pro-inflammatory cytokines and chemokines including IFNγ, TNFα, IL-1β and IL-6 (Hoozemans et al., 2006; Wyss-Coray, 2006; Heneka and O'Banion, 2007; Rojo et al., 2008). Aβ can interact with microglial receptors and induce inflammatory responses. It has been reported that CD40-CD40L system is a critical enhancer of microglial activation in a mouse model of AD and is involved in promoting the acute-phase inflammatory response in the CNS. In fact, studies have shown that CD40 ligation and nanomolar levels of Aβ synergistically induce microglial activation as measured by TNFα production (Tan et al., 1999). CD36 is also related to downstream activation of pro-inflammatory responses (Sheedy et al., 2013). Unfortunately, even though our results show morphological microglial alterations indicative of reactive microglia, we did not observe any changes in the expression of inflammatory cytokines in our models, probably due to the large variability observed both *in vitro* and *in vivo*.

MCSF has the capacity to polarize microglia towards both pro-inflammatory and anti-inflammatory profiles depending on the microenvironment and other inflammatory molecules (Hamilton et al., 2014). On the one hand, MCSF increases the expression of CD40, TNFα, IL-6 and TGFβ1 in macrophages (Vogel et al., 2014). However, MCSF and IL-4, IL-10, IL-13, or a mixture of these mediators induce anti-inflammatory function (Mantovani et al., 2004; Durafourt et al., 2012). Notwithstanding, microglia activation by MCSF can generate inflammatory response. Murphy et al. (1998) observed an increase in MCSF levels in AD which could magnify Aβ-induced production of microglial inflammatory cytokines and nitric oxide, which in turn could intensify the cerebral inflammatory state. Moreover, in experiments using neuronal-microglial co-cultures MCSF and 10 μM fibrillar Aβ treatments induced an enhancement of neurotoxicity mediated by ROS production (Li et al., 2004).

Under our experimental conditions, MCSF treatment promoted microglia towards a pro-inflammatory, rather than anti-inflammatory, phenotype. CD40 and pro-inflammatory cytokines TNFα, IL-6 and TGFβ1 were upregulated in our transcriptomic analysis. However, the anti-inflammatory receptor MSR1 as well as CD36 gene expression was upregulated. CD36 protein levels, however, were downregulated. Interestingly, under Aβ-associated pathological conditions, MCSF seems to promote an anti-inflammatory status. MCSF treatment reduced the levels of IL-1β observed in the 5XFAD *ex vivo* model and mitigated micro- and astrogliosis both *ex vivo* and *in vivo* in 3xTg-AD mice.

The complement system plays an essential role in maintaining brain homeostasis as it participates in host defense by quickly recognizing and eliminating pathogens, cellular debris, and misfolded proteins (Gomez-Arboledas et al., 2021). During development, the complement system participates on refining the synaptic circuits. This process is mainly mediated by microglia and the classical complement cascade (Stevens et al., 2007). Interestingly, in AD mouse models, C1q and C3 are highly upregulated, paralleling Aβ deposition (Reichwald et al., 2009). Furthermore, C4 has also been implicated in mediating synaptic removal (Sekar et al., 2016). Any role presumably played by MCSF in modulating the complement system is currently unknown. Our transcriptomic analysis showed that 1 µM oAβ was not sufficient to induce alterations in complement components, but MCSF decreased the expression of C2 and a led to a minor reduction in the expression of C3 and C4a genes. Although highly speculative, this may be consistent with our data supporting absence of microglial pruning in our *in vitro* AD model. We cannot discard the possibility that 24 h incubation leads to a complete degradation of synaptic components by microglía. Detailed studies are needed to further evaluate the role of MCSF in modulating the complement system.

Overall, MCSF signaling seems very versatile, with potential to act in pro-inflammatory or anti-inflammatory ways. Exogenous supplementation of MCSF shows beneficial results against Aβ-related pathology.

6. oAβ interferes with the MCSF-activated microglial response.

Our results indicate that even though MCSF alone has the capacity to turn microglia into reactive cells, it generally induces a rather anti-inflammatory state, which is protective against pathology.

However, our data also showed that the presence of oAβ interferes with the effect of MCSF in microglia, particularly in relation to MSR1 and Tyrobp expression and TFEB nuclear localization. While MCSF alone reduces the expression of microglial CSF-1R, and increments the expression of microglial MSR1, Tyrobp, the presence of oAβ diminishes these effects. MCSF treatment increases nuclear TFEB localization, and again oAβ reduces this effect. Whether these observations are due to oAβ alone or to the dynamic, interchangeable roles played by MCSF under pathological conditions is not known.

7. Exploring biomarkers for Alzheimer's disease.

Discovery of biomarkers for different stages of the diseases is of key importance in the development of more efficient therapies against AD.

Previous reports described that, following MCSF treatment, CSF-1R induced a signaling cascade leading to degradation of the receptor by the proteasome (Guilbert and Stanley, 1986; Lee, 1999). Our *in vitro* results are consistent with this observation, since MCSF treatment reduced CSF-1R levels in microglia primary cultures, which is suggestive of receptor internalization and MCSF/CSF-1R axis activation.

However, under AD pathological conditions, MCSF and/or CSF-1R levels are altered. Low levels of MCSF were measured in patients with MCI, which, together with low levels of other hematopoietic cytokines, predicted a rapid progression of the disease towards a dementia diagnosis (Ray et al., 2007; Hume and MacDonald, 2012). In contrast, a recent study reported increased mRNA expression of MCSF and CSF-1R in AD (Walker et al., 2017). According to our data, MCSF/CSF-1R axis is less activated in the *post-mortem* brain hippocampus of AD patients compared with healthy individuals since there is less ligand and more receptor available. Thus, the levels of MCSF are reduced whereas CSF-1R is increased. Although additional studies are needed, the use of

MCSF/CSF-1R axis as biomarker of AD may constitute a promising new avenue of research.

Another potential biomarker proposed by our studies is TFEB. High levels of microRNA-128 (miR-128) (Lukiw, 2007), a microRNA that targets TFEB mRNA, have been reported in hippocampus of AD patients and that lower expression of TFEB and lysosomal genes (Sardiello and Ballabio, 2009). Moreover, increased phosphorylation of TFEB in AD is consistent with its observed progressive nuclear exclusion in brain samples from AD patients (Wang et al., 2016a). Our results also point towards TFEB levels being altered during the progression of AD. Although oAβ did not modified TFEB expression *in vitro*, TFEB protein expression was increased in hippocampus of AD patients at late Braak stages. Our *in vitro* experiments did show that TFEB expression increased in nuclear compartment after MCSF treatment, suggesting that MCSF promotes TFEB nuclear traslocation. Interestingly, oAβ abrogated this effect. Again, we see how the presence of Aβ interferes with MCSF-activated microglial function. Overall, TFEB expression is altered in AD and MCSF is able to modulate its activation *in vitro*. Further studies are necessary to understand the mechanism behind this activation.

8. Are microglia beneficial or detrimental in AD?

Different strategies have been used to evaluate the role played by microglia in AD. This project focuses on the MCSF/CSF-1R axis as a key modulator of microglia against AD progression. However, other strategies targeting CSF-1R have also yielded positive results. One of those strategies is based on the ablation of microglia. The specific CSF-1R inhibitor PLX5622 eliminates microglia from brain parenchyma, preventing microglial association with plaques and improving cognition in aged 3xTg-AD mice (Dagher et al., 2015). Absence of microglia prevent plaque formation in the 5XFAD mice (Spangenberg et al., 2019) . This strategy implies the removal of the microglia from CNS, a drastic and provocative strategy that could result in the loss of essential brain functions. Another approach targets microglia by inhibiting their proliferation. A selective inhibitor of CSF-1R tyrosine kinase activity, GW2580, blocks microglia proliferation and shifts microglia towards an anti-inflammatory phenotype (Olmos-Alonso et al., 2016). This treatment slowed neuronal damage and disease progression in a mouse model of chronic

neurodegeneration (Gomez-Nicola et al., 2013). Importantly, these two strategies highlight the negative contribution of microglia to AD pathogenesis. A third strategy used by us and others, is based on the extracellular supplementation of MCSF. Boissonneault et al. (2008) previously reported the beneficial effects of MCSF *in vivo* on ameliorating cognitive performance and mitigating histopathology in APP/PS1 mice. Majumdar et al., (2011) showed that, surveillant microglia are not able to degrade fibrillar forms of Aβ efficiently unless they are treated with MCSF. Herein we report that exogenous supplementation with MCSF activates several microglial functions that mitigate Aβ-induced synaptic pathology, improve microglial surveillance, and reduce the inflammatory state in our AD models. This third strategy implies that microglia under pathological conditions contribute to the disease progression but can be targeted and modulated to act against it.

Conclusions

1. MCSF upregulates transcription and protein expression of a number of microglial receptors. The presence of oAβ partially reduces this effect for some of the receptors.

2. MCSF modulates microglial inflammatory profile by effecting gene expression for a number of pro- and anti-inflammatory cytokines.

3. MCSF contributes to the removal of both extracellular oAβ *in vitro* and Aβ plaques *in vivo*.

4. Microglia are not able to improve synaptic pathology induced by synthetic oAβ unless activated by MCSF.

5. MCSF treatment revert micro- and astrogliosis observed in adult 3xTg-AD model mice.

6. Microglia surveillance and motility are reduced in AD, and MCSF mitigates this effect in *ex vivo* models.

7. The use of the MCSF/CSF-1R axis as biomarker for AD may constitute an attractive new avenue of research.

Altogether, the results included in this doctoral thesis suggest that MCSF treatment can modify transcriptomics and proteomics in microglia and therefore modulate important microglial functions, namely mainly, we studied Aβ clearance capacity, surveillance, and inflammation functions in MCSF-activated microglia. Overall, we have observed a number of beneficial effects promoted by MCSF treatment of microglia in the context of AD using a variety of models -*in vitro*, *ex vivo* and *in vivo*. Importantly, MCSF treatment in 3xTg-AD adult mice was shown to be beneficial in reducing Aβ plaque load, ameliorating synaptic pathology and mitigating micro- and astrogliosis. This suggests the MCSF/CSF1-R signaling cascade as a potential therapeutic target to treat AD. Additionally, considering that MCSF, CSF-1R and TFEB levels are altered in AD patients, their use as biomarkers for AD could constitute an attractive new avenue of research. The relevance of these findings to AD progression warrants further investigation.

Bibliography

Aguzzi A, Barres BA, Bennett ML (2013) Microglia: Scapegoat, Saboteur, or Something Else? Science 339:156–161 Available at: https://www.science.org/doi/10.1126/science.1227901.

Ajami B, Bennett JL, Krieger C, Tetzlaff W, Rossi FM v (2007) Local self-renewal can sustain CNS microglia maintenance and function throughout adult life. Nature Neuroscience 10:1538–1543 Available at: http://www.nature.com/articles/nn2014.

Akiyama H, Nishimura T, Kondo H, Ikeda K, Hayashi Y, McGeer PL (1994) Expression of the receptor for macrophage colony stimulating factor by brain microglia and its upregulation in brains of patients with Alzheimer's disease and amyotrophic lateral sclerosis. Brain Research 639:171–174 Available at: https://linkinghub.elsevier.com/retrieve/pii/0006899394917795.

Alberdi E, Sánchez-Gómez MV, Cavaliere F, Pérez-Samartín A, Zugaza JL, Trullas R, Domercq M, Matute C (2010) Amyloid β oligomers induce Ca2+ dysregulation and neuronal death through activation of ionotropic glutamate receptors. Cell Calcium 47:264–272 Available at: https://linkinghub.elsevier.com/retrieve/pii/S0143416009002048.

Almeida CG (2006) beta-Amyloid Accumulation Impairs Multivesicular Body Sorting by Inhibiting the Ubiquitin-Proteasome System. Journal of Neuroscience 26:4277–4288.

Almeida CG, Tampellini D, Takahashi RH, Greengard P, Lin MT, Snyder EM, Gouras GK (2005) Beta-amyloid accumulation in APP mutant neurons reduces PSD-95 and GluR1 in synapses. Neurobiology of Disease 20:187–198 Available at: https://linkinghub.elsevier.com/retrieve/pii/S0969996105000720.

Alzheimer A (1907) über eine eigenartige Erkrankung der Hirnrinde. Allgemeine Zeitschrift fur Psychiatrie und Psychisch-gerichtliche Medizin 64:146–148.

Arosio B, Trabattoni D, Galimberti L, Bucciarelli P, Fasano F, Calabresi C, Cazzullo CL, Vergani C, Annoni G, Clerici M (2004) Interleukin-10 and interleukin-6 gene polymorphisms as risk factors for Alzheimer's disease. Neurobiology of Aging 25:1009–1015 Available at: https://linkinghub.elsevier.com/retrieve/pii/S0197458003002380.

Asakura E, Tojo N, Tanabe T (1999) Monocyte proliferation induced by modified serum is associated with endogenous M-CSF production: evidence for involvement of a signalling pathway via scavenger receptors. Cell Proliferation 32:185–194.

Ashe KH, Zahs KR (2010) Probing the Biology of Alzheimer's Disease in Mice. Neuron 66:631–645.

Askew K, Li K, Olmos-Alonso A, Garcia-Moreno F, Liang Y, Richardson P, Tipton T, Chapman MA, Riecken K, Beccari S, Sierra A, Molnár Z, Cragg MS, Garaschuk O, Perry VH, Gomez-Nicola D (2017) Coupled Proliferation and Apoptosis Maintain the Rapid Turnover of Microglia in the Adult Brain. Cell Reports 18:391–405.

Baccarini M, Li W, dello Sbarba P, Stanley ER (1991) Increased phosphorylation of the colony stimulating factor-1 receptor following transmembrane signaling. Receptor 1:243–259 Available at: http://www.ncbi.nlm.nih.gov/pubmed/1843210 [Accessed October 19, 2021].

Bajaj L, Lotfi P, Pal R, Ronza A di, Sharma J, Sardiello M (2019) Lysosome biogenesis in health and disease. Journal of Neurochemistry 148:573–589.

Bao F, Wicklund L, Lacor PN, Klein WL, Nordberg A, Marutle A (2012) Different β-amyloid oligomer assemblies in Alzheimer brains correlate with age of disease onset and impaired cholinergic activity. Neurobiology of Aging 33:825–838.

Barger SW, Harmon AD (1997) Microglial activation by Alzheimer amyloid precursor protein and modulation by apolipoprotein E. Nature 388:878–881 Available at: http://www.nature.com/articles/42257.

Barrachina M, Maes T, Buesa C, Ferrer I (2006) Lysosome-associated membrane protein 1 (LAMP-1) in Alzheimer's disease. Neuropathology and Applied Neurobiology 32:505–516.

Benzing WC, Wujek JR, Ward EK, Shaffer D, Ashe KH, Younkin SG, Brunden KR (1999) Evidence for glial-mediated inflammation in aged APPSW transgenic mice. Neurobiology of Aging 20:581–589.

Bertram L, McQueen MB, Mullin K, Blacker D, Tanzi RE (2007) Systematic meta-analyses of Alzheimer disease genetic association studies: the AlzGene database. Nature Genetics 39.

Billings LM, Oddo S, Green KN, McGaugh JL, LaFerla FM (2005) Intraneuronal Aβ Causes the Onset of Early Alzheimer's Disease-Related Cognitive Deficits in Transgenic Mice. Neuron 45:675–688.

Blennow K, Bogdanovic N, Alafuzoff I, Ekman R, Davidsson P (1996) Synaptic pathology in Alzheimer's disease: Relation to severity of dementia, but not to senile plaques, neurofibrillary tangles, or the ApoE4 allele. Journal of Neural Transmission 103:603–618 Available at: http://link.springer.com/10.1007/BF01273157.

Bloom GS (2014) Amyloid-β and Tau. JAMA Neurology 71:505 Available at: http://archneur.jamanetwork.com/article.aspx?doi=10.1001/jamaneurol.2013.5847.

Boissonneault V, Filali M, Lessard M, Relton J, Wong G, Rivest S (2008) Powerful beneficial effects of macrophage colony-stimulating factor on -amyloid deposition and cognitive impairment in Alzheimer's disease. Brain 132:1078–1092 Available at: https://academic.oup.com/brain/article-lookup/doi/10.1093/brain/awn331.

Boocock CA, Jones GE, Stanley ER, Pollard JW (1989) Colony-stimulating factor-1 induces rapid behavioural responses in the mouse macrophage cell line, BAC1.2F5. Journal of cell science 93 (Pt 3):447–456.

Bornemann KD, Wiederhold K-H, Pauli C, Ermini F, Stalder M, Schnell L, Sommer B, Jucker M, Staufenbiel M (2001) Aβ-Induced Inflammatory Processes in Microglia Cells of APP23 Transgenic Mice. The American Journal of Pathology 158:63–73.

Braak H, Alafuzoff I, Arzberger T, Kretzschmar H, del Tredici K (2006) Staging of Alzheimer disease-associated neurofibrillary pathology using paraffin sections and immunocytochemistry. Acta Neuropathologica 112:389–404.

Braak H, Braak E (1991) Neuropathological stageing of Alzheimer-related changes. Acta Neuropathologica 82:239–259.

Braak H, Braak E (1995) Staging of alzheimer's disease-related neurofibrillary changes. Neurobiology of Aging 16:271–278 Available at: https://linkinghub.elsevier.com/retrieve/pii/0197458095000216 [Accessed October 17, 2021].

Braak H, Braak E (1997) Frequency of Stages of Alzheimer-Related Lesions in Different Age Categories. Neurobiology of Aging 18:351–357.

Braak H, Thal DR, Ghebremedhin E, del Tredici K (2011) Stages of the Pathologic Process in Alzheimer Disease: Age Categories From 1 to 100 Years. Journal of Neuropathology & Experimental Neurology 70:960–969.

Bryan KJ, Zhu X, Harris PL, Perry G, Castellani RJ, Smith MA, Casadesus G (2008) Expression of CD74 is increased in neurofibrillary tangles in Alzheimer's disease. Molecular Neurodegeneration 3:13 Available at: https://molecularneurodegeneration.biomedcentral.com/articles/10.1186/1750-1326-3-13.

Bu G (2009) Apolipoprotein E and its receptors in Alzheimer's disease: pathways, pathogenesis and therapy. Nature Reviews Neuroscience 10:333–344.

Buttgereit A, Lelios I, Yu X, Vrohlings M, Krakoski NR, Gautier EL, Nishinakamura R, Becher B, Greter M (2016) Sall1 is a transcriptional regulator defining microglia identity and function. Nature Immunology 17:1397–1406.

Cacace R, Sleegers K, van Broeckhoven C (2016) Molecular genetics of early-onset Alzheimer's disease revisited. Alzheimer's & Dementia 12:733–748.

Caescu CI, Guo X, Tesfa L, Bhagat TD, Verma A, Zheng D, Stanley ER (2015) Colony stimulating factor-1 receptor signaling networks inhibit mouse macrophage inflammatory responses by induction of microRNA-21. Blood 125:e1–e13 Available at: https://ashpublications.org/blood/article/125/8/e1/34208/Colony-stimulating-factor1-receptor-signaling.

Calingasan NY, Erdely HA, Anthony Altar C (2002) Identification of CD40 ligand in Alzheimer's disease and in animal models of Alzheimer's disease and brain injury. Neurobiology of Aging 23:31–39.

Calsolaro V, Edison P (2016) Neuroinflammation in Alzheimer's disease: Current evidence and future directions. Alzheimer's & Dementia 12:719–732.

Capetillo-Zarate E, Gracia L, Tampellini D, Gouras GK (2012) Intraneuronal Aß Accumulation, Amyloid Plaques, and Synapse Pathology in Alzheimer's Disease. Neurodegenerative Diseases 10:56–59 Available at: https://www.karger.com/Article/FullText/334762 [Accessed October 22, 2021].

Capetillo-Zarate E, Staufenbiel M, Abramowski D, Haass C, Escher A, Stadelmann C, Yamaguchi H, Wiestler OD, Thal DR (2006) Selective vulnerability of different types of commissural neurons for amyloid -protein-induced neurodegeneration in APP23 mice correlates with dendritic tree morphology. Brain 129:2992–3005 Available at: https://academic.oup.com/brain/article-lookup/doi/10.1093/brain/awl176 [Accessed October 20, 2021].

Cataldo AM, Barnett JL, Berman SA, Li J, Quarless S, Bursztajn S, Lippa C, Nixon RA (1995) Gene expression and cellular content of cathepsin D in Alzheimer's disease brain: Evidence for early up-regulation of the endosomal-lysosomal system. Neuron 14:671–680 Available at: https://linkinghub.elsevier.com/retrieve/pii/0896627395903240.

Cataldo AM, Barnett JL, Mann DMA, Nixon RA (1996) Colocalization of Lysosomal Hydrolase and β-Amyloid in Diffuse Plaques of the Cerebellum and Striatum in Alzheimer's Disease and Down's Syndrome. Journal of Neuropathology and Experimental Neurology 55:704–715.

Cataldo AM, Barnett JL, Pieroni C, Nixon RA (1997) Increased Neuronal Endocytosis and Protease Delivery to Early Endosomes in Sporadic Alzheimer's Disease: Neuropathologic Evidence for a Mechanism of Increased β-Amyloidogenesis. The Journal of Neuroscience 17:6142–6151.

Cataldo AM, Paskevich PA, Kominami E, Nixon RA (1991) Lysosomal hydrolases of different classes are abnormally distributed in brains of patients with Alzheimer disease. Proceedings of the National Academy of Sciences 88:10998–11002.

Cataldo AM, Peterhoff CM, Schmidt SD, Terio NB, Duff K, Beard M, Mathews PM, Nixon RA (2004) Presenilin Mutations in Familial Alzheimer Disease and Transgenic Mouse Models Accelerate Neuronal Lysosomal Pathology. Journal of Neuropathology & Experimental Neurology 63:821–830.

Chao CC, Ala TA, Hu S, Crossley KB, Sherman RE, Peterson PK, Frey WH (1994) Serum cytokine levels in patients with Alzheimer's disease. Clinical Diagnostic Laboratory Immunology 1:433–436 Available at: https://journals.asm.org/doi/10.1128/cdli.1.4.433-436.1994.

Chao CC, Hu S, Molitor TW, Shaskan EG, Peterson PK (1992) Activated microglia mediate neuronal cell injury via a nitric oxide mechanism. Journal of immunology (Baltimore, Md : 1950) 149:2736–2741 Available at: http://www.ncbi.nlm.nih.gov/pubmed/1383325.

Checchin D, Sennlaub F, Levavasseur E, Leduc M, Chemtob S (2006) Potential Role of Microglia in Retinal Blood Vessel Formation. Investigative Opthalmology & Visual Science 47:3595 Available at: http://iovs.arvojournals.org/article.aspx?doi=10.1167/iovs.05-1522.

Chitu V, Gokhan Ş, Nandi S, Mehler MF, Stanley ER (2016) Emerging Roles for CSF-1 Receptor and its Ligands in the Nervous System. Trends in Neurosciences 39:378–393 Available at: https://linkinghub.elsevier.com/retrieve/pii/S0166223616000539.

Chitu V, Pixley FJ, Macaluso F, Larson DR, Condeelis J, Yeung Y-G, Stanley ER (2005) The PCH Family Member MAYP/PSTPIP2 Directly Regulates F-Actin Bundling and Enhances Filopodia Formation and Motility in Macrophages. Molecular Biology of the Cell 16:2947–2959 Available at: https://www.molbiolcell.org/doi/10.1091/mbc.e04-10-0914.

Cho M-H, Cho K, Kang H-J, Jeon E-Y, Kim H-S, Kwon H-J, Kim H-M, Kim D-H, Yoon S-Y (2014) Autophagy in microglia degrades extracellular β-amyloid fibrils and regulates the NLRP3 inflammasome. Autophagy 10:1761–1775.

Chong Y (1997) Effect of a carboxy-terminal fragment of the alzheimer's amyloid precursor protein on expression of proinflammatory cytokines in rat glial cells. Life Sciences 61:2323–2333.

Choucair-Jaafar N, Laporte V, Levy R, Poindron P, Lombard Y, Gies J-P (2011) Complement receptor 3 (CD11b/CD18) is implicated in the elimination of β-amyloid peptides. Fundamental & Clinical Pharmacology 25:115–122.

Christensen DZ, Bayer TA, Wirths O (2009) Formic acid is essential for immunohistochemical detection of aggregated intraneuronal Aβ peptides in mouse models of Alzheimer's disease. Brain Research 1301:116–125 Available at: https://linkinghub.elsevier.com/retrieve/pii/S0006899309018885 [Accessed October 20, 2021].

Christie R, Freeman M, Hyman B (1996) Expression of the macrophage scavenger receptor, a multifunctional lipoprotein receptor, in microglia associated with senile plaques in Alzheimer's disease. American journal of pathology 148:399–403.

Cline EN, Bicca MA, Viola KL, Klein WL (2018) The Amyloid-β Oligomer Hypothesis: Beginning of the Third Decade Perry G, Avila J, Moreira PI, Sorensen AA, Tabaton M, eds. Journal of Alzheimer's Disease 64:S567–S610 Available at: https://www.medra.org/servlet/aliasResolver?alias=iospress&doi=10.3233/JAD-179941.

Colom-Cadena M, Spires-Jones T, Zetterberg H, Blennow K, Caggiano A, DeKosky ST, Fillit H, Harrison JE, Schneider LS, Scheltens P, de Haan W, Grundman M, van Dyck CH, Izzo NJ, Catalano SM (2020) The clinical promise of biomarkers of synapse damage or loss in Alzheimer's disease. Alzheimer's Research & Therapy 12:21–33.

Colonna M (2003) TREMs in the immune system and beyond. Nature Reviews Immunology 3:445–453.

Combs CK, Karlo JC, Kao S-C, Landreth GE (2001) β-Amyloid Stimulation of Microglia and Monocytes Results in TNFα-Dependent Expression of Inducible Nitric Oxide Synthase and Neuronal Apoptosis. The Journal of Neuroscience 21:1179–1188.

Coraci IS, Husemann J, Berman JW, Hulette C, Dufour JH, Campanella GK, Luster AD, Silverstein SC, el Khoury JB (2002) CD36, a Class B Scavenger Receptor, Is Expressed on Microglia in Alzheimer's Disease Brains and Can Mediate Production of Reactive Oxygen Species in Response to β-Amyloid Fibrils. The American Journal of Pathology 160.

Crehan H, Holton P, Wray S, Pocock J, Guerreiro R, Hardy J (2012) Complement receptor 1 (CR1) and Alzheimer's disease. Immunobiology 217:244–250.

Cruts M, Hendriks L, van Broeckhoven C (1996) The presenilin genes: a new gene family involved in Alzheimer disease pathology. Human Molecular Genetics 5:1449–1455.

Cruts M, Theuns J, van Broeckhoven C (2012) Locus-specific mutation databases for neurodegenerative brain diseases. Human Mutation 33:1340–1344.

Cunningham CL, Martínez-Cerdeño V, Noctor SC (2013) Microglia regulate the number of neural precursor cells in the developing cerebral cortex. The Journal of neuroscience : the official journal of the Society for Neuroscience 33:4216–4233.

Daborg J, Andreasson U, Pekna M, Lautner R, Hanse E, Minthon L, Blennow K, Hansson O, Zetterberg H (2012) Cerebrospinal fluid levels of complement proteins C3, C4 and CR1 in Alzheimer's disease. Journal of Neural Transmission 119:789–797.

Dagher NN, Najafi AR, Kayala KMN, Elmore MRP, White TE, Medeiros R, West BL, Green KN (2015) Colony-stimulating factor 1 receptor inhibition prevents microglial plaque association and improves cognition in 3xTg-AD mice. Journal of Neuroinflammation 12:139–153.

Dahlgren KN, Manelli AM, Stine WB, Baker LK, Krafft GA, LaDu MJ (2002) Oligomeric and Fibrillar Species of Amyloid-β Peptides Differentially Affect Neuronal Viability. Journal of Biological Chemistry 277:32046–32053 Available at: https://linkinghub.elsevier.com/retrieve/pii/S0021925820700633 [Accessed October 17, 2021].

Davalos D, Grutzendler J, Yang G, Kim J v, Zuo Y, Jung S, Littman DR, Dustin ML, Gan W-B (2005) ATP mediates rapid microglial response to local brain injury in vivo. Nature Neuroscience 8:752–758.

Davis N, Mota BC, Stead L, Palmer EOC, Lombardero L, Rodríguez-Puertas R, de Paola V, Barnes SJ, Sastre M (2021) Pharmacological ablation of astrocytes reduces Aβ degradation and synaptic connectivity in an ex vivo model of Alzheimer's disease. Journal of Neuroinflammation 18:73–85.

de Calignon A, Polydoro M, Suárez-Calvet M, William C, Adamowicz DH, Kopeikina KJ, Pitstick R, Sahara N, Ashe KH, Carlson GA, Spires-Jones TL, Hyman BT (2012) Propagation of Tau Pathology in a Model of Early Alzheimer's Disease. Neuron 73:685–697 Available at: https://linkinghub.elsevier.com/retrieve/pii/S0896627312000384.

Demuro A, Mina E, Kayed R, Milton SC, Parker I, Glabe CG (2005) Calcium Dysregulation and Membrane Disruption as a Ubiquitous Neurotoxic Mechanism of Soluble Amyloid Oligomers*◆. Journal of Biological Chemistry 280:17294–17300.

Doens D, Fernández PL (2014) Microglia receptors and their implications in the response to amyloid β for Alzheimer's disease pathogenesis. Journal of Neuroinflammation 11:48–62.

Durafourt BA, Moore CS, Zammit DA, Johnson TA, Zaguia F, Guiot M-C, Bar-Or A, Antel JP (2012) Comparison of polarization properties of human adult microglia and blood-derived macrophages. Glia 60:717–727.

Duyckaerts C, Delaère P, Poulain V, Brion J-P, Hauw J-J (1988) Does amyloid precede paired helical filaments in the senile plaque? A study of 15 cases with graded intellectual status in aging and Alzheimer disease. Neuroscience Letters 91:354–359 Available at: https://linkinghub.elsevier.com/retrieve/pii/0304394088907069 [Accessed October 23, 2021].

el Khoury JB, Moore KJ, Means TK, Leung J, Terada K, Toft M, Freeman MW, Luster AD (2003) CD36 Mediates the Innate Host Response to β-Amyloid. Journal of Experimental Medicine 197:1657–1666.

Eugenin EA, Eckardt D, Theis M, Willecke K, Bennett MVL, Saez JC (2001) Microglia at brain stab wounds express connexin 43 and in vitro form functional gap junctions after treatment with interferon- and tumor necrosis factor-. Proceedings of the National Academy of Sciences 98:4190–4195.

Fernandez-Albarral J, Ramírez A, de Hoz R, Salazar J (2022) Retinal microglial activation in glaucoma: evolution over time in a unilateral ocular hypertension model. Neural Regeneration Research 17:797–799.

Fernández-López D, Faustino J, Klibanov AL, Derugin N, Blanchard E, Simon F, Leib SL, Vexler ZS (2016) Microglial Cells Prevent Hemorrhage in Neonatal Focal Arterial Stroke. The Journal of neuroscience : the official journal of the Society for Neuroscience 36:2881–2893.

Filipov NM (2019) Overview of peripheral and central inflammatory responses and their contribution to neurotoxicity. In, pp 169–193.

Fillit H, Ding W, Buee L, Kalman J, Altstiel L, Lawlor B, Wolf-Klein G (1991) Elevated circulating tumor necrosis factor levels in Alzheimer's disease. Neuroscience Letters 129:318–320.

Fonseca MI, Chu S-H, Hernandez MX, Fang MJ, Modarresi L, Selvan P, MacGregor GR, Tenner AJ (2017) Cell-specific deletion of C1qa identifies microglia as the dominant source of C1q in mouse brain. Journal of Neuroinflammation 14:48 Available at: https://jneuroinflammation.biomedcentral.com/articles/10.1186/s12974-017-0814-9 [Accessed October 25, 2021].

Fonseca MI, Kawas CH, Troncoso JC, Tenner AJ (2004) Neuronal localization of C1q in preclinical Alzheimer's disease. Neurobiology of Disease 15:40–46.

Frank S, Burbach GJ, Bonin M, Walter M, Streit W, Bechmann I, Deller T (2008) TREM2 is upregulated in amyloid plaque-associated microglia in aged APP23 transgenic mice. Glia 56:1438–1447.

Frautschy SA, Yang F, Irrizarry M, Hyman B, Saido TC, Hsiao K, Cole GM (1998) Microglial response to amyloid plaques in APPsw transgenic mice. The American journal of pathology 152:307–317.

Frenkel D, Wilkinson K, Zhao L, Hickman SE, Means TK, Puckett L, Farfara D, Kingery ND, Weiner HL, el Khoury J (2013) Scara1 deficiency impairs clearance of soluble amyloid-β by mononuclear phagocytes and accelerates Alzheimer's-like disease progression. Nature Communications 4:2030–2049.

Fu H, Liu B, Frost JL, Hong S, Jin M, Ostaszewski B, Shankar GM, Costantino IM, Carroll MC, Mayadas TN, Lemere CA (2012) Complement component C3 and complement receptor type 3 contribute to the phagocytosis and clearance of fibrillar Aβ by microglia. Glia 60:993–1003 Available at: https://onlinelibrary.wiley.com/doi/10.1002/glia.22331.

Fu R, Shen Q, Xu P, Luo JJ, Tang Y (2014) Phagocytosis of Microglia in the Central Nervous System Diseases. Molecular Neurobiology 49:1422–1434.

Gehrmann J, Matsumoto Y, Kreutzberg GW (1995) Microglia: Intrinsic immuneffector cell of the brain. Brain Research Reviews 20:269–287.

Ginhoux F, Greter M, Leboeuf M, Nandi S, See P, Gokhan S, Mehler MF, Conway SJ, Ng LG, Stanley ER, Samokhvalov IM, Merad M (2010) Fate Mapping Analysis Reveals That Adult Microglia Derive from Primitive Macrophages. Science 330:841–845.

Ginhoux F, Lim S, Hoeffel G, Low D, Huber T (2013) Origin and differentiation of microglia. Frontiers in Cellular Neuroscience 7:45–59 Available at: http://journal.frontiersin.org/article/10.3389/fncel.2013.00045/abstract.

Glabe CC (2005) Amyloid Accumulation and Pathogensis of Alzheimer's Disease: Significance of Monomeric, Oligomeric and Fibrillar Aβ. In: Alzheimer's Disease, pp 167–177. Springer US.

Glenner GG, Wong CW (1984) Alzheimer's disease: Initial report of the purification and characterization of a novel cerebrovascular amyloid protein. Biochemical and Biophysical Research Communications 120.

Goate A et al. (1991) Segregation of a missense mutation in the amyloid precursor protein gene with familial Alzheimer's disease. Nature 349:704–706.

Goedert M, Jakes R, Vanmechelen E (1995) Monoclonal antibody AT8 recognises tau protein phosphorylated at both serine 202 and threonine 205. Neuroscience Letters 189:167–170.

Gomez-Arboledas A, Acharya MM, Tenner AJ (2021) The Role of Complement in Synaptic Pruning and Neurodegeneration. ImmunoTargets and Therapy Volume 10:373–386.

Gomez-Nicola D, Fransen NL, Suzzi S, Perry VH (2013) Regulation of Microglial Proliferation during Chronic Neurodegeneration. Journal of Neuroscience 33:2481–2493.

Gouras GK, Tsai J, Naslund J, Vincent B, Edgar M, Checler F, Greenfield JP, Haroutunian V, Buxbaum JD, Xu H, Greengard P, Relkin NR (2000) Intraneuronal Aβ42 Accumulation in Human Brain. The American Journal of Pathology 156:15–20.

Griciuc A, Federico AN, Natasan J, Forte AM, McGinty D, Nguyen H, Volak A, LeRoy S, Gandhi S, Lerner EP, Hudry E, Tanzi RE, Maguire CA (2020) Gene therapy for Alzheimer's disease targeting CD33 reduces amyloid beta accumulation and neuroinflammation. Human Molecular Genetics 29:2920–2935.

Griciuc A, Serrano-Pozo A, Parrado AR, Lesinski AN, Asselin CN, Mullin K, Hooli B, Choi SH, Hyman BT, Tanzi RE (2013) Alzheimer's Disease Risk Gene CD33 Inhibits Microglial Uptake of Amyloid Beta. Neuron 78:631–643.

Griffin WST, Sheng JG, Royston MC, Gentleman SM, McKenzie JE, Graham DI, Roberts GW, Mrak RE (2006) Glial-Neuronal Interactions in Alzheimer's Disease: The Potential Role of a 'Cytokine Cycle' in Disease Progression. Brain Pathology 8:65–72.

Gruber MF, Williams CC, Gerrard TL (1994) Macrophage-colony-stimulating factor expression by anti-CD45 stimulated human monocytes is transcriptionally up-regulated by IL-1 beta and inhibited by IL-4 and IL-10. Journal of immunology (Baltimore, Md : 1950) 152:1354–1361.

Grundke-Iqbal I, Iqbal K, Tung YC, Quinlan M, Wisniewski HM, Binder LI (1986) Abnormal phosphorylation of the microtubule-associated protein tau (tau) in Alzheimer cytoskeletal pathology. Proceedings of the National Academy of Sciences 83:4913–4917 Available at: http://www.pnas.org/cgi/doi/10.1073/pnas.83.13.4913.

Gu D, Liu F, Meng M, Zhang L, Gordon ML, Wang Y, Cai L, Zhang N (2020) Elevated matrix metalloproteinase-9 levels in neuronal extracellular vesicles in Alzheimer's disease. Annals of Clinical and Translational Neurology 7:1681–1691.

Guerreiro R et al. (2013) *TREM2* Variants in Alzheimer's Disease. New England Journal of Medicine 368:117–127.

Guilbert LJ, Stanley ER (1986) The interaction of 125I-colony-stimulating factor-1 with bone marrow-derived macrophages. The Journal of biological chemistry 261:4024–4032 Available at: http://www.ncbi.nlm.nih.gov/pubmed/3485098 [Accessed October 19, 2021].

Guo X, Tang P, Chen L, Liu P, Hou C, Zhang X, Liu Y, Chong L, Li X, Li R (2017) Amyloid β-Induced Redistribution of Transcriptional Factor EB and Lysosomal Dysfunction in Primary Microglial Cells. Frontiers in Aging Neuroscience 9:228–238 Available at: http://journal.frontiersin.org/article/10.3389/fnagi.2017.00228/full [Accessed October 17, 2021].

Gyoneva S, Swanger SA, Zhang J, Weinshenker D, Traynelis SF (2016) Altered motility of plaque-associated microglia in a model of Alzheimer's disease. Neuroscience 330:410–420 Available at: http://linkinghub.elsevier.com/retrieve/pii/S0306452216302202.

Haass C, Selkoe DJ (2007) Soluble protein oligomers in neurodegeneration: lessons from the Alzheimer's amyloid β-peptide. Nature Reviews Molecular Cell Biology 8:101–112.

Hamilton TA, Zhao C, Pavicic PG, Datta S (2014) Myeloid Colony-Stimulating Factors as Regulators of Macrophage Polarization. Frontiers in Immunology 5:554–560.

Hanisch U-K, Kettenmann H (2007) Microglia: active sensor and versatile effector cells in the normal and pathologic brain. Nature Neuroscience 10:1387–1394.

Hardy J (2002) The Amyloid Hypothesis of Alzheimer's Disease: Progress and Problems on the Road to Therapeutics. Science 297:353–356.

Hardy J, Allsop D (1991) Amyloid deposition as the central event in the aetiology of Alzheimer's disease. Trends in Pharmacological Sciences 12:383–388.

Hardy JA, Higgins GA (1992) Alzheimer's Disease: The Amyloid Cascade Hypothesis. Science 256:184–185.

Hemonnot A-L, Hua J, Ulmann L, Hirbec H (2019) Microglia in Alzheimer Disease: Well-Known Targets and New Opportunities. Frontiers in Aging Neuroscience 11:233–253.

Heneka MT, O'Banion MK (2007) Inflammatory processes in Alzheimer's disease. Journal of neuroimmunology 184:69–91.

Herms J, Anliker B, Heber S, Ring S, Fuhrmann M, Kretzschmar H, Sisodia S, Müller U (2004) Cortical dysplasia resembling human type 2 lissencephaly in mice lacking all three APP family members. The EMBO Journal 23:4106–4015.

Hershey CL, Fisher DE (2004) Mitf and Tfe3: members of a b-HLH-ZIP transcription factor family essential for osteoclast development and function. Bone 34:689–696.

Holcomb L, Gordon MN, McGowan E, Yu X, Benkovic S, Jantzen P, Wright K, Saad I, Mueller R, Morgan D, Sanders S, Zehr C, O'Campo K, Hardy J, Prada C-M, Eckman C, Younkin S, Hsiao K, Duff K (1998) Accelerated Alzheimer-type phenotype in transgenic mice carrying both mutant amyloid precursor protein and presenilin 1 transgenes. Nature Medicine 4:97–100 Available at: http://www.nature.com/articles/nm0198-097 [Accessed October 20, 2021].

Holtzman DM, Herz J, Bu G (2012) Apolipoprotein E and Apolipoprotein E Receptors: Normal Biology and Roles in Alzheimer Disease. Cold Spring Harbor Perspectives in Medicine 2:a006312–a006312.

Hong S, Beja-Glasser VF, Nfonoyim BM, Frouin A, Li S, Ramakrishnan S, Merry KM, Shi Q, Rosenthal A, Barres BA, Lemere CA, Selkoe DJ, Stevens B (2016) Complement and microglia mediate early synapse loss in Alzheimer mouse models. Science 352:712–716.

Hoozemans JJM, Veerhuis R, Rozemuller JM, Eikelenboom P (2006) Neuroinflammation and regeneration in the early stages of Alzheimer's disease pathology. International Journal of Developmental Neuroscience 24:157–165.

Hsia AY, Masliah E, McConlogue L, Yu G-Q, Tatsuno G, Hu K, Kholodenko D, Malenka RC, Nicoll RA, Mucke L (1999) Plaque-independent disruption of neural circuits in Alzheimer's disease mouse models. Proceedings of the National Academy of Sciences 96:3228–3233 Available at: http://www.pnas.org/cgi/doi/10.1073/pnas.96.6.3228 [Accessed October 20, 2021].

Huang Y (2006) Apolipoprotein E and Alzheimer disease. Neurology 66:79–85.

Hume DA, MacDonald KPA (2012) Therapeutic applications of macrophage colony-stimulating factor-1 (CSF-1) and antagonists of CSF-1 receptor (CSF-1R) signaling. Blood 119.

Ingelsson M, Fukumoto H, Newell KL, Growdon JH, Hedley-Whyte ET, Frosch MP, Albert MS, Hyman BT, Irizarry MC (2004) Early A accumulation and progressive synaptic loss, gliosis, and tangle formation in AD brain. Neurology 62:925–931.

Itagaki S, Mcgeer P, Akiyama H, Zhu S, Selkoe D (1989) Relationship of microglia and astrocytes to amyloid deposits of Alzheimer disease. Journal of Neuroimmunology 24:173–182.

Jack CR, Knopman DS, Jagust WJ, Petersen RC, Weiner MW, Aisen PS, Shaw LM, Vemuri P, Wiste HJ, Weigand SD, Lesnick TG, Pankratz VS, Donohue MC, Trojanowski JQ (2013) Tracking pathophysiological processes in Alzheimer's disease: an updated hypothetical model of dynamic biomarkers. The Lancet Neurology 12:207–216.

Jack CR, Lowe VJ, Senjem ML, Weigand SD, Kemp BJ, Shiung MM, Knopman DS, Boeve BF, Klunk WE, Mathis CA, Petersen RC (2008) 11C PiB and structural MRI provide complementary information in imaging of Alzheimer's disease and amnestic mild cognitive impairment. Brain 131:665–680.

Jack CR, Lowe VJ, Weigand SD, Wiste HJ, Senjem ML, Knopman DS, Shiung MM, Gunter JL, Boeve BF, Kemp BJ, Weiner M, Petersen RC (2009) Serial PIB and MRI in normal, mild cognitive impairment and Alzheimer's disease: implications for sequence of pathological events in Alzheimer's disease. Brain 132:1355–1365.

Jackson RJ, Rudinskiy N, Herrmann AG, Croft S, Kim JM, Petrova V, Ramos-Rodriguez JJ, Pitstick R, Wegmann S, Garcia-Alloza M, Carlson GA, Hyman BT, Spires-Jones TL (2016) Human tau increases amyloid β plaque size but not amyloid β-mediated synapse loss in a novel mouse model of Alzheimer's disease. European Journal of Neuroscience 44:3056–3066.

Jawhar S, Trawicka A, Jenneckens C, Bayer TA, Wirths O (2012) Motor deficits, neuron loss, and reduced anxiety coinciding with axonal degeneration and intraneuronal Aβ aggregation in the 5XFAD mouse model of Alzheimer's disease. Neurobiology of Aging 33:196.e29-196.e40.

Jones RS, Minogue AM, Connor TJ, Lynch MA (2013) Amyloid-β-Induced Astrocytic Phagocytosis is Mediated by CD36, CD47 and RAGE. Journal of Neuroimmune Pharmacology 8:301–311.

Jung S, Aliberti J, Graemmel P, Sunshine MJ, Kreutzberg GW, Sher A, Littman DR (2000) Analysis of Fractalkine Receptor CX $_3$ CR1 Function by Targeted Deletion and Green Fluorescent Protein Reporter Gene Insertion. Molecular and Cellular Biology 20:4106–4114.

Kamphuis W, Kooijman L, Orre M, Stassen O, Pekny M, Hol EM (2015) GFAP and vimentin deficiency alters gene expression in astrocytes and microglia in wild-type mice and changes the transcriptional response of reactive glia in mouse model for Alzheimer's disease. Glia 63:1036–1056.

Kamphuis W, Kooijman L, Schetters S, Orre M, Hol EM (2016) Transcriptional profiling of CD11c-positive microglia accumulating around amyloid plaques in a mouse model for Alzheimer's disease. Biochimica et Biophysica Acta (BBA) - Molecular Basis of Disease 1862:1847–1860.

Karch CM, Goate AM (2015) Alzheimer's Disease Risk Genes and Mechanisms of Disease Pathogenesis. Biological Psychiatry 77:43–51.

Keren-Shaul H, Spinrad A, Weiner A, Matcovitch-Natan O, Dvir-Szternfeld R, Ulland TK, David E, Baruch K, Lara-Astaiso D, Toth B, Itzkovitz S, Colonna M, Schwartz M, Amit I (2017) A Unique Microglia Type Associated with Restricting Development of Alzheimer's Disease. Cell 169:1276-1290.e17.

Khoury J el, Hickman SE, Thomas CA, Cao L, Silverstein SC, Loike JD (1996) Scavenger receptor-mediated adhesion of microglia to β-amyloid fibrils. Nature 382:716–719.

Kidd PM (2008) Alzheimer's disease, amnestic mild cognitive impairment, and age-associated memory impairment: current understanding and progress toward integrative prevention. Alternative medicine review : a journal of clinical therapeutic 13:85–115.

Kierdorf K et al. (2013) Microglia emerge from erythromyeloid precursors via Pu.1- and Irf8-dependent pathways. Nature Neuroscience 16:273–280.

Kim J-W, Jung S-Y, Kim Y, Heo H, Hong C-H, Seo S-W, Choi S-H, Son S-J, Lee S, Chang J (2021) Identification of Cathepsin D as a Plasma Biomarker for Alzheimer's Disease. Cells 10:138–151.

Kimberly WT, Zheng JB, Guénette SY, Selkoe DJ (2001) The Intracellular Domain of the β-Amyloid Precursor Protein Is Stabilized by Fe65 and Translocates to the Nucleus in a Notch-like Manner. Journal of Biological Chemistry 276:40288–40292.

Klein WL (2002) Aβ toxicity in Alzheimer's disease: globular oligomers (ADDLs) as new vaccine and drug targets. Neurochemistry International 41:345–352.

Koenigsknecht J (2004) Microglial Phagocytosis of Fibrillar -Amyloid through a 1 Integrin-Dependent Mechanism. Journal of Neuroscience 24:9838–9846.

Koenigsknecht-Talboo J, Meyer-Luehmann M, Parsadanian M, Garcia-Alloza M, Finn MB, Hyman BT, Bacskai BJ, Holtzman DM (2008) Rapid Microglial Response Around Amyloid Pathology after Systemic Anti-A Antibody Administration in PDAPP Mice. Journal of Neuroscience 28:14156–14164.

Koffie RM, Hashimoto T, Tai H-C, Kay KR, Serrano-Pozo A, Joyner D, Hou S, Kopeikina KJ, Frosch MP, Lee VM, Holtzman DM, Hyman BT, Spires-Jones TL (2012) Apolipoprotein E4 effects in Alzheimer's disease are mediated by synaptotoxic oligomeric amyloid-β. Brain 135:2155–2168 Available at: https://academic.oup.com/brain/article-lookup/doi/10.1093/brain/aws127 [Accessed October 20, 2021].

Koffie RM, Meyer-Luehmann M, Hashimoto T, Adams KW, Mielke ML, Garcia-Alloza M, Micheva KD, Smith SJ, Kim ML, Lee VM, Hyman BT, Spires-Jones TL (2009) Oligomeric amyloid associates with postsynaptic densities and correlates with excitatory synapse loss near senile plaques. Proceedings of the National Academy of Sciences 106:4012–4017.

Kosik KS, Joachim CL, Selkoe DJ (1986) Microtubule-associated protein tau (tau) is a major antigenic component of paired helical filaments in Alzheimer disease. Proceedings of the National Academy of Sciences 83:4044–4048.

Krabbe G, Halle A, Matyash V, Rinnenthal JL, Eom GD, Bernhardt U, Miller KR, Prokop S, Kettenmann H, Heppner FL (2013) Functional Impairment of Microglia Coincides with Beta-Amyloid Deposition in Mice with Alzheimer-Like Pathology Priller J, ed. PLoS ONE 8:e60921 Available at: https://dx.plos.org/10.1371/journal.pone.0060921.

Krasemann S et al. (2017) The TREM2-APOE Pathway Drives the Transcriptional Phenotype of Dysfunctional Microglia in Neurodegenerative Diseases. Immunity 47:566-581.e9.

Krieger M, Krieger J (1994) STRUCTURES AND FUNCTIONS OF MULTILIGAND LIPOPROTEIN RECEPTORS: Macrophage Scavenger Receptors and LDL Receptor-Related Protein (LRP). Annual Review of Biochemistry 63:601–637.

Kubota Y, Takubo K, Shimizu T, Ohno H, Kishi K, Shibuya M, Saya H, Suda T (2009) M-CSF inhibition selectively targets pathological angiogenesis and lymphangiogenesis. The Journal of experimental medicine 206:1089–1102.

Lacombe J, Karsenty G, Ferron M (2013) Regulation of lysosome biogenesis and functions in osteoclasts. Cell Cycle 12:2744–2752.

Lambert MP, Barlow AK, Chromy BA, Edwards C, Freed R, Liosatos M, Morgan TE, Rozovsky I, Trommer B, Viola KL, Wals P, Zhang C, Finch CE, Krafft GA, Klein WL (1998) Diffusible, nonfibrillar ligands derived from A 1-42 are potent central nervous system neurotoxins. Proceedings of the National Academy of Sciences 95:6448–6452.

Lane CA, Hardy J, Schott JM (2018) Alzheimer's disease. European Journal of Neurology 25:59–70.

Lange PF, Wartosch L, Jentsch TJ, Fuhrmann JC (2006) ClC-7 requires Ostm1 as a β-subunit to support bone resorption and lysosomal function. Nature 440:220–223.

Laske C, Stransky E, Hoffmann N, Maetzler W, Straten G, Eschweiler GW, Leyhe T (2010) Macrophage Colony-Stimulating Factor (M-CSF) in Plasma and CSF of Patients with Mild Cognitive Impairment and Alzheimers Disease. Current Alzheimer Research 7:409–414.

Lautner R, Mattsson N, Schöll M, Augutis K, Blennow K, Olsson B, Zetterberg H (2011) Biomarkers for Microglial Activation in Alzheimer's Disease. International Journal of Alzheimer's Disease 2011:939426–939431.

Lawson LJ, Perry VH, Dri P, Gordon S (1990) Heterogeneity in the distribution and morphology of microglia in the normal adult mouse brain. Neuroscience 39:151–170.

Lee CYD, Landreth GE (2010) The role of microglia in amyloid clearance from the AD brain. Journal of Neural Transmission 117:949–960 Available at: http://link.springer.com/10.1007/s00702-010-0433-4.

Lee PSW (1999) The Cbl protooncoprotein stimulates CSF-1 receptor multiubiquitination and endocytosis, and attenuates macrophage proliferation. The EMBO Journal 18:3616–3628.

Li H, Chen C, Dou Y, Wu H, Liu Y, Lou H-F, Zhang J, Li X, Wang H, Duan S (2013) P2Y4 receptor-mediated pinocytosis contributes to amyloid beta-induced self-uptake by microglia. Molecular and cellular biology 33:4282–4293 Available at: http://www.ncbi.nlm.nih.gov/pubmed/24001770 [Accessed October 21, 2021].

Li M, Pisalyaput K, Galvan M, Tenner AJ (2004) Macrophage colony stimulatory factor and interferon-gamma trigger distinct mechanisms for augmentation of beta-amyloid-induced microglia-mediated neurotoxicity. Journal of Neurochemistry 91:623–633.

Li W, Stanley ER (1991) Role of dimerization and modification of the CSF-1 receptor in its activation and internalization during the CSF-1 response. The EMBO journal 10:277–288.

Lim NK-H, Moestrup V, Zhang X, Wang W-A, Møller A, Huang F-D (2018) An Improved Method for Collection of Cerebrospinal Fluid from Anesthetized Mice. JoVE (Journal of Visualized Experiments) 2018:e56774 Available at: https://www.jove.com/v/56774/an-improved-method-for-collection-cerebrospinal-fluid-from [Accessed October 17, 2021].

Lin H, Lee E, Hestir K, Leo C, Huang M, Bosch E, Halenbeck R, Wu G, Zhou A, Behrens D, Hollenbaugh D, Linnemann T, Qin M, Wong J, Chu K, Doberstein SK, Williams LT (2008) Discovery of a Cytokine and Its Receptor by Functional Screening of the Extracellular Proteome. Science 320:807–811.

Lio D, Licastro F, Scola L, Chiappelli M, Grimaldi LM, Crivello A, Colonna-Romano G, Candore G, Franceschi C, Caruso C (2003) Interleukin-10 promoter polymorphism in sporadic Alzheimer's disease. Genes & Immunity 4:234–238.

Lowell CA (2011) Src-family and Syk Kinases in Activating and Inhibitory Pathways in Innate Immune Cells: Signaling Cross Talk. Cold Spring Harbor Perspectives in Biology 3:a002352–a002352 Available at: http://cshperspectives.cshlp.org/lookup/doi/10.1101/cshperspect.a002352.

Lübke T, Lobel P, Sleat DE (2009) Proteomics of the lysosome. Biochimica et Biophysica Acta (BBA) - Molecular Cell Research 1793:625–635.

Lue L-F, Walker DG, Brachova L, Beach TG, Rogers J, Schmidt AM, Stern DM, Yan S du (2001) Involvement of Microglial Receptor for Advanced Glycation Endproducts (RAGE) in Alzheimer's Disease: Identification of a Cellular Activation Mechanism. Experimental Neurology 171:29–45.

Lukiw WJ (2007) Micro-RNA speciation in fetal, adult and Alzheimer's disease hippocampus. NeuroReport 18:297–300.

Lyman M, Lloyd DG, Ji X, Vizcaychipi MP, Ma D (2014) Neuroinflammation: The role and consequences. Neuroscience Research 79:1–12.

Madry C, Kyrargyri V, Arancibia-Cárcamo IL, Jolivet R, Kohsaka S, Bryan RM, Attwell D (2018) Microglial Ramification, Surveillance, and Interleukin-1β Release Are Regulated by the Two-Pore Domain K+ Channel THIK-1. Neuron 97:299-312.e6 Available at: http://www.ncbi.nlm.nih.gov/pubmed/29290552 [Accessed October 17, 2021].

Maier M, Peng Y, Jiang L, Seabrook TJ, Carroll MC, Lemere CA (2008) Complement C3 Deficiency Leads to Accelerated Amyloid Plaque Deposition and Neurodegeneration and Modulation of the Microglia/Macrophage Phenotype in Amyloid Precursor Protein Transgenic Mice. Journal of Neuroscience 28:6333–6341.

Majumdar A, Capetillo-Zarate E, Cruz D, Gouras GK, Maxfield FR (2011) Degradation of Alzheimer's amyloid fibrils by microglia requires delivery of ClC-7 to lysosomes. Molecular Biology of the Cell 22:1664–1676.

Majumdar A, Cruz D, Asamoah N, Buxbaum A, Sohar I, Lobel P, Maxfield FR (2007) Activation of Microglia Acidifies Lysosomes and Leads to Degradation of Alzheimer Amyloid Fibrils. Molecular Biology of the Cell 18:1490–1496.

Malia TJ, Teplyakov A, Ernst R, Wu S, Lacy ER, Liu X, Vandermeeren M, Mercken M, Luo J, Sweet RW, Gilliland GL (2016) Epitope mapping and structural basis for the recognition of phosphorylated tau by the anti-tau antibody AT8. Proteins: Structure, Function, and Bioinformatics 84:427–434.

Manterola L, Hernando-Rodríguez M, Ruiz A, Apraiz A, Arrizabalaga O, Vellón L, Alberdi E, Cavaliere F, Lacerda HM, Jimenez S, Parada LA, Matute C, Zugaza JL (2013) 1–42 β-Amyloid peptide requires PDK1/nPKC/Rac 1 pathway to induce neuronal death. Translational Psychiatry 3:e219–e219 Available at: http://www.nature.com/articles/tp2012147 [Accessed October 17, 2021].

Mantovani A, Sica A, Sozzani S, Allavena P, Vecchi A, Locati M (2004) The chemokine system in diverse forms of macrophage activation and polarization. Trends in Immunology 25:677–686.

Martina JA, Diab HI, Li H, Puertollano R (2014) Novel roles for the MiTF/TFE family of transcription factors in organelle biogenesis, nutrient sensing, and energy homeostasis. Cellular and Molecular Life Sciences 71:2483–2497.

Masliah E, Hansen L, Albright T, Mallory M, Terry RD (1991) Immunoelectron microscopic study of synaptic pathology in Alzheimer's disease. Acta Neuropathologica 81:428–433.

Mathys H, Adaikkan C, Gao F, Young JZ, Manet E, Hemberg M, De Jager PL, Ransohoff RM, Regev A, Tsai LH (2017) Temporal Tracking of Microglia Activation in Neurodegeneration at Single-Cell Resolution. Cell Reports 21:366–380.

Matza D (2003) Invariant chain, a chain of command. Trends in Immunology 24:264–268.

Maxfield FR, Willard JM, Lu S (2016) Lysosomes : biology, diseases, and therapeutics. Wiley, Hoboken, NJ Available at: https://www.wiley.com/en-ie/Lysosomes%3A+Biology%2C+Diseases%2C+and+Therapeutics+-p-9781118645154 [Accessed February 17, 2022].

McCarthy KD, de Vellis J (1980) Preparation of separate astroglial and oligodendroglial cell cultures from rat cerebral tissue. Journal of Cell Biology 85:890–902 Available at: https://rupress.org/jcb/article/85/3/890/21108/Preparation-of-separate-astroglial-and [Accessed October 17, 2021].

Meadows NA, Sharma SM, Faulkner GJ, Ostrowski MC, Hume DA, Cassady AI (2007) The Expression of Clcn7 and Ostm1 in Osteoclasts Is Coregulated by Microphthalmia Transcription Factor. Journal of Biological Chemistry 282:1891–1904.

Medeiros R, Kitazawa M, Passos GF, Baglietto-Vargas D, Cheng D, Cribbs DH, LaFerla FM (2013) Aspirin-Triggered Lipoxin A4 Stimulates Alternative Activation of Microglia and Reduces Alzheimer Disease–Like Pathology in Mice. The American Journal of Pathology 182:1780–1789.

Mena R, Edwards PC, Harrington CR, Mukaetova-Ladinska EB, Wischik CM (1996) Staging the pathological assembly of truncated tau protein into paired helical filaments in Alzheimer's disease. Acta Neuropathologica 91:633–641.

Meyer-Luehmann M, Spires-Jones TL, Prada C, Garcia-Alloza M, de Calignon A, Rozkalne A, Koenigsknecht-Talboo J, Holtzman DM, Bacskai BJ, Hyman BT (2008) Rapid appearance and local toxicity of amyloid-β plaques in a mouse model of Alzheimer's disease. Nature 451:720–724.

Milà-Alomà M, Salvadó G, Gispert JD, Vilor-Tejedor N, Grau-Rivera O, Sala-Vila A, Sánchez-Benavides G, Arenaza-Urquijo EM, Crous-Bou M, González-de-Echávarri JM, Minguillon C, Fauria K, Simon M, Kollmorgen G, Zetterberg H, Blennow K, Suárez-Calvet M, Molinuevo JL (2020) Amyloid beta, tau, synaptic, neurodegeneration, and glial biomarkers in the preclinical stage of the Alzheimer's *continuum*. Alzheimer's & Dementia 16:1358–1371 Available at: https://onlinelibrary.wiley.com/doi/10.1002/alz.12131.

Min S-W, Cho S-H, Zhou Y, Schroeder S, Haroutunian V, Seeley WW, Huang EJ, Shen Y, Masliah E, Mukherjee C, Meyers D, Cole PA, Ott M, Gan L (2010) Acetylation of Tau Inhibits Its Degradation and Contributes to Tauopathy. Neuron 67:953–966.

Mirra SS, Heyman A, McKeel D, Sumi SM, Crain BJ, Brownlee LM, Vogel FS, Hughes JP, Belle G v., Berg L (1991) The Consortium to Establish a Registry for Alzheimer's Disease (CERAD): Part II. Standardization of the neuropathologic assessment of Alzheimer's disease. Neurology 41:479–479.

Mitrasinovic O (2003) Microglial overexpression of the M-CSF receptor augments phagocytosis of opsonized Aβ. Neurobiology of Aging 24:807–815.

Mitrasinovic OM (2005) Microglia Overexpressing the Macrophage Colony-Stimulating Factor Receptor Are Neuroprotective in a Microglial-Hippocampal Organotypic Coculture System. Journal of Neuroscience 25:4442–4451.

Mitrasinovic OM, Murphy GM (2002) Accelerated Phagocytosis of Amyloid-β by Mouse and Human Microglia Overexpressing the Macrophage Colony-stimulating Factor Receptor. Journal of Biological Chemistry 277:29889–29896.

Mitrasinovic OM, Perez G v., Zhao F, Lee YL, Poon C, Murphy GM (2001) Overexpression of Macrophage Colony-stimulating Factor Receptor on Microglial Cells Induces an Inflammatory Response. Journal of Biological Chemistry 276:30142–30149.

Mitrasinovic OM, Vincent VAM, Simsek D, Murphy GM (2003) Macrophage colony stimulating factor promotes phagocytosis by murine microglia. Neuroscience Letters 344:185–188.

Mittelbronn M, Dietz K, Schluesener HJ, Meyermann R (2001) Local distribution of microglia in the normal adult human central nervous system differs by up to one order of magnitude. Acta Neuropathologica 101:249–255.

Moechars D, Dewachter I, Lorent K, Reversé D, Baekelandt V, Naidu A, Tesseur I, Spittaels K, Haute C van den, Checler F, Godaux E, Cordell B, van Leuven F (1999) Early Phenotypic Changes in Transgenic Mice That Overexpress Different Mutants of Amyloid Precursor Protein in Brain. Journal of Biological Chemistry 274:6483–6492 Available at: https://linkinghub.elsevier.com/retrieve/pii/S002192581987610X [Accessed October 20, 2021].

Mohana T, Navin AV, Jamuna S, Sakeena Sadullah MS, Niranjali Devaraj S (2015) Inhibition of differentiation of monocyte to macrophages in atherosclerosis by oligomeric proanthocyanidins –In-vivo and in-vitro study. Food and Chemical Toxicology 82:96–105.

Monsonego A, Imitola J, Petrovic S, Zota V, Nemirovsky A, Baron R, Fisher Y, Owens T, Weiner HL (2006) Abeta-induced meningoencephalitis is IFN- -dependent and is associated with T cell-dependent clearance of Abeta in a mouse model of Alzheimer's disease. Proceedings of the National Academy of Sciences 103:5048–5053.

Moolman DL, Vitolo O v., Vonsattel J-PG, Shelanski ML (2004) Dendrite and dendritic spine alterations in alzheimer models. Journal of Neurocytology 33:377–387 Available at: http://link.springer.com/10.1023/B:NEUR.0000044197.83514.64 [Accessed October 20, 2021].

Mormino EC, Kluth JT, Madison CM, Rabinovici GD, Baker SL, Miller BL, Koeppe RA, Mathis CA, Weiner MW, Jagust WJ (2009) Episodic memory loss is related to hippocampal-mediated -amyloid deposition in elderly subjects. Brain 132:1310–1323.

Motyckova G, Weilbaecher KN, Horstmann M, Rieman DJ, Fisher DZ, Fisher DE (2001) Linking osteopetrosis and pycnodysostosis: Regulation of cathepsin K expression by the microphthalmia transcription factor family. Proceedings of the National Academy of Sciences 98:5798–5803.

Mueller-Steiner S, Zhou Y, Arai H, Roberson ED, Sun B, Chen J, Wang X, Yu G, Esposito L, Mucke L, Gan L (2006) Antiamyloidogenic and Neuroprotective Functions of Cathepsin B: Implications for Alzheimer's Disease. Neuron 51:703–714.

Müller UC, Deller T, Korte M (2017) Not just amyloid: physiological functions of the amyloid precursor protein family. Nature Reviews Neuroscience 18:281–298.

Murphy GM, Yang L, Cordell B (1998) Macrophage Colony-stimulating Factor Augments β-Amyloid-induced Interleukin-1, Interleukin-6, and Nitric Oxide Production by Microglial Cells. Journal of Biological Chemistry 273:20967–20971.

Nandi S, Akhter MP, Seifert MF, Dai X-M, Stanley ER (2006) Developmental and functional significance of the CSF-1 proteoglycan chondroitin sulfate chain. Blood 107:786–795.

Nandi S, Gokhan S, Dai X-M, Wei S, Enikolopov G, Lin H, Mehler MF, Stanley ER (2012) The CSF-1 receptor ligands IL-34 and CSF-1 exhibit distinct developmental brain expression patterns and regulate neural progenitor cell maintenance and maturation. Developmental Biology 367:100–113.

Napolitano G, Esposito A, Choi H, Matarese M, Benedetti V, Malta C di, Monfregola J, Medina DL, Lippincott-Schwartz J, Ballabio A (2018) mTOR-dependent phosphorylation controls TFEB nuclear export. Nature Communications 9:3312–3322 Available at: /pmc/articles/PMC6098152/ [Accessed October 17, 2021].

Nelson PT et al. (2012) Correlation of Alzheimer Disease Neuropathologic Changes With Cognitive Status: A Review of the Literature. Journal of Neuropathology & Experimental Neurology 71:362–381.

Neumann H, Kotter MR, Franklin RJM (2008) Debris clearance by microglia: an essential link between degeneration and regeneration. Brain 132:288–295.

Nicoll JAR, Wilkinson D, Holmes C, Steart P, Markham H, Weller RO (2003) Neuropathology of human Alzheimer disease after immunization with amyloid-β peptide: a case report. Nature Medicine 9:448–452.

Nijholt DAT, de Graaf TR, van Haastert ES, Oliveira AO, Berkers CR, Zwart R, Ovaa H, Baas F, Hoozemans JJM, Scheper W (2011) Endoplasmic reticulum stress activates autophagy but not the proteasome in neuronal cells: implications for Alzheimer's disease. Cell Death & Differentiation 18:1071–1081.

Nikolic L, Shen W, Nobili P, Virenque A, Ulmann L, Audinat E (2018) Blocking TNFα-driven astrocyte purinergic signaling restores normal synaptic activity during epileptogenesis. Glia 66:2673–2683 Available at: https://onlinelibrary.wiley.com/doi/10.1002/glia.23519 [Accessed October 17, 2021].

Nimmerjahn A (2005) Resting Microglial Cells Are Highly Dynamic Surveillants of Brain Parenchyma in Vivo. Science 308:1314–1318.

Nishida M, Ando M, Iwamoto Y, Tsuchiya K, Nitta K (2016) New Insight into Atherosclerosis in Hemodialysis Patients: Overexpression of Scavenger Receptor and Macrophage Colony-Stimulating Factor Genes. Nephron Extra 6:22–30.

Nixon RA, Yang D-S, Lee J-H (2008) Neurodegenerative lysosomal disorders: A continuum from development to late age. Autophagy 4:590–599.

Oakley H, Cole SL, Logan S, Maus E, Shao P, Craft J, Guillozet-Bongaarts A, Ohno M, Disterhoft J, Eldik L van, Berry R, Vassar R (2006a) Intraneuronal β-Amyloid Aggregates, Neurodegeneration, and Neuron Loss in Transgenic Mice with Five Familial Alzheimer's Disease Mutations: Potential Factors in Amyloid Plaque Formation. The Journal of Neuroscience 26:10129 Available at: /pmc/articles/PMC6674618/ [Accessed October 17, 2021].

Oddo S, Caccamo A, Shepherd JD, Murphy MP, Golde TE, Kayed R, Metherate R, Mattson MP, Akbari Y, LaFerla FM (2003) Triple-Transgenic Model of Alzheimer's Disease with Plaques and Tangles. Neuron 39:409–421.

Oddo S, Caccamo A, Tran L, Lambert MP, Glabe CG, Klein WL, LaFerla FM (2006) Temporal Profile of Amyloid-β (Aβ) Oligomerization in an in Vivo Model of Alzheimer Disease. Journal of Biological Chemistry 281:1599–1604.

Oh K-J, Perez SE, Lagalwar S, Vana L, Binder L, Mufson EJ (2010) Staging of Alzheimer's Pathology in Triple Transgenic Mice: A Light and Electron Microscopic Analysis. International Journal of Alzheimer's Disease 2010:1–24 Available at: http://www.hindawi.com/journals/ijad/2010/780102/.

Oh S, Hong HS, Hwang E, Sim HJ, Lee W, Shin SJ, Mook-Jung I (2005) Amyloid peptide attenuates the proteasome activity in neuronal cells. Mechanisms of Ageing and Development 126:1292–1299.

Olmos-Alonso A, Schetters STT, Sri S, Askew K, Mancuso R, Vargas-Caballero M, Holscher C, Perry VH, Gomez-Nicola D (2016) Pharmacological targeting of CSF1R inhibits microglial proliferation and prevents the progression of Alzheimer's-like pathology. Brain 139:891–907 Available at: https://academic.oup.com/brain/article-lookup/doi/10.1093/brain/awv379.

Orr ME, Oddo S (2013) Autophagic/lysosomal dysfunction in Alzheimer's disease. Alzheimer's Research & Therapy 5:53 Available at: http://alzres.biomedcentral.com/articles/10.1186/alzrt217.

Orre M, Kamphuis W, Dooves S, Kooijman L, Chan ET, Kirk CJ, Dimayuga Smith V, Koot S, Mamber C, Jansen AH, Ovaa H, Hol EM (2013) Reactive glia show increased immunoproteasome activity in Alzheimer's disease. Brain 136:1415–1431.

Otero K, Turnbull IR, Poliani PL, Vermi W, Cerutti E, Aoshi T, Tassi I, Takai T, Stanley SL, Miller M, Shaw AS, Colonna M (2009) Macrophage colony-stimulating factor induces the proliferation and survival of macrophages via a pathway involving DAP12 and β-catenin. Nature Immunology 10:734–743 Available at: http://www.nature.com/articles/ni.1744 [Accessed October 19, 2021].

Palmieri M, Impey S, Kang H, di Ronza A, Pelz C, Sardiello M, Ballabio A (2011) Characterization of the CLEAR network reveals an integrated control of cellular clearance pathways. Human Molecular Genetics 20:3852–3866.

Pan X, Zhu Y, Lin N, Zhang J, Ye Q, Huang H, Chen X (2011) Microglial phagocytosis induced by fibrillar β-amyloid is attenuated by oligomeric β-amyloid: implications for Alzheimer's disease. Molecular Neurodegeneration 6:45 Available at: https://molecularneurodegeneration.biomedcentral.com/articles/10.1186/1750-1326-6-45.

Paresce DM, Ghosh RN, Maxfield FR (1996) Microglial Cells Internalize Aggregates of the Alzheimer's Disease Amyloid β-Protein Via a Scavenger Receptor. Neuron 17:553–565 Available at: https://linkinghub.elsevier.com/retrieve/pii/S0896627300801877 [Accessed October 21, 2021].

Pastore N, Brady OA, Diab HI, Martina JA, Sun L, Huynh T, Lim J-A, Zare H, Raben N, Ballabio A, Puertollano R (2016) TFEB and TFE3 cooperate in the regulation of the innate immune response in activated macrophages. Autophagy 12:1240–1258.

Perez SE, He B, Muhammad N, Oh K-J, Fahnestock M, Ikonomovic MD, Mufson EJ (2011) Cholinotrophic basal forebrain system alterations in 3xTg-AD transgenic mice. Neurobiology of Disease 41:338–352.

Perrin RJ, Fagan AM, Holtzman DM (2009) Multimodal techniques for diagnosis and prognosis of Alzheimer's disease. Nature 461:916–922.

Pfeiffer T, Avignone E, Nägerl UV (2016) Induction of hippocampal long-term potentiation increases the morphological dynamics of microglial processes and prolongs their contacts with dendritic spines. Scientific Reports 6:32422 Available at: http://www.nature.com/articles/srep32422 [Accessed October 17, 2021].

Pillai S, Netravali IA, Cariappa A, Mattoo H (2012) Siglecs and Immune Regulation. Annual Review of Immunology 30:357–392.

Prehn JH, Bindokas VP, Jordán J, Galindo MF, Ghadge GD, Roos RP, Boise LH, Thompson CB, Krajewski S, Reed JC, Miller RJ (1996) Protective effect of transforming growth factor-beta 1 on beta-amyloid neurotoxicity in rat hippocampal neurons. Molecular pharmacology 49:319–328 Available at: http://www.ncbi.nlm.nih.gov/pubmed/8632765.

Prokop S, Miller KR, Heppner FL (2013) Microglia actions in Alzheimer's disease. Acta Neuropathologica 126:461–477.

Qin S (2006) System Xc- and Apolipoprotein E Expressed by Microglia Have Opposite Effects on the Neurotoxicity of Amyloid-beta Peptide 1-40. Journal of Neuroscience 26:3345–3356.

Querol-Vilaseca M, Colom-Cadena M, Pegueroles J, Nuñez-Llaves R, Luque-Cabecerans J, Muñoz-Llahuna L, Andilla J, Belbin O, Spires-Jones TL, Gelpi E, Clarimon J, Loza-Alvarez P, Fortea J, Lleó A (2019) Nanoscale structure of amyloid-β plaques in Alzheimer's disease. Scientific Reports 9:5181.

Raivich G, Haas S, Werner A, Klein MA, Kloss C, Kreutzberg GW (1998) Regulation of MSCF receptors on microglia in the normal and injured mouse central nervous system: A quantitative immunofluorescence study using confocal laser microscopy. The Journal of Comparative Neurology 395:342–358.

Ray S et al. (2007) Classification and prediction of clinical Alzheimer's diagnosis based on plasma signaling proteins. Nature Medicine 13:1359–1362.

Raychaudhuri M, Mukhopadhyay D (2007) AICD and its Adaptors – In Search of New Players. Journal of Alzheimer's Disease 11:343–358.

Reichwald J, Danner S, Wiederhold K-H, Staufenbiel M (2009) Expression of complement system components during aging and amyloid deposition in APP transgenic mice. Journal of Neuroinflammation 6:35 Available at: https://jneuroinflammation.biomedcentral.com/articles/10.1186/1742-2094-6-35.

Richard BC, Kurdakova A, Baches S, Bayer TA, Weggen S, Wirths O (2015) Gene Dosage Dependent Aggravation of the Neurological Phenotype in the 5XFAD Mouse Model of Alzheimer's Disease. Journal of Alzheimer's Disease 45:1223–1236.

Ries M, Sastre M (2016) Mechanisms of Aβ Clearance and Degradation by Glial Cells. Frontiers in Aging Neuroscience 8:160 Available at: http://journal.frontiersin.org/Article/10.3389/fnagi.2016.00160/abstract.

Río-Hortega P (1919) El "Tercer Elemento" de los Centros Nerviosos".III. Naturaleza Probable de la Microglía, Boletín de la Sociedad Española de Biología VIII. :108–121.

Rodríguez JJ, Jones VC, Tabuchi M, Allan SM, Knight EM, LaFerla FM, Oddo S, Verkhratsky A (2008) Impaired Adult Neurogenesis in the Dentate Gyrus of a Triple Transgenic Mouse Model of Alzheimer's Disease. PLoS ONE 3:e2935.

Rojo LE, Fernández JA, Maccioni AA, Jimenez JM, Maccioni RB (2008) Neuroinflammation: implications for the pathogenesis and molecular diagnosis of Alzheimer's disease. Archives of medical research 39:1–16.

Ruiz A, Matute C, Alberdi E (2009) Endoplasmic reticulum Ca2+ release through ryanodine and IP3 receptors contributes to neuronal excitotoxicity. Cell Calcium 46:273–281 Available at: https://linkinghub.elsevier.com/retrieve/pii/S014341600900150X [Accessed October 17, 2021].

Ryan GR, Dai X-M, Dominguez MG, Tong W, Chuan F, Chisholm O, Russell RG, Pollard JW, Stanley ER (2001) Rescue of the colony-stimulating factor 1 (CSF-1)–nullizygous mouse (Csf1op/Csf1op) phenotype with a CSF-1 transgene and identification of sites of local CSF-1 synthesis. Blood 98:74–84.

Saito T, Matsuba Y, Mihira N, Takano J, Nilsson P, Itohara S, Iwata N, Saido TC (2014) Single App knock-in mouse models of Alzheimer's disease. Nature Neuroscience 17:661–663.

Sala Frigerio C, Wolfs L, Fattorelli N, Thrupp N, Voytyuk I, Schmidt I, Mancuso R, Chen WT, Woodbury ME, Srivastava G, Möller T, Hudry E, Das S, Saido T, Karran E, Hyman B, Perry VH, Fiers M, De Strooper B (2019) The Major Risk Factors for Alzheimer's Disease: Age, Sex, and Genes Modulate the Microglia Response to Aβ Plaques. Cell Reports 27:1293-1306.e6.

Santos AN, Ewers M, Minthon L, Simm A, Silber R-E, Blennow K, Prvulovic D, Hansson O, Hampel H (2012) Amyloid-β Oligomers in Cerebrospinal Fluid are Associated with Cognitive Decline in Patients with Alzheimer's Disease. Journal of Alzheimer's Disease 29:171–176 Available at: https://www.medra.org/servlet/aliasResolver?alias=iospress&doi=10.3233/JAD-2012-111361.

Sardiello M, Ballabio A (2009) Lysosomal enhancement: A CLEAR answer to cellular degradative needs. Cell Cycle 8:4021–4022 Available at: http://www.tandfonline.com/doi/abs/10.4161/cc.8.24.10263.

Sasaguri H, Nilsson P, Hashimoto S, Nagata K, Saito T, de Strooper B, Hardy J, Vassar R, Winblad B, Saido TC (2017) <scp>APP</scp> mouse models for Alzheimer's disease preclinical studies. The EMBO Journal 36:2473–2487 Available at: https://onlinelibrary.wiley.com/doi/10.15252/embj.201797397.

Schafer DP, Lehrman EK, Kautzman AG, Koyama R, Mardinly AR, Yamasaki R, Ransohoff RM, Greenberg ME, Barres BA, Stevens B (2012) Microglia Sculpt Postnatal Neural Circuits in an Activity and Complement-Dependent Manner. Neuron 74:691–705 Available at: https://linkinghub.elsevier.com/retrieve/pii/S0896627312003340 [Accessed October 25, 2021].

Scheff SW, Price DA, Schmitt FA, Mufson EJ (2006) Hippocampal synaptic loss in early Alzheimer's disease and mild cognitive impairment. Neurobiology of Aging 27:1372–1384.

Schindelin J, Arganda-Carreras I, Frise E, Kaynig V, Longair M, Pietzsch T, Preibisch S, Rueden C, Saalfeld S, Schmid B, Tinevez J-Y, White DJ, Hartenstein V, Eliceiri K, Tomancak P, Cardona A (2012) Fiji: an open-source platform for biological-image analysis. Nature Methods 9:676–682 Available at: http://www.nature.com/articles/nmeth.2019 [Accessed October 17, 2021].

Schwabe T, Srinivasan K, Rhinn H (2020) Shifting paradigms: The central role of microglia in Alzheimer's disease. Neurobiology of Disease 143:104962 Available at: https://linkinghub.elsevier.com/retrieve/pii/S0969996120302370.

Ségaliny AI, Tellez-Gabriel M, Heymann M-F, Heymann D (2015) Receptor tyrosine kinases: Characterisation, mechanism of action and therapeutic interests for bone cancers. Journal of Bone Oncology 4:1–12 Available at: https://linkinghub.elsevier.com/retrieve/pii/S2212137415200188.

Sekar A, Bialas AR, de Rivera H, Davis A, Hammond TR, Kamitaki N, Tooley K, Presumey J, Baum M, van Doren V, Genovese G, Rose SA, Handsaker RE, Schizophrenia Working Group of the Psychiatric Genomics Consortium, Daly MJ, Carroll MC, Stevens B, McCarroll SA (2016) Schizophrenia risk from complex variation of complement component 4. Nature 530:177–183 Available at: http://www.ncbi.nlm.nih.gov/pubmed/26814963 [Accessed October 25, 2021].

Selkoe DJ (1991) The molecular pathology of Alzheimer's disease. Neuron 6:487–498 Available at: https://linkinghub.elsevier.com/retrieve/pii/0896627391900522.

Selkoe DJ (2002) Alzheimer's Disease Is a Synaptic Failure. Science 298:789–791 Available at: https://www.science.org/doi/10.1126/science.1074069.

Selkoe DJ, Hardy J (2016) The amyloid hypothesis of Alzheimer's disease at 25 years. EMBO Molecular Medicine 8:595–608 Available at: https://onlinelibrary.wiley.com/doi/10.15252/emmm.201606210.

Serrano-Pozo A, Frosch MP, Masliah E, Hyman BT (2011) Neuropathological Alterations in Alzheimer Disease. Cold Spring Harbor Perspectives in Medicine 1:a006189–a006189 Available at: http://perspectivesinmedicine.cshlp.org/lookup/doi/10.1101/cshperspect.a006189.

Shah A, Kishore U, Shastri A (2021) Complement System in Alzheimer's Disease. International Journal of Molecular Sciences 22:13647 Available at: https://www.mdpi.com/1422-0067/22/24/13647.

Sharma J, di Ronza A, Lotfi P, Sardiello M (2018) Lysosomes and Brain Health. Annual Review of Neuroscience 41:255–276 Available at: https://www.annualreviews.org/doi/10.1146/annurev-neuro-080317-061804.

Sheedy FJ, Grebe A, Rayner KJ, Kalantari P, Ramkhelawon B, Carpenter SB, Becker CE, Ediriweera HN, Mullick AE, Golenbock DT, Stuart LM, Latz E, Fitzgerald KA, Moore KJ (2013) CD36 coordinates NLRP3 inflammasome activation by facilitating intracellular nucleation of soluble ligands into particulate ligands in sterile inflammation. Nature Immunology 14:812–820 Available at: http://www.nature.com/articles/ni.2639.

Sheng JG, Mrak RE, Bales KR, Cordell B, Paul SM, Jones RA, Woodward S, Zhou XQ, McGinness JM, Griffin WST (2001) Overexpression of the Neuritotrophic Cytokine S100β Precedes the Appearance of Neuritic β-Amyloid Plaques in APPV717F Mice. Journal of Neurochemistry 74:295–301 Available at: http://doi.wiley.com/10.1046/j.1471-4159.2000.0740295.x.

Sherrington R et al. (1995) Cloning of a gene bearing missense mutations in early-onset familial Alzheimer's disease. Nature 375:754–760 Available at: http://www.nature.com/articles/375754a0.

Shibata N, Kawarai T, Meng Y, Lee JH, Lee H-S, Wakutani Y, Shibata E, Pathan N, Bi A, Sato C, Sorbi S, Bruni AC, Duara R, Mayeux R, Farrer LA, George-Hyslop P st., Rogaeva E (2007) Association studies between the plasmin genes and late-onset Alzheimer's disease. Neurobiology of Aging 28:1041–1043 Available at: https://linkinghub.elsevier.com/retrieve/pii/S0197458006001837.

Sierra A, Paolicelli RC, Kettenmann H (2019) Cien Años de Microglía: Milestones in a Century of Microglial Research. Trends in Neurosciences 42:778–792 Available at: http://www.cell.com/article/S0166223619301754/fulltext [Accessed October 21, 2021].

Smith AM, Gibbons HM, Oldfield RL, Bergin PM, Mee EW, Curtis MA, Faull RLM, Dragunow M (2013) M-CSF increases proliferation and phagocytosis while modulating receptor and transcription factor expression in adult human microglia. Journal of Neuroinflammation 10:859 Available at: https://jneuroinflammation.biomedcentral.com/articles/10.1186/1742-2094-10-85.

Smith ME (1999) Phagocytosis of myelin in demyelinative disease: a review. Neurochemical Research 24:261–268.

Solé-Domènech S, Cruz DL, Capetillo-Zarate E, Maxfield FR (2016) The endocytic pathway in microglia during health, aging and Alzheimer's disease. Ageing Research Reviews 32:89–103 Available at: https://linkinghub.elsevier.com/retrieve/pii/S1568163716301428.

Solé-Domènech S, Rojas A v., Maisuradze GG, Scheraga HA, Lobel P, Maxfield FR (2018) Lysosomal enzyme tripeptidyl peptidase 1 destabilizes fibrillar Aβ by multiple endoproteolytic cleavages within the β-sheet domain. Proceedings of the National Academy of Sciences 115:1493–1498 Available at: http://www.pnas.org/lookup/doi/10.1073/pnas.1719808115.

Soulet D, Rivest S (2008) Bone-marrow-derived microglia: myth or reality? Current Opinion in Pharmacology 8:508–518 Available at: https://linkinghub.elsevier.com/retrieve/pii/S147148920800043X.

Spampanato C, Feeney E, Li L, Cardone M, Lim J, Annunziata F, Zare H, Polishchuk R, Puertollano R, Parenti G, Ballabio A, Raben N (2013) Transcription factor EB (TFEB) is a new therapeutic target for Pompe disease. EMBO Molecular Medicine 5:691–706 Available at: https://onlinelibrary.wiley.com/doi/10.1002/emmm.201202176.

Spangenberg E et al. (2019) Sustained microglial depletion with CSF1R inhibitor impairs parenchymal plaque development in an Alzheimer's disease model. Nature Communications 10:3758 Available at: http://www.nature.com/articles/s41467-019-11674-z.

Spires TL (2005) Dendritic Spine Abnormalities in Amyloid Precursor Protein Transgenic Mice Demonstrated by Gene Transfer and Intravital Multiphoton Microscopy. Journal of Neuroscience 25:7278–7287 Available at: https://www.jneurosci.org/lookup/doi/10.1523/JNEUROSCI.1879-05.2005.

Stanley ER, Chitu V (2014) CSF-1 Receptor Signaling in Myeloid Cells. Cold Spring Harbor Perspectives in Biology 6:a021857–a021857 Available at: http://cshperspectives.cshlp.org/lookup/doi/10.1101/cshperspect.a021857.

Stanley ER, Cifone M, Heard PM, Defendi V (1976) Factors regulating macrophage production and growth: identity of colony-stimulating factor and macrophage growth factor. Journal of Experimental Medicine 143:631–647 Available at: https://rupress.org/jem/article/143/3/631/22039/Factors-regulating-macrophage-production-and.

Stanley ER, Heard PM (1977) Factors regulating macrophage production and growth. Purification and some properties of the colony stimulating factor from medium conditioned by mouse L cells. The Journal of biological chemistry 252:4305–4312 Available at: http://www.ncbi.nlm.nih.gov/pubmed/301140.

Steingrimsson E, Tessarollo L, Pathak B, Hou L, Arnheiter H, Copeland NG, Jenkins NA (2002) Mitf and Tfe3, two members of the Mitf-Tfe family of bHLH-Zip transcription factors, have important but functionally redundant roles in osteoclast development. Proceedings of the National Academy of Sciences 99:4477–4482 Available at: http://www.pnas.org/cgi/doi/10.1073/pnas.072071099.

Stence N, Waite M, Dailey ME (2001) Dynamics of microglial activation: a confocal time-lapse analysis in hippocampal slices. Glia 33:256–266 Available at: http://www.ncbi.nlm.nih.gov/pubmed/11241743.

Stevens B, Allen NJ, Vazquez LE, Howell GR, Christopherson KS, Nouri N, Micheva KD, Mehalow AK, Huberman AD, Stafford B, Sher A, Litke AM, Lambris JD, Smith SJ, John SWM, Barres BA (2007) The Classical Complement Cascade Mediates CNS Synapse Elimination. Cell 131:1164–1178 Available at: https://linkinghub.elsevier.com/retrieve/pii/S0092867407013554 [Accessed October 25, 2021].

Stoppini L, Buchs P-A, Muller D (1991) A simple method for organotypic cultures of nervous tissue. Journal of Neuroscience Methods 37:173–182.

Streit WJ, Mrak RE, Griffin WST (2004) Microglia and neuroinflammation: a pathological perspective. Journal of Neuroinflammation 1.

Sun Y, Rong X, Lu W, Peng Y, Li J, Xu S, Wang L, Wang X (2015) Translational Study of Alzheimer's Disease (AD) Biomarkers from Brain Tissues in AβPP/PS1 Mice and Serum of AD Patients. Journal of Alzheimer's Disease 45:269–282 Available at: https://www.medra.org/servlet/aliasResolver?alias=iospress&doi=10.3233/JAD-142805.

T. Griffin WS, Sheng JG, Roberts GW, Mrak RE (1995) Interleukin-1 Expression in Different Plaque Types in Alzheimer's Disease. Journal of Neuropathology and Experimental Neurology 54:276–281 Available at: https://academic.oup.com/jnen/article-lookup/doi/10.1097/00005072-199503000-00014.

Takami M, Nagashima Y, Sano Y, Ishihara S, Morishima-Kawashima M, Funamoto S, Ihara Y (2009) -Secretase: Successive Tripeptide and Tetrapeptide Release from the Transmembrane Domain of -Carboxyl Terminal Fragment. Journal of Neuroscience 29:13042–13052 Available at: https://www.jneurosci.org/lookup/doi/10.1523/JNEUROSCI.2362-09.2009.

Tan J, Town T, Paris D, Mori T, Suo Z, Crawford F, Mattson MP, Flavell RA, Mullan M (1999a) Microglial activation resulting from CD40-CD40L interaction after beta-amyloid stimulation. Science (New York, NY) 286:2352–2355.

Tarkowski E, Blennow K, Wallin A, Tarkowski A (1999) Intracerebral production of tumor necrosis factor-alpha, a local neuroprotective agent, in Alzheimer disease and vascular dementia. Journal of Clinical Immunology 19.

Tenner AJ (2020) Complement-Mediated Events in Alzheimer's Disease: Mechanisms and Potential Therapeutic Targets. Journal of immunology (Baltimore, Md : 1950) 204:306–315.

Thal DR, Rüb U, Orantes M, Braak H (2002) Phases of Aβ-deposition in the human brain and its relevance for the development of AD. Neurology 58:1791–1800 Available at: https://www.neurology.org/lookup/doi/10.1212/WNL.58.12.1791.

Togo T, Akiyama H, Kondo H, Ikeda K, Kato M, Iseki E, Kosaka K (2000) Expression of CD40 in the brain of Alzheimer's disease and other neurological diseases. Brain research 885:117–121.

Tomiyama T, Matsuyama S, Iso H, Umeda T, Takuma H, Ohnishi K, Ishibashi K, Teraoka R, Sakama N, Yamashita T, Nishitsuji K, Ito K, Shimada H, Lambert MP, Klein WL, Mori H (2010) A Mouse Model of Amyloid Oligomers: Their Contribution to Synaptic Alteration, Abnormal Tau Phosphorylation, Glial Activation, and Neuronal Loss In Vivo. Journal of Neuroscience 30:4845–4856 Available at: https://www.jneurosci.org/lookup/doi/10.1523/JNEUROSCI.5825-09.2010.

Tremblay M-È, Lowery RL, Majewska AK (2010) Microglial Interactions with Synapses Are Modulated by Visual Experience Dalva M, ed. PLoS Biology 8:e1000527 Available at: https://dx.plos.org/10.1371/journal.pbio.1000527.

Tremblay M-E, Stevens B, Sierra A, Wake H, Bessis A, Nimmerjahn A (2011) The Role of Microglia in the Healthy Brain. Journal of Neuroscience 31:16064–16069.

Tseng BP, Green KN, Chan JL, Blurton-Jones M, LaFerla FM (2008) Aβ inhibits the proteasome and enhances amyloid and tau accumulation. Neurobiology of Aging 29:1607–1618.

van der Wal EA, Gómez-Pinilla F, Cotman CW (1993) Transforming growth factor-β1 is in plaques in Alzheimer and Down pathologies. NeuroReport 4:69–72 Available at: http://journals.lww.com/00001756-199301000-00018.

Vandenabeele P, Fiers W (1991) Is amyloidogenesis during Alzheimer's disease due to an IL-1-/IL-6-mediated 'acute phase response' in the brain? Immunology Today 12:217–219 Available at: https://linkinghub.elsevier.com/retrieve/pii/016756999190032O.

Vincent V (2002) Proinflammatory effects of M-CSF and Aβ in hippocampal organotypic cultures. Neurobiology of Aging 23:349–362 Available at: https://linkinghub.elsevier.com/retrieve/pii/S0197458001003384.

Vincent VAM, Robinson CC, Simsek D, Murphy GM (2002) Macrophage colony stimulating factor prevents NMDA-induced neuronal death in hippocampal organotypic cultures. Journal of Neurochemistry 82:1388–1397 Available at: http://doi.wiley.com/10.1046/j.1471-4159.2002.01087.x.

Viola KL, Klein WL (2015) Amyloid β oligomers in Alzheimer's disease pathogenesis, treatment, and diagnosis. Acta Neuropathologica 129.

Vogel DYS, Glim JE, Stavenuiter AWD, Breur M, Heijnen P, Amor S, Dijkstra CD, Beelen RHJ (2014) Human macrophage polarization in vitro: Maturation and activation methods compared. Immunobiology 219:695–703 Available at: https://linkinghub.elsevier.com/retrieve/pii/S0171298514000862.

von Holst A (2006) The Unique 473HD-Chondroitinsulfate Epitope Is Expressed by Radial Glia and Involved in Neural Precursor Cell Proliferation. Journal of Neuroscience 26:4082–4094 Available at: https://www.jneurosci.org/lookup/doi/10.1523/JNEUROSCI.0422-06.2006.

von Rotz RC, Kohli BM, Bosset J, Meier M, Suzuki T, Nitsch RM, Konietzko U (2004) The APP intracellular domain forms nuclear multiprotein complexes and regulates the transcription of its own precursor. Journal of Cell Science 117:4435–4448 Available at: https://journals.biologists.com/jcs/article/117/19/4435/27774/The-APP-intracellular-domain-forms-nuclear.

Wake H, Moorhouse AJ, Jinno S, Kohsaka S, Nabekura J (2009) Resting Microglia Directly Monitor the Functional State of Synapses In Vivo and Determine the Fate of Ischemic Terminals. Journal of Neuroscience 29:3974–3980 Available at: https://www.jneurosci.org/lookup/doi/10.1523/JNEUROSCI.4363-08.2009.

Walker DG, Tang TM, Lue L-F (2017) Studies on Colony Stimulating Factor Receptor-1 and Ligands Colony Stimulating Factor-1 and Interleukin-34 in Alzheimer's Disease Brains and Human Microglia. Frontiers in Aging Neuroscience 9 Available at: http://journal.frontiersin.org/article/10.3389/fnagi.2017.00244/full.

Walton NM, Sutter BM, Laywell ED, Levkoff LH, Kearns SM, Marshall GP, Scheffler B, Steindler DA (2006) Microglia instruct subventricular zone neurogenesis. Glia 54:815–825 Available at: https://onlinelibrary.wiley.com/doi/10.1002/glia.20419.

Wang H, Huang L, Wu L, Lan J, Feng X, Li P, Peng Y (2020) The MMP-2/TIMP-2 System in Alzheimer Disease. CNS & Neurological Disorders - Drug Targets 19:402–416 Available at: https://www.eurekaselect.com/184815/article.

Wang H, Wang R, Xu S, Lakshmana MK (2016a) Transcription Factor EB Is Selectively Reduced in the Nuclear Fractions of Alzheimer's and Amyotrophic Lateral Sclerosis Brains. Neuroscience Journal 2016:1–8 Available at: https://www.hindawi.com/journals/neuroscience/2016/4732837/.

Wang J-Z, Grundke-Iqbal I, Iqbal K (1996) Glycosylation of microtubule–associated protein tau: An abnormal posttranslational modification in Alzheimer's disease. Nature Medicine 2:871–875 Available at: http://www.nature.com/articles/nm0896-871.

Wang Q (2004) Block of Long-Term Potentiation by Naturally Secreted and Synthetic Amyloid -Peptide in Hippocampal Slices Is Mediated via Activation of the Kinases c-Jun N-Terminal Kinase, Cyclin-Dependent Kinase 5, and p38 Mitogen-Activated Protein Kinase as well as Metabotropic Glutamate Receptor Type 5. Journal of Neuroscience 24:3370–3378 Available at: https://www.jneurosci.org/lookup/doi/10.1523/JNEUROSCI.1633-03.2004.

Wang S, Wang R, Chen L, Bennett DA, Dickson DW, Wang D-S (2010) Expression and functional profiling of neprilysin, insulin-degrading enzyme, and endothelin-converting enzyme in prospectively studied elderly and Alzheimer's brain. Journal of Neurochemistry 115:47–57 Available at: https://onlinelibrary.wiley.com/doi/10.1111/j.1471-4159.2010.06899.x [Accessed October 21, 2021].

Wang Y, Cella M, Mallinson K, Ulrich JD, Young KL, Robinette ML, Gilfillan S, Krishnan GM, Sudhakar S, Zinselmeyer BH, Holtzman DM, Cirrito JR, Colonna M (2015) TREM2 Lipid Sensing Sustains the Microglial Response in an Alzheimer's Disease Model. Cell 160:1061–1071.

Wang Y, Ulland TK, Ulrich JD, Song W, Tzaferis JA, Hole JT, Yuan P, Mahan TE, Shi Y, Gilfillan S, Cella M, Grutzendler J, DeMattos RB, Cirrito JR, Holtzman DM, Colonna M (2016b) TREM2-mediated early microglial response limits diffusion and toxicity of amyloid plaques. Journal of Experimental Medicine 213:667–675.

Wang Y, Yeung YG, Stanley ER (1999) CSF-1 stimulated multiubiquitination of the CSF-1 receptor and of Cbl follows their tyrosine phosphorylation and association with other signaling proteins. Journal of cellular biochemistry 72:119–134 Available at: http://www.ncbi.nlm.nih.gov/pubmed/10025673 [Accessed October 19, 2021].

Webb SE, Pollard JW, Jones GE (1996) Direct observation and quantification of macrophage chemoattraction to the growth factor CSF-1. Journal of cell science 109 (Pt 4):793–803 Available at: http://www.ncbi.nlm.nih.gov/pubmed/8718671.

Wei S, Nandi S, Chitu V, Yeung Y-G, Yu W, Huang M, Williams LT, Lin H, Stanley ER (2010) Functional overlap but differential expression of CSF-1 and IL-34 in their CSF-1 receptor-mediated regulation of myeloid cells. Journal of Leukocyte Biology 88:495–505 Available at: http://doi.wiley.com/10.1189/jlb.1209822.

Weidemann A, Eggert S, Reinhard FBM, Vogel M, Paliga K, Baier G, Masters CL, Beyreuther K, Evin G (2002) A Novel ε-Cleavage within the Transmembrane Domain of the Alzheimer Amyloid Precursor Protein Demonstrates Homology with Notch Processing. Biochemistry 41:2825–2835 Available at: https://pubs.acs.org/doi/10.1021/bi015794o.

Weilbaecher KN, Motyckova G, Huber WE, Takemoto CM, Hemesath TJ, Xu Y, Hershey CL, Dowland NR, Wells AG, Fisher DE (2001) Linkage of M-CSF Signaling to Mitf, TFE3, and the

Osteoclast Defect in Mitfmi/mi Mice. Molecular Cell 8:749–758 Available at: https://linkinghub.elsevier.com/retrieve/pii/S1097276501003604.

Wertkin AM, Turner RS, Pleasure SJ, Golde TE, Younkin SG, Trojanowski JQ, Lee VM (1993) Human neurons derived from a teratocarcinoma cell line express solely the 695-amino acid amyloid precursor protein and produce intracellular beta-amyloid or A4 peptides. Proceedings of the National Academy of Sciences 90:9513–9517 Available at: http://www.pnas.org/cgi/doi/10.1073/pnas.90.20.9513.

Wharton SB, Minett T, Drew D, Forster G, Matthews F, Brayne C, Ince PG (2016) Epidemiological pathology of Tau in the ageing brain: application of staging for neuropil threads (BrainNet Europe protocol) to the MRC cognitive function and ageing brain study. Acta Neuropathologica Communications 4:11 Available at: http://actaneurocomms.biomedcentral.com/articles/10.1186/s40478-016-0275-x.

Wilcock DM (2004) Passive Amyloid Immunotherapy Clears Amyloid and Transiently Activates Microglia in a Transgenic Mouse Model of Amyloid Deposition. Journal of Neuroscience 24:6144–6151.

Wilde MC de, Overk CR, Sijben JW, Masliah E (2016) Meta-analysis of synaptic pathology in Alzheimer's disease reveals selective molecular vesicular machinery vulnerability. Alzheimer's & Dementia 12:633–644 Available at: https://onlinelibrary.wiley.com/doi/full/10.1016/j.jalz.2015.12.005 [Accessed October 20, 2021].

Wilkinson K BJGMMKEKJ (2011) A high content drug screen identifies ursolic acid as an inhibitor of amyloid beta protein interactions with its recep- tor CD36. Journal of Biological Chemistry 286:34914–34922.

Wilkinson K, el Khoury J (2012) Microglial Scavenger Receptors and Their Roles in the Pathogenesis of Alzheimer's Disease. International Journal of Alzheimer's Disease 2012:1–10 Available at: http://www.hindawi.com/journals/ijad/2012/489456/.

Wlodarczyk A, Holtman IR, Krueger M, Yogev N, Bruttger J, Khorooshi R, Benmamar-Badel A, Boer-Bergsma JJ, Martin NA, Karram K, Kramer I, Boddeke EW, Waisman A, Eggen BJ, Owens T (2017) A novel microglial subset plays a key role in myelinogenesis in developing brain. The EMBO Journal 36:3292–3308 Available at: https://onlinelibrary.wiley.com/doi/10.15252/embj.201696056.

Wolfe DM, Lee J, Kumar A, Lee S, Orenstein SJ, Nixon RA (2013) Autophagy failure in Alzheimer's disease and the role of defective lysosomal acidification. European Journal of Neuroscience 37:1949–1961 Available at: https://onlinelibrary.wiley.com/doi/10.1111/ejn.12169.

Wong E, Cuervo AM (2010) Autophagy gone awry in neurodegenerative diseases. Nature Neuroscience 13:805–811 Available at: http://www.nature.com/articles/nn.2575.

Wood JG, Mirra SS, Pollock NJ, Binder LI (1986) Neurofibrillary tangles of Alzheimer disease share antigenic determinants with the axonal microtubule-associated protein tau (tau). Proceedings of the National Academy of Sciences 83:4040–4043 Available at: http://www.pnas.org/cgi/doi/10.1073/pnas.83.11.4040.

Wyss-Coray T (2006) Inflammation in Alzheimer disease: driving force, bystander or beneficial response? Nature medicine 12:1005–1015.

Wyss-Coray T, Mucke L (2002) Inflammation in Neurodegenerative Disease—A Double-Edged Sword. Neuron 35:419–432.

Xinze S, Xuan W, Longze S, Qi X (2018) Comparison of β-Amyloid Plaque Labeling Methods: Antibody Staining, Gallyas Silver Staining, and Thioflavin-S Staining. cmsj 33:167–173 Available at: http://cmsj.cams.cn/EN/10.24920/03476.

Xu J, Yu T, Pietronigro EC, Yuan J, Arioli J, Pei Y, Luo X, Ye J, Constantin G, Mao C, Xiao Y (2020) Peli1 impairs microglial Aβ phagocytosis through promoting C/EBPβ degradation Daneman R, ed. PLOS Biology 18:e3000837 Available at: https://dx.plos.org/10.1371/journal.pbio.3000837.

Yang AJ, Chandswangbhuvana D, Shu T, Henschen A, Glabe CG (1999) Intracellular Accumulation of Insoluble, Newly Synthesized Aβn-42 in Amyloid Precursor Protein-transfected Cells That Have Been Treated with Aβ1–42. Journal of Biological Chemistry 274:20650–20656 Available at: https://linkinghub.elsevier.com/retrieve/pii/S0021925819726982.

Yang C-N, Shiao Y-J, Shie F-S, Guo B-S, Chen P-H, Cho C-Y, Chen Y-J, Huang F-L, Tsay H-J (2011) Mechanism mediating oligomeric Aβ clearance by naïve primary microglia. Neurobiology of Disease 42:221–230 Available at: https://linkinghub.elsevier.com/retrieve/pii/S0969996111000064.

Yoshiyama Y, Higuchi M, Zhang B, Huang S-M, Iwata N, Saido TC, Maeda J, Suhara T, Trojanowski JQ, Lee VM-Y (2007) Synapse Loss and Microglial Activation Precede Tangles in a P301S Tauopathy Mouse Model. Neuron 53:337–351.

Young AMH et al. (2021) A map of transcriptional heterogeneity and regulatory variation in human microglia. Nature Genetics.

Young K, Morrison H (2018) Quantifying Microglia Morphology from Photomicrographs of Immunohistochemistry Prepared Tissue Using ImageJ. Journal of Visualized Experiments 2018 Available at: https://www.jove.com/video/57648/quantifying-microglia-morphology-from-photomicrographs.

Yu Y, Jans DC, Winblad B, Tjernberg LO, Schedin-Weiss S (2018) Neuronal Aβ42 is enriched in small vesicles at the presynaptic side of synapses. Life Science Alliance 1:e201800028 Available at: https://www.life-science-alliance.org/lookup/doi/10.26508/lsa.201800028.

Yu Y, Ye RD (2015) Microglial Aβ Receptors in Alzheimer's Disease. Cellular and Molecular Neurobiology 35:71–83 Available at: http://link.springer.com/10.1007/s10571-014-0101-6.

Zhang Y, Zhao J (2015) TFEB Participates in the Aβ-Induced Pathogenesis of Alzheimer's Disease by Regulating the Autophagy-Lysosome Pathway. DNA and Cell Biology 34:661–668 Available at: http://www.liebertpub.com/doi/10.1089/dna.2014.2738.

Zhao Z, Xiang Z, Haroutunian V, Buxbaum JD, Stetka B, Pasinetti GM (2007) Insulin degrading enzyme activity selectively decreases in the hippocampal formation of cases at high risk to develop Alzheimer's disease. Neurobiology of Aging 28:824–830 Available at: https://linkinghub.elsevier.com/retrieve/pii/S0197458006001412.

Zheng H, Koo EH (2011) Biology and pathophysiology of the amyloid precursor protein. Molecular Neurodegeneration 6:27 Available at: http://molecularneurodegeneration.biomedcentral.com/articles/10.1186/1750-1326-6-27.